Cornwall FLOW Accelerator

THE SOUTH-WEST TRANSMISSION NETWORK AND FLOATING OFFSHORE WIND IN THE CELTIC SEA

Document Title		THE SOUTH-WEST TRANSMISSION NETWORK AND FLOATING OFFSHORE WIND IN THE CELTIC SEA	
Document Reference		PN000463 CFAR-OC-039-14022023	
Date of Issue		20230316	
Lead Author		Bradley McKay	
Co-Author		Nathan Haley	
Revision History	**Date**	**Reviewed / Approved by**	**Authorised by**
First Draft			
Second Draft			
First Issue	20230214	Chunjiang Jia	Simon Cheeseman
Addendum	20230316		Simon Cheeseman
Rev 1	20221031		
Rev 2	20221112		
Rev 3	20221201		
Rev 4	20221208		
Rev 5	20221216		
Rev 6	20230210		

HM Government

European Union
European Regional Development Fund

CATAPULT
Offshore Renewable Energy

CORNWALL FLOW ACCELERATOR PROJECT Innovation in Low Carbon Design and Manufacturability

The South-West Transmission Network and Floating Offshore Wind Optimization in the Celtic Sea

REPORT - Floating Offshore Wind Electrical Infrastructure and Grid Connections

Photo Source: HVDC technology for offshore wind is maturing | ABB (DolWin2 platform en route)

ACKNOWLEDGEMENT

The study was jointly supported by the Celtic Sea Cluster (CSC) under the part ERDF funded Cornwall FLOW Accelerator Project, led by Celtic Sea Power (CSP), supported by University of Exeter (UoE), University of Plymouth (UoP), Offshore Renewable Energy (ORE) Catapult, and delivered by ORE Catapult.

The Pembrokeshire Demonstration Zone (PDZ) project is being led by Celtic Sea Power Ltd, a 100% subsidiary of Cornwall Council. Funded by the Welsh European Funding Office (WEFO) and the Swansea Bay City Deal (SBCD), and the development of PDZ is part of the Pembroke Dock Marine programme. Partners to Pembroke Dock Marine include Port of Milford Haven, Pembrokeshire County Council, ORE Catapult and Marine Energy Wales.

ORE Catapult is a not-for-profit research organisation, established in 2013 by the UK Government as one of a network of Catapults in high growth industries. It is the UK's leading innovation centre for offshore renewable energy and helps to create UK economic benefit in the sector by using its test assets, engineering and ORE market expertise to drive down the cost of offshore renewable energy and support the growth of the industry.

Lead Author: Bradley McKay (BM) – Research Engineer Electrical (FOW Accelerator) MRE

Co-Author: Nathan Haley (NH) – Research Engineer Electrical - Floating Wind

Published Date: 16/03/2023

The authors and Contributors would like to thank a number of individuals at ORE Catapult for their support through expert group meetings.

DISCLAIMER

Front Cover Source: DolWin2 platform en route ABB HVDC DolWin2 - Wikipedia and HVDC technology for offshore wind is maturing | ABB

DOCUMENT HISTORY

Revision	Date	Authors	Reviewer	Approver	Authoriser	Revision History
Rev 1	20221031	BM, NH				Version Rev-1.1

Rev 2	20221112	BM, NH				Version Rev-1.2
Rev 3	20221201	BM				Version Rev-1.3
Rev 4	20221208	BM				Version Rev-1.4
Rev 5	20221216	BM, NH	Simon Cheeseman			Version Rev-1.5
Rev 6	20230210	BM, NH	Chunjiang Jia	Chunjiang Jia	Simon Cheeseman	Version Rev-2.0
Final	20230214	BM	Chunjiang Jia	Chunjiang Jia	Simon Cheeseman	Version Rev-2.0
Addendum	20230316	BM			Simon Cheeseman	Version Rev-2.1

PREFACE

ORE Catapult is the UK's flagship technology innovation and research centre for offshore wind, wave and tidal energy. ORE Catapult is playing a leading role in the delivery of the offshore wind sector deal (partnership between UK Government and offshore wind industry), including the Offshore Wind Growth Partnership, focused on enhancing the competitiveness of UK supply chain companies for supplying into the domestic and export markets. ORE Catapult has developed and actively maintains technology roadmaps to co-ordinate Research and Development funding and activity across agreed industry priorities. This provides ORE Catapult with a unique broad and objective perspective on the UK and global offshore wind industry.

We are an independent, not-for-profit business that exists to accelerate the development of offshore wind, wave and tidal technologies. Our team of over 300 people has extensive technical and research capabilities, industry experience and a proven track record. Through our world-class testing and research programmes, we work for industry, academia and government to improve technology reliability and enhance knowledge, directly impacting upon the cost of offshore renewable energy. We organise our activities around key areas for future innovation and developing local Centres of Excellence that will support the transformation of our coastal communities. These areas include: floating wind; marine energy; testing and demonstration; operations and maintenance.

The Centres of Excellence champion innovation in robotics, autonomous systems, big data and artificial intelligence, balance of plant – especially foundations – and next-generation technologies. To date, we have supported more than 800 small to medium-sized enterprise, contributed to 328 active and completed research projects, and supported over 180 companies in their product development.

CONTENTS

LIST OF FIGURES

LIST OF TABLES

NOMENCLATURE

AMSL	Above Mean Sea Level
BEIS	The Department for Business, Energy and Industrial Strategy
B-F	Bottom Fixed
CCGT	Combined Cycle Gas Turbine
CFA	Cornwall FLOW Accelerator
CfD	Contracts for Difference
CIGRE	The International Council on Large Electric Systems
CoG	Centre of Gravity
CSA	Cross-Sectional Area
CSC	Celtic Sea Cluster
DND	Detailed Network Design
EoL	End of Life
FOW	Floating Offshore Wind
FOWT	Floating Offshore Wind Turbine

HND	Holistic Network Design
HV	High Voltage
HVAC	High Voltage Alternating Current
HVDC	High Voltage Direct Current
IEC	The International Electrotechnical Commission
IGBT	Insulate-Gate Bipolar Gate Transistors
LCC	Line-Commutated Converter
LEP	Local Enterprise Partnership
LiDAR	Light Detection and Ranging
MH:EK	Milford Haven Energy Kingdom
MOS	Multipurpose Offshore Substation
MRE	Marine Renewable Energy
MSW	Mean Sea Water
NGESO	National Grid Electricity System Operator
O&G	Oil and Gas
O&M	Operation and Maintenance
ORE	Offshore Renewable Energy
OSS	Offshore Substation
OW	Offshore Wind
OTNR	Offshore Transmission Network Review
PDA	Project Development Areas
PDZ	Pembrokeshire Demonstration Zone
PE	Polyethylene
PMSG	Permanent Magnet Synchronous Generator
R&D	Research and Development
RE	Renewable Energy
RPM	Revolutions Per Minute
SoL	Start of Life
TCE	The Crown Estate
VSC	Voltage Source Converter
XLPE	Cross-Linked Polyethylene

SYMBOLS AND UNITS

$°C$	degree Celsius
λ	tip speed ratio lambda
ω	angular frequency in radian per second (rad/s)
η	efficiency
A	wind turbine swept area (m^2)
Al	aluminium
C	capacitance in farad (F)
CF	capacity factor
C_P	wind turbine power coefficient

Cu	copper
f	frequency in hertz (Hz)
GW	giga-watt
GWh	giga-watt hours
GWh/yr	energy in giga-watt hours per year
I_n	nominal current in ampere (A)
K	temperature (Kelvin)
kg/m^3	air density
km	kilometer
$K.m/W$	thermal resistivity
kV	kilo-volt
L	inductance in Henry (H)
m	meter
m^2	meter squared
mm^2	milli meter squared
MW	mega-watt
MWh	mega-watt hours
MWh/yr	energy in mega-watt hours per year
ρ	air density (kg/m^3)
P	active power (W)
P_{in}	wind power available or theoretical wind kinetic energy per unit time in Watt (W)
P_n	nominal active power of wind turbine in Watt (W)
P_{out}	actual electrical power produced in Watt (W)
pf	power factor
puV	per unit voltage
Q	reactive power in volt ampere reactive (VAr)
R	resistance in ohms (Ω
S	apparent power volt ampere (VA)
S_n	nominal apparent power of wind turbine (Volt Ampere)
U	phase-to-phase voltage (V)
$U_{correct}$	phase-to-phase voltage correction (V)
$U_{op.min}$	minimum phase-to-phase voltage the turbine can ride through in per unit
U_n	nominal phase-to-phase voltage (V)
u^3	velocity cubed in metres per second (m/s)
v_{cut-in}	cut-in wind speed in metres per second (m/s)
$v_{cut-out}$	cut-out wind speed in metres per second (m/s)
W/m	conductor losses (Watt per metre)
X	reactance in ohm (Ω)

EXECUTIVE SUMMARY

The Cornwall Flow Accelerator work package 4 led by ORE Catapult details innovation in low carbon design and manufacturability that lays the groundwork for development of low carbon strategies, across design, manufacturing, and operations & maintenance. Within this work package, the goal of this specific task 6 analysis, is for the electrical infrastructure for floating offshore wind in the Celtic Sea to identify opportunities in the UK's South West region. This research will build on earlier considerations of how floating offshore wind can be integrated into the South Wales and South West UK transmission network.

This research will take the format of two distinct sections. Firstly, it begins with an overview of electrical system from regional network down to single turbine output power, and focuses on a scenario based on a 500 MW floating offshore wind farm, comparing 66 kV and 132 kV submarine cable to increase the flexibility and importance of floating wind farms and substation designs for Celtic Sea. Secondly, a holistic view of electrical infrastructure is followed to identify the technical challenges in dynamic inter-array cables and collector systems, and comparison is made between high-voltage alternating current and high-voltage direct current for offshore energy transmission.

To build on earlier considerations of how floating offshore wind can be integrated into the South Wales and South West UK transmission network, this report considers how best to deliver the distribution of energy from near-term and long-term floating wind deployments, both technically and spatially. What types of major infrastructure requirements, possible alternative solutions, Celtic Sea electrical scenarios, models and investment that are required for integrating future floating wind developments into the Celtic Sea energy network are also considered. Currently in the Celtic Sea there are no offshore cable routes to connect wind farms onshore, nor direct offshore links to South Wales and South West England, although around this region there are approximately six 400 kV substations onshore, namely: Pembroke, Swansea North, Rhigos, Cilfynydd, Hinkley Point and Alverdiscott for possible connections. The Pembroke substation is located very close to the Celtic Sea and is a focal point for the offshore-onshore connection suitable for floating offshore wind. In addition, a new option has been proposed by the Cornwall Council and Cornwall and Isles of Scilly Local Enterprise Partnership to the National Grid ESO offering Aerohub as a site to be considered for an additional substation to help alleviate pressure on the existing infrastructure and provide energy direct to Cornish industry.

As outlined in the Holistic Network Design, Ofgem has announced details on how it will accelerate delivery of the unprecedented volume of onshore transmission network aiming to support delivery of up to 50 GW of offshore wind by 2030. Under a new streamlined regulatory framework known as 'The Accelerated Strategic Transmission Investment', Ofgem will expedite 26 projects at a cost of £20 bn [1]. Projects will be built by geographically incumbent Transmission System Operators against target dates and constraint costs via incentives for a timely delivery through a reward and penalty system.

The Business, Energy, and Industrial Strategy in collaboration with Ofgem, have launched the Offshore Coordination Support Scheme. The scheme will coordinate offshore transmission between offshore wind farm projects, reducing transmission infrastructure needs, costs and environmental impact. In addition, the scheme will create early opportunities and capture lessons learned to shape the Offshore Transmission Network Review.

The specifics to this report are to collect top-level information about the South West transmission network for floating offshore wind in the Celtic sea for the Cornwall FLOW Accelerator Project. Research in Section 1 will focus on South Wales & South West UK electrical network offshore, wind farm array cable configurations, single turbine electrical output power, offshore interconnection cable design. These research contents are bases on the following facts. The Holistic Network Design will need to be revisited for the Celtic Sea and should be considered in the next phase of the National Grid Electricity System Operator - Detailed Network Design strategy. The Celtic Sea is a large area of interest for the development of floating offshore wind technologies due to the reliable wind resource, relatively shallow and links for floating wind from regions in South Wales, South West England, and the potential collaboration with Ireland. The Celtic Sea for future design scenarios is considering reaching the 4 GW of floating offshore wind by 2035 (that are based on scenarios that range from 2026 to 2035).

Within this section, array connections of wind turbines in offshore wind farms are also reviewed with four topology options, namely tapered radial strings (daisy-chain), tee's (branches), tapered ring loops and redundant rings. Fundamental requirements are also discussed to establish the electrical power output from a wind turbine, such as power curve versus wind speed or rotor angular velocity. Since array cables currently deployed are with either 33 or 66 kV voltage, a higher voltage level of 132 kV is also reviewed for array cables of higher power turbine and/or farm capacity.

Research in Section 2 will focus on offshore substation and collector system, the optimisation in dynamic cable systems, and high-voltage direct current and high-voltage alternating current transmission. Dynamic cable resilience and longevity over the project lifetime to floating offshore structures and anchor point on the seabed are compared. Further requirements for a feasible dynamic cable are also explored. These cable requirements are defined early in the wind farm design process depending on the floating offshore wind turbine used, array configuration design, and wind farm capacity.

As transmission decisions come to fruition for floating offshore wind, consideration to focus on the use of either high-voltage direct current and/or high-voltage alternating current transmission will be vital for offshore wind farms. The decision will be judged by distance and electrical losses through the cable. It must be noted that high-voltage alternating current has an important limitation, the high-voltage alternating current cable. This type of cable has a high capacitance per length, measured in micro-Farads per km (µF/km). There is a capacitive charging current in addition to the power delivery current through the cable, requiring excessive reactive power to function with limitation in transmission distance, which, however, is not found in high-voltage direct current. New high-voltage direct current innovation and the benefits to this form of transmission are now being considered for floating offshore wind. Research has shown that high-voltage direct current has overwhelming advantages in long-distance electricity transmission. Floating offshore wind farms more than 50 km from shore are recommended to use high-voltage direct current transmission.

Finally, there are three previous publications to support the research that are all based on the electrical infrastructure for the Celtic Sea by Offshore Renewable Energy Catapult. They can be found under the Celtic Sea Cluster for the Cornwall FLOW Accelerator Project, titled as followed, (1) 'Optimised cable connection options for floating offshore wind', (2) 'Exploring the Potential Interactions between Floating Offshore Wind and Hydrogen', and (3) 'The Future Potential Role of Offshore Multipurpose Connectors'.

1 INTRODUCTION

The government's 50 giga-watt (GW) target for offshore wind energy by 2030, which includes up to 5 GW of floating offshore wind power (FOW), provides a clear message now under our new Prime Minister Rishi Sunak for confidence to investors [1]. According to The Department for Business, Energy, and Industrial Strategy (BEIS) during 2021 alone there were over £1 billion of inward investment to the UK's supply chain [2]. The UK currently holds a competitive advantage in FOW innovative technology, which is set to overtake conventional fixed offshore wind power by 2050. Therefore, by using synergies from the oil and gas (O&G) sectors all related to floating offshore structures, subsea cabling and their challenges faced. This should aid in potential solutions to FOW electrical infrastructure for the future in lessons learnt. Setting clear, medium to long term ambition in the Celtic Sea for FOW that will help to focus intellectuals to overcome policy barriers across government and industry. This will secure the UK's competitive advantage in the FOW industry to deliver greater investor confidence.

According to The UK Government's Ten Point Plan for Green Industrial Revolution, new offshore wind (OW) developments are now the cheapest form of renewable energy (RE) we can build, although bottom-fixed (B-F) offshore wind does have its limitations [1]. Therefore, by raising ambitions on FOW from 4 GW to 20 GW in the Celtic Sea in the coming decades this would support cheaper domestic RE and it would secure the UK's competitive advantage.

This report is to collect top-level information about the South West transmission network for floating offshore wind in the Celtic sea for the Cornwall FLOW Accelerator (CFA) Project. The research will focus around two parts, namely: Section 1 – South Wales & South West UK electrical network offshore; wind array configurations; electrical output power; and offshore interconnection cable design. In Section 2 – focus will be around offshore substation and collector systems; optimisation in dynamic cable systems; and high-voltage direct current (HVDC) and high-voltage alternating current (HVAC) transmission comparisons.

Moreover, discussions will also identify the definitions related to floaters, their failure rates and challenges, and new improved wet mate connector technology (adding more research and knowledge from a previous publication through the Celtic Sea Cluster (CSC), namely *'Optimised cable connection option for floating offshore wind'*). Lastly, added key areas discussed and calculated in the appendices will focus on apparent power; conductor losses in subsea cable; voltage management for AC frequency; reactive power; inductive and capacitive reactance in HV transmission systems.

1.1 Objectives of the research

With OW energy projects located in hostile environments, especially FOW installations with challenges like operation and maintenance (O&M) and weather dependant deployment. The South West transmission network will play a vital and reliable role to optimise FOW in the Celtic Sea. Failures are inevitable, due to the dynamic environment, but proper planning and the correct multipurpose connection options being used will add to required solutions, to cause minimal delays.

This research will build on earlier considerations of how FOW can be integrated into the South Wales and South West UK transmission network.

This research will address:

- Integrating future floating wind development(s) into the South West and South Wales energy network.
- To differentiate both technically and spatially how the distribution of energy from both short and long-term floating wind deployments can best be delivered.
- Investigate types of major electrical infrastructure, alternative solutions and investment that may be required, linking the importance of inter-array cable arrangements, dynamic array and export cable routes by definition.
- Solutions to connecting FOW electrical infrastructure in the Celtic Sea to the national electrical grid network.

2 SOUTH WALES & SOUTH WEST UK ELECTRICAL NETWORK

2.1 Introduction

The Offshore Transmission Network Review (OTNR) was launched by BEIS in July 2020, and in July 2022, the National Grid published work of their Holistic Network Design (HND) to set out the required network to facilitate the future connection of offshore wind projects. The Celtic Sea has the potential for tens of GWs, maybe in the hundreds of GW in the future with its ideal location and wind resource available. Therefore, the HND facilitates the connection necessary to shore and for the transmission to all areas of the UK with a focus on the needs of social, economic and environment considerations. Based on these objectives the HND recommends the optimal transmission network for the connection of offshore wind to the national grid.

This section details the HND proposed in the South West UK and South Wales regions with existing and planned network, including alternate based scenarios.

The HND is designed with the assumption of only 1 GW of floating wind in the Celtic Sea, however the Celtic Sea has the potential for much more generation which will require the HND to be revisited for this region. This should be considered in the Detailed Network Design (DND) which is the National Grid's next phase of work following the HND.

2.2 Existing Network

The South Wales (SW1), South West (B13), national grid regions are shown in Figure 1, identifying how the regions are connected by 400 kV and 275 kV transmission circuits [3]. It is clear there are adequate onshore points to connect offshore renewable projects in the Celtic Sea, however, there are currently no offshore cable routes to connect wind farms onshore, nor to connect South Wales to South West England directly without an onshore transmission grid.

Around South Wales and South West England, there are about six 400 kV substations onshore, namely: Pembroke, Swansea North, Rhigos, Cilfynydd, Hinkley Point and Alverdiscott. The Pembroke substation is located very close to the Celtic Sea and is a focal point for offshore – onshore connection, however it will not be able to cope with the additional future generations from offshore projects as well as the adjacent 2,200 MW combined cycle gas turbine (CCGT) Pembroke Power Station. Currently, the only two Celtic Sea FOW projects (Erebus and Valorous) are planned to connect to the Welsh grid through Pembroke.

There are currently few energy storage technologies being utilised in Wales with most used in the North Wales region. Energy storage systems implemented in the South Wales and South West England regions could reduce future upgrading of the National Grid to support the future offshore wind generation in the Celtic Sea.

2.3 Proposed new Grid Supply Point for FOW in Cornwall

Cornwall Council and Cornwall and Isles of Scilly Local Enterprise Partnership (LEP) recognise the enormous opportunity that FOW presents for the regions bounding the Celtic Sea. They recently co-signed a letter to the National Grid ESO offering Aerohub as a site to be considered for an additional substation

enabling Cornwall to host at least one of the major onshore substations connecting directly into the National Grid Electricity Transmission system. To help alleviate pressure on the grid network and enable Cornwall to benefit from the energy into its regional industry. Aerohub is owned by the Cornwall Council which would give more certainty to the development process. The benefits are the available 21.5 hectares that form part of Aerohub one of the UK's largest designated Enterprise Zones. The site is located near to Cornwall's Airport Newquay, circa 8 km from the National Grid Indian Queens substation and 3.5 km from Watergate Bay in the north coast, classified as a suitable cable landing point for FOW generated in the Celtic Sea.

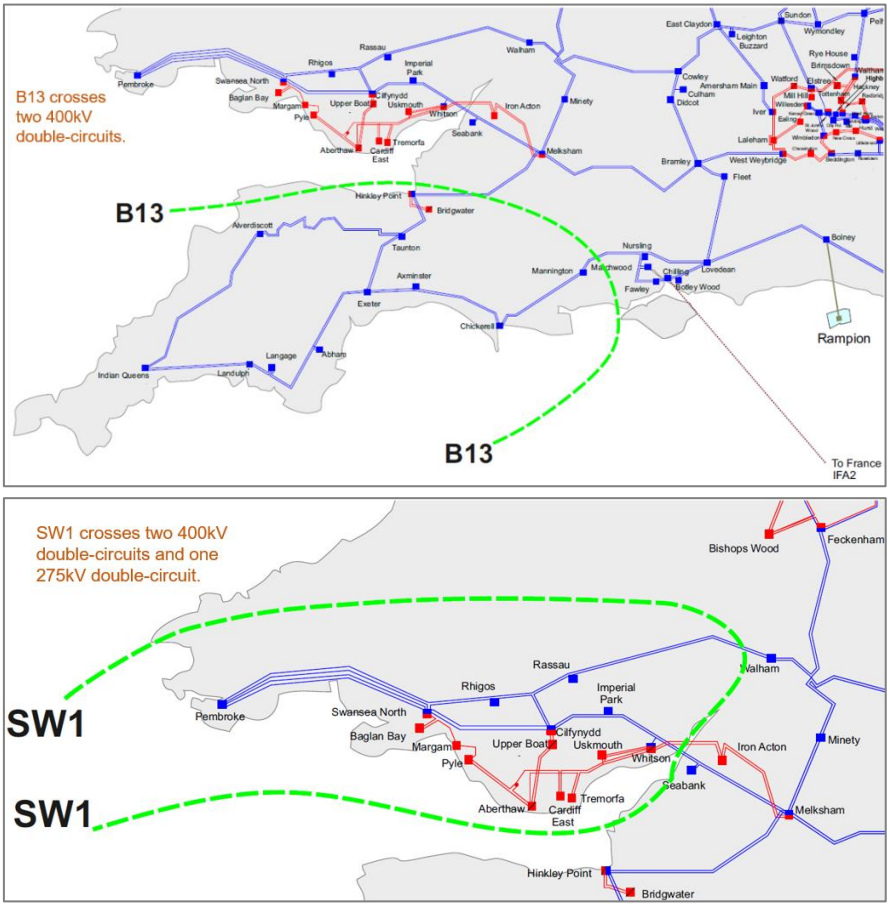

Figure 1: Maps of South Wales and South West England National Grid boundaries. Top: The grid in South West (B13) crosses two 400 kV double-circuits. Bottom: The grid in South Wales (SW1) consists of a 400 kV ring from Walham to Pembroke, and from there to Melksham; (SW1) crosses two 400 kV double-circuits and one 275 kV double-circuit. There is a meshed 275 kV network that connects to this 400 kV ring at Swansea North, Cilfynydd and Melksham [3].

2.4 Holistic Network Design

The HND developed by the National Grid is a design to provide onshore and offshore recommendations to facilitate the UK Governments ambition for 50 GW of offshore wind power by 2030 around the UK. It assumes that the Celtic Sea will facilitate just 1 GW of floating wind. But, the Celtic Sea has the potential for much more capacity.

There are three assumed projects with a combined capacity of only 1 GW proposed so far, with a coordinated and radial design recommended to connect the offshore wind farms to shore, these are

shown in Figure 2. The coordinated design connects all three wind farms in a string via HVAC cables to the substation located onshore at Pembroke on the Coordinated map in Figure 2. Whereas in the Radial design the connections to each wind farm are connected separately via HVAC cables to two onshore locations, Pembroke substation and the Baglan Bay substation on the Radial design map in Figure 2.

This section explores the HND for the South Wales and South West England regions.

Figure 2: Recommended coordinated map (left) and radial design map (right) for the South West region [4].

The design has gone from a single 100 MW test and demonstration lease to four (five if the repurposed Wavehub site off Hayle is included), and an increase in project scale for the next phase from 300 MW developments to four by 1 GW to meet the Energy Security Strategy (ESS) of the UK which are currently being expected to be built out in phases. Exploration following the leasing round in the Celtic Sea by The Crown Estate (TCE) with rights awarded by the end of 2023, as seen in Figure 3, hence the HND was developed through assumptions of capacity and location [5]. The preferred coordinated design, from Figure 2, would assume HVAC cables built on the following criteria, as found in Table 1.

Table 1: Recommended HND coordinated cable rating, number of cables and type, to the design in the Celtic Sea.

Route	Rating (MW)	No. of Cables	Type
1 – Pembroke	2 circuits of 500 each	2	275 kV = 2 circuits of 1 cable
1 – 2a	2 circuits of 360 each	2	275 kV = 2 circuits of 1 cable
2a – 2b	2 circuits of 200 each	2	275 kV = 2 circuits of 1 cable
The HVAC cable route numbers assume 500 MW is possible at 275 kV, longer distances may require an additional parallel cable to account for the reactive power losses.			

Onshore works to facilitate the HND include a substation for new connections at Pembroke and uprating circuits and installing flow control devices to manage power flow. Alternative designs recommended by the National Grid included using HVDC links between one of the wind farms to a substation at Alverdiscott but investigations found the design did not perform compared to the recommended HND [6]. Further alternative scenarios are explored in Section 2.6 which assumes a greater, more realistic capacity in the Celtic Sea by 2030.

In summary to this section, by making the case for stakeholders to back an approach to BEIS under their co-ordination fund to support a Celtic Sea project in parallel to the Celtic Sea leasing round process as shown in Figure 3. There are key fundamentals worth mentioning as follows, that the refined areas of

search (A & B) will be more than likely under a HVAC cable option. However, the refined areas of search (C, D & E), would be technically in HVDC territory, due to the long distance offshore.

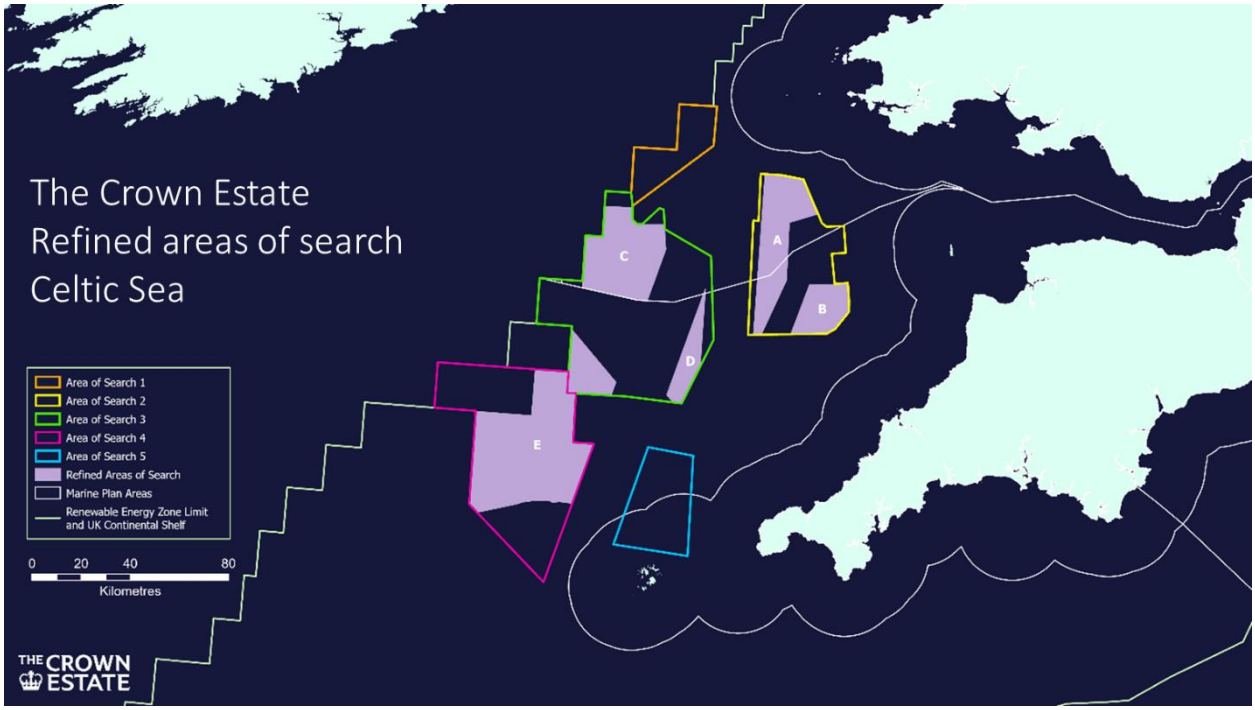

Figure 3: Presented by The Crown Estate the five Refined Areas of Search located within three of the original five broad Areas of Search [5].

2.5 Offshore Wind in the Celtic Sea

The Celtic Sea is an area of interest for the development of offshore wind technologies due to the reliable wind resource, size, water depths, and availability from the South Wales and South West England regions, as well as potential collaboration with Ireland.

Due to water depths in the Celtic Sea (average water depth between 90 and 100 m (300 – 330 ft)), the B-F offshore wind projects have been overlooked, however with the development of FOW, the Celtic Sea is a popular area of interest for projects to contribute to government targets of wind energy generation [7].

The Crown Estate are the forerunners in the development in the Celtic Sea with ambitions to develop up to 4 GW of offshore wind, specifically in FOW, for build out between 2030 – 2035. Four project development areas (PDAs) are expected to produce a minimum and maximum power capacity of 300 MW and 1 GW respectively, that relate to the TCEs refined areas of search [5].

There have been several floating offshore wind projects announced in the region including Erebus (96 MW), Valorous (300 MW), Whitecross (100 MW) and the Pembroke Demonstration Zone (PDZ) (90 MW); potentially building out to 1.2 GW on the PDZ, proposed as a multipurpose offshore substation (MOS) [8]. The onshore coastline surrounding the Celtic Sea is well suited to maximise supply chain opportunities and feasible routes for connectivity to the onshore National Grid.

With the electrical infrastructure of the onshore National Grid needs upgrading to incorporate future offshore wind development. Alternative proposals are being explored with the direct transmission of electricity, or the use of offshore electrolysers to produce hydrogen for export to shore. Which is a focus

of the Milford Haven Energy Kingdom (MH:EK) project in the Celtic Sea. Further detail can be found in a previous publication in this series by Offshore Renewable Energy Catapult, for the Celtic Sea Cluster (under the Cornwall FLOW Accelerator Project) titled: '*Optimised cable connection options for floating offshore wind*' and '*Exploring the Potential Interactions between Floating Offshore Wind and Hydrogen*'.

2.6 Novel Approach to Future FOW Development

2.6.1 Energy Storage Systems

At times of peak demand when generation from renewable resource(s) is low, energy storage technologies can be applied to absorb energy when generation is higher than the demand; and released back into the grid when generation is inadequate to meet demand needs. By developing the energy storage technology around the South Wales and South West England regions, upgrades to the existing National Grid could be reduced. Technologies that are used to store energy include pumped hydro storage which requires large areas for reservoirs, and battery storage [9]; with the cost that has reduced significantly, and that the UK is expanding in the development of large-scale battery storage. These systems mean the National Grid reduces the need for further substations and high-capacity cables, as well as reducing the discarded load.

2.6.2 Hydrogen Production

Although the Cornwall FLOW Accelerator (CFA) Project does not focus on the use of hydrogen technology in the Celtic Sea, it is important to note the potential of this technology. Energy generated from offshore wind turbines can be used directly in electrolysers which convert electrical energy into chemical energy with the production of green hydrogen gas [9]. Hydrogen has a very high energy content and is an emerging energy source in hydrogen turbine generators and hydrogen powered vehicles. The Milford Haven Energy Kingdom [10] Project focuses on the use of offshore wind in the Celtic Sea for hydrogen production and its uses. The use of offshore wind for hydrogen production reduces the upgrade requirements of the National Grid, however, it introduces additional costs to provide electrolysis and hydrogen storage technologies onshore and offshore.

2.6.3 Interconnection To Other Countries

By interconnecting the Celtic Sea and the South Wales and South West England regions to other countries, the National Grid constraints can be reduced by exporting overloaded power to countries with unconstrained grids like continental Europe [9]. As well as other countries, offshore wind projects in the Celtic Sea can be interconnected to each other and to other ports around the region, not just a central Pembroke onshore substation as outlined in the HND. This will be explored in more detail which can be found in the work conducted in this series by Offshore Renewable Energy Catapult, for the Celtic Sea Cluster (under the Cornwall FLOW Accelerator Project) titled: *'The Future Potential Role of Offshore Multipurpose Connectors'*.

2.6.4 Holistic Network Design Alternative Scenarios (Part 1)

Alternative scenarios for what the Celtic Sea FOW could look like compared to the HND have been developed by Celtic Sea Power and ORE Catapult [11]; which incorporate a more realistic interpretation of the future potential projects in the Celtic Sea and how they might look to be connected to the National

Grid. As the HND assumes only 1 GW of offshore wind in the Celtic Sea, the alternative scenarios offer increased capacity of up to 4 GW which is expected in the future by the Government's ESS.

The work the National Grid Electricity System Operator (NG ESO) are progressing to define what and where the offshore electrical network should look like, are taking shape, to meet The Crown Estate's aspirations. As of July 2022, which showed that multiple projects of precommercial scale connecting via a HVAC Network into Pembroke, could be a solution. This alignment coincides with the PDZ, or MOS, as seen in the graphical representation in Figure 4. In the coordinated design, from Figure 2 and Table 1, the assumption would be to lay two by 275 kV HVAC cables; for the first leg (1-Pembroke) 2 circuits of 500 MW each; for the second leg (1 – 2a) 2 circuits of 360 MW each; and for the third leg (2a – 2b) 2 circuits of 200 MW each. All cable lengths will assume 275 kV, and longer distances may require an additional parallel cable to account for reactive power losses, discussed in more detail later.

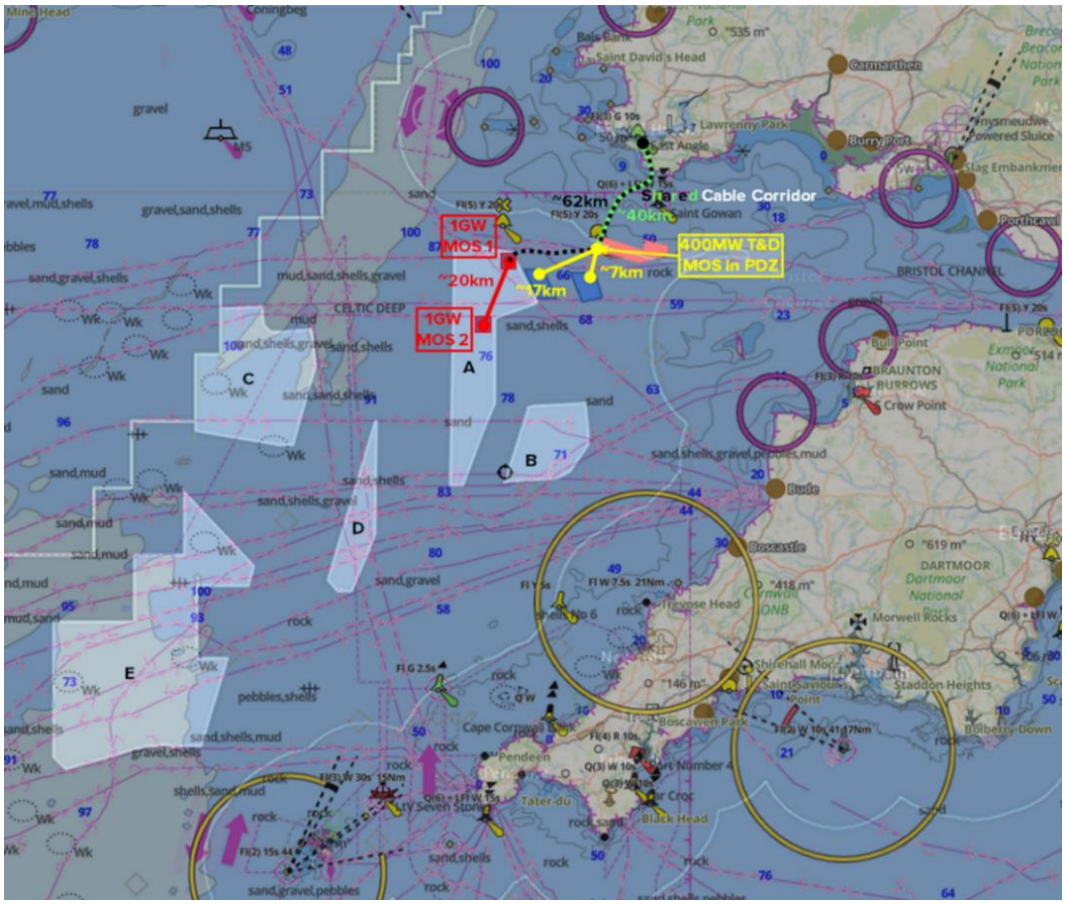

Figure 4: Graphical representation of external influences and how the Celtic Sea Cluster are proposing to maintain a project that will continue to support the R&D activity; and the needs of both the test and demonstration and commercial phase projects.

As an illustrative indicative example, found on the map of the Celtic Sea in Figure 4, illustrating the proposed work under the HND, and PDZ, that could benefit the FOW sector for the Celtic Sea. Taking the indicative designs for the commercial projects – coordinating them with a potential test and demonstration phase platform, and associated infrastructure back to a suitable point of connection. Whilst this map represents Pembroke, including the complexities to environmental surveys. The Celtic Sea Cluster (CSC) will still be seeking to look at all potential points of connection in the Swansea Bay City Region. Further work conducted in this series by Offshore Renewable Energy Catapult is to support offshore

substations (OSS), under the Cornwall FLOW Accelerator Project that can be found in the publication titled: *'The Future Potential Role of Offshore Multipurpose Connectors'.*

2.6.5 Holistic Network Design Alternative Scenarios (Part 2)

For completeness to the Celtic Sea for future design scenarios, various proposals have been thought of by the Celtic Sea Power and ORE Catapult, in line with the HND from the NG ESO about what the future may hold to reach the 4 GW FOW by 2035 (these scenarios range from a timescale from 2026 to 2035).

The *first scenario* includes several more OWFs with varying capacity of up to 1 GW and all connected individually to onshore substations at Pembroke, Swansea North (Wales) and the North coast of Devon (England). Scenario (1A) and (1B) shown in

Finally, the *fourth scenario*, found in (4A), shown in Figure 8, is that of scenario 1, however introduces the integration of green hydrogen at a fixed offshore substation. However, electrolysis in the near future might require onshore electrolysis due to the constraints of motion, clean air and water limitations. The question about electrolysis onshore vs offshore is an interesting argument. Industry thinking currently is that it would be difficult to put an electrolyser offshore. However, would expect that near-shore electrolyser will still need to get its water from the sea via desalination, and to have filters for the air purification. There is also the point of motion, that electrolyser companies are starting to tackle. Offshore electrolysis is a relatively new field, and, tentatively, perhaps the current industry is thinking of offshore wind to electrolysis projects in the short term are going to have onshore electrolysers.

Scenario 1:

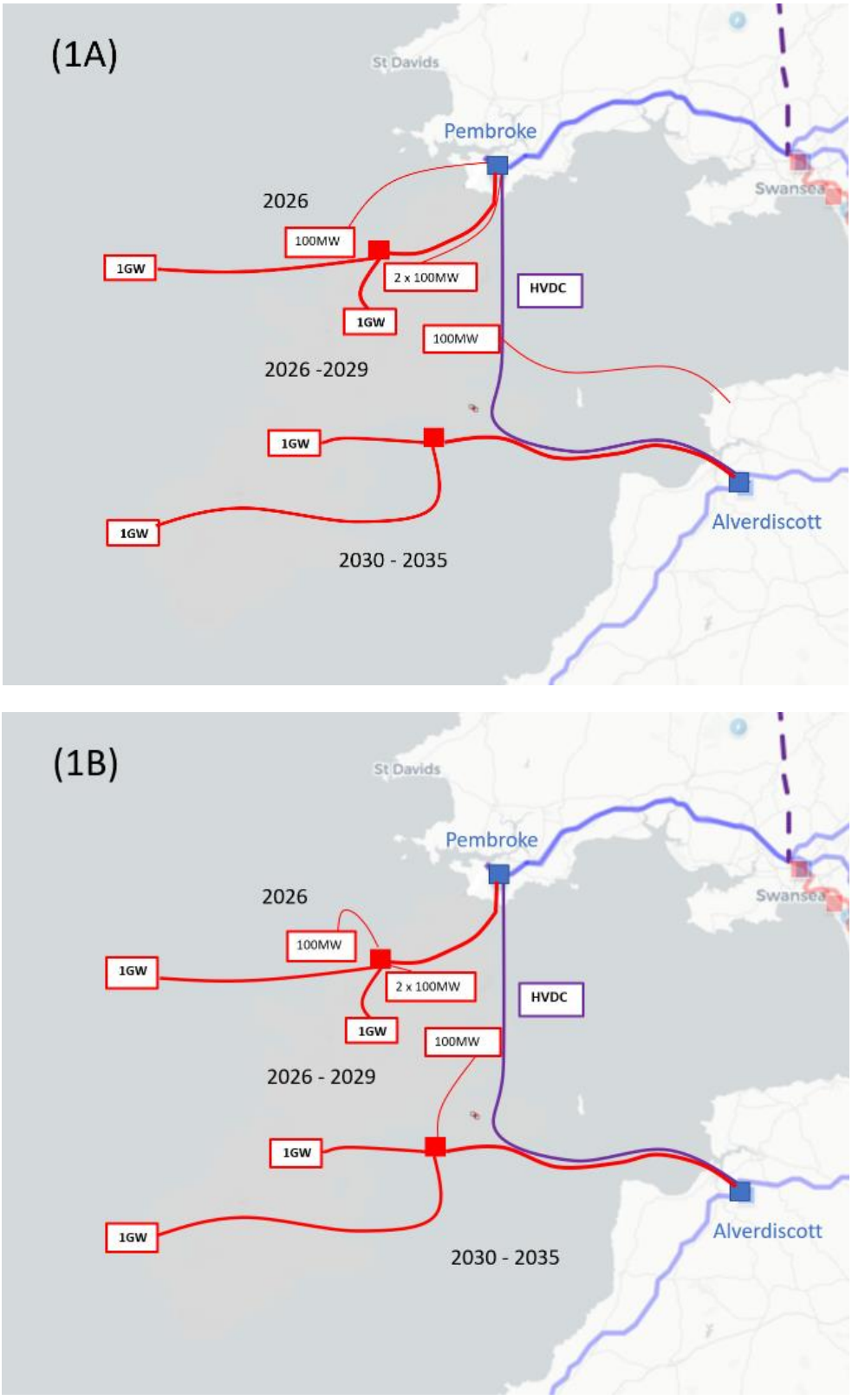

Figure 5: (1A) Alternative scenario (individual developer led & commercially co-ordinated): by 2026 system 2x 100 MW; 2026-2029 system 2x 100 MW; 2030-2035 system 4x 1 GW; including a HVDC interconnection. (1B) Alternative Scenario (all co-ordinated): by 2026 system 2x 100 MW; 2026-2029 system 2x 100 MW; 2030-2035 system 4x 1 GW; including a HVDC interconnection.

Scenario 2:

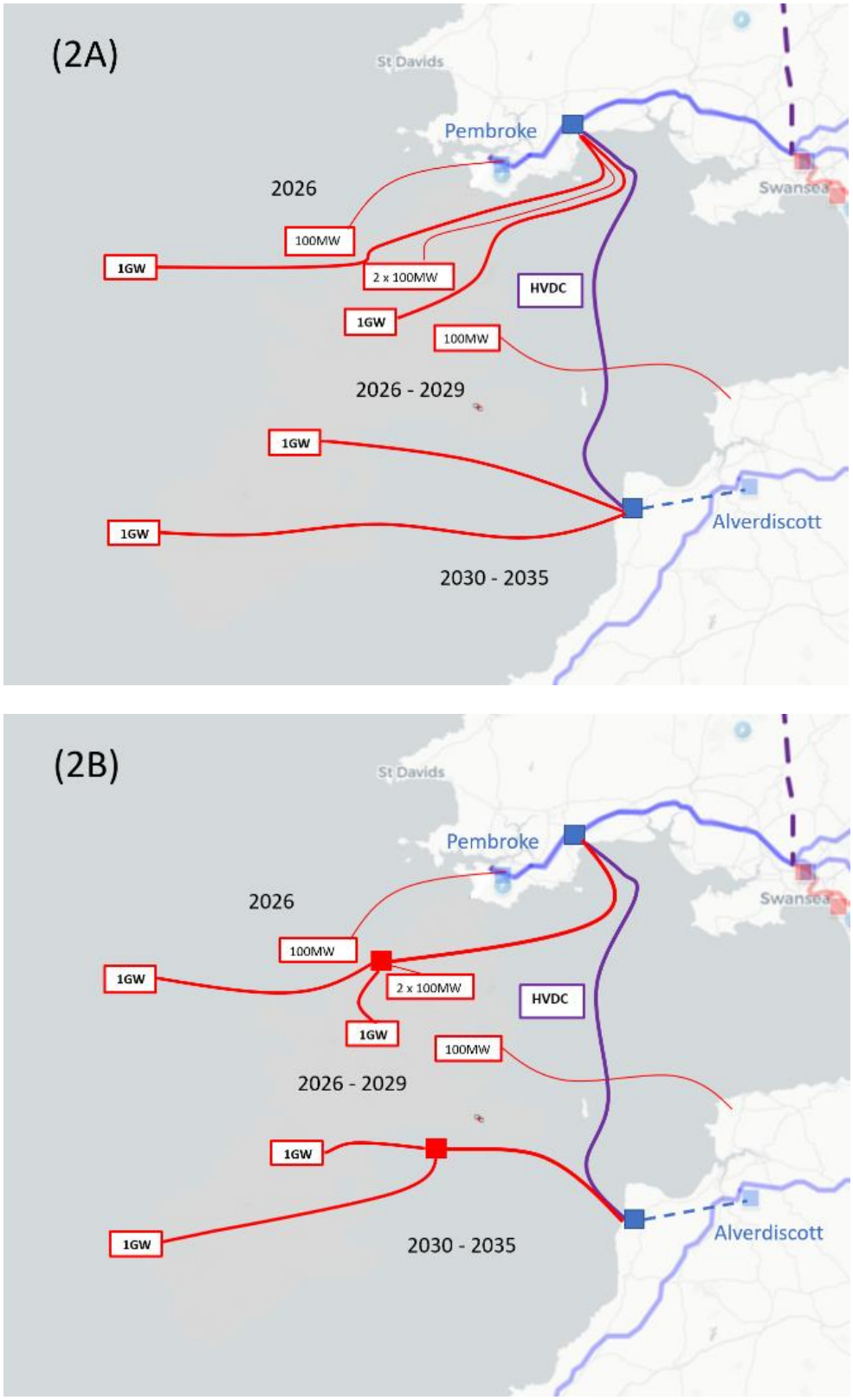

Figure 6: (2A) Alternative scenario (point of connection change onshore): by 2026 system 2x 100 MW; 2026-2029 system 2x 100 MW; 2030-2035 system 4x 1 GW; including a HVDC interconnection. (2B) Alternative Scenario (point of connection change both onshore & offshore): by 2026 system 2x 100 MW; 2026-2029 system 2x 100 MW; 2030-2035 system 4x 1 GW; including a HVDC interconnection.

Scenario 3:

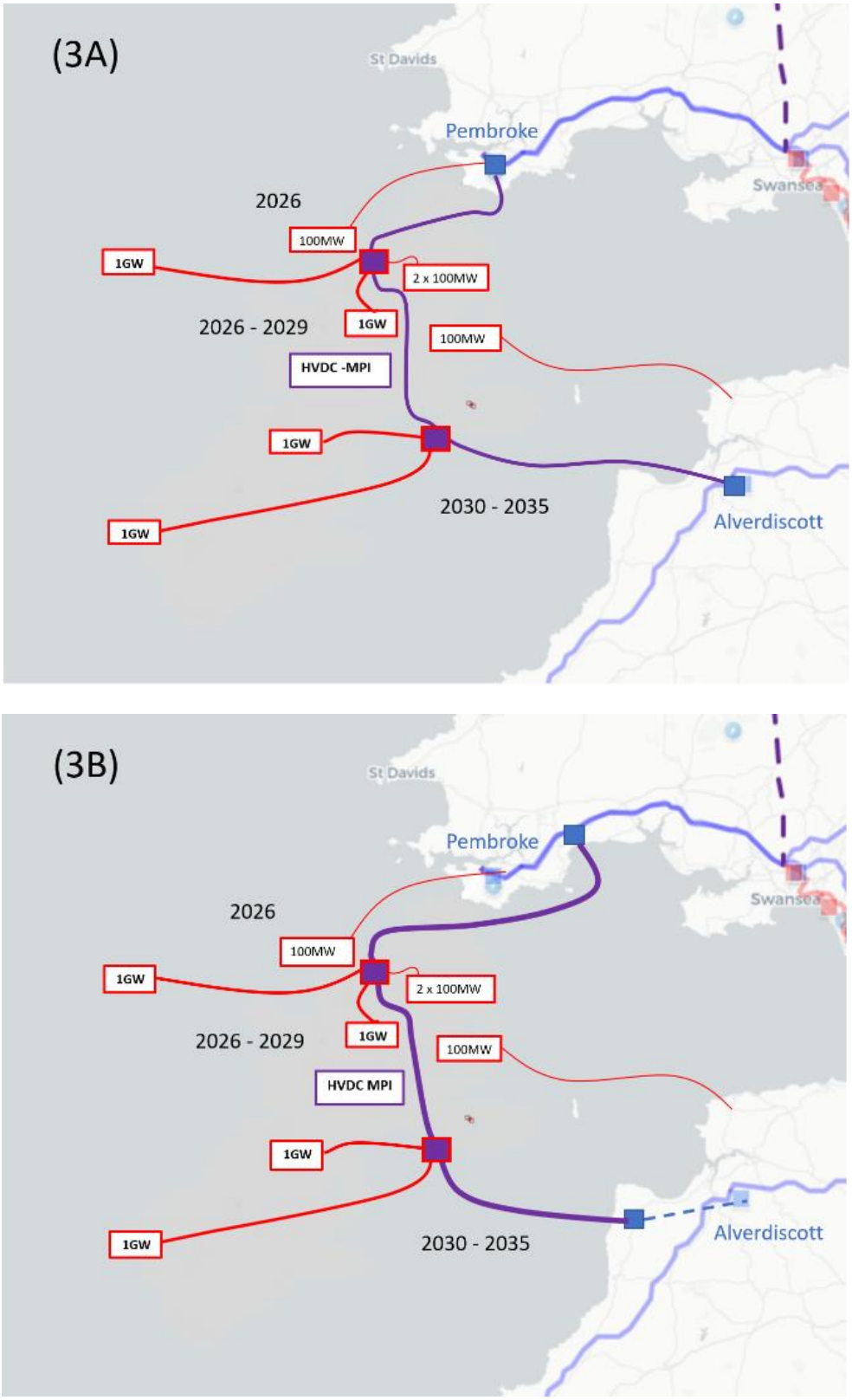

Figure 7: (3A) Alternative scenario (point of connection & introduction to multipurpose connector HVDC): by 2026 system 2x 100 MW; 2026-2029 system 2x 100 MW; 2030-2035 system 4x 1 GW + MPI. (3B) Alternative Scenario (point of connection change onshore & introduction to multipurpose connector HVDC): by 2026 system 2x 100 MW; 2026-2029 system 2x 100 MW; 2030-2035 system 4x 1 GW + MPI.

Scenario 4:

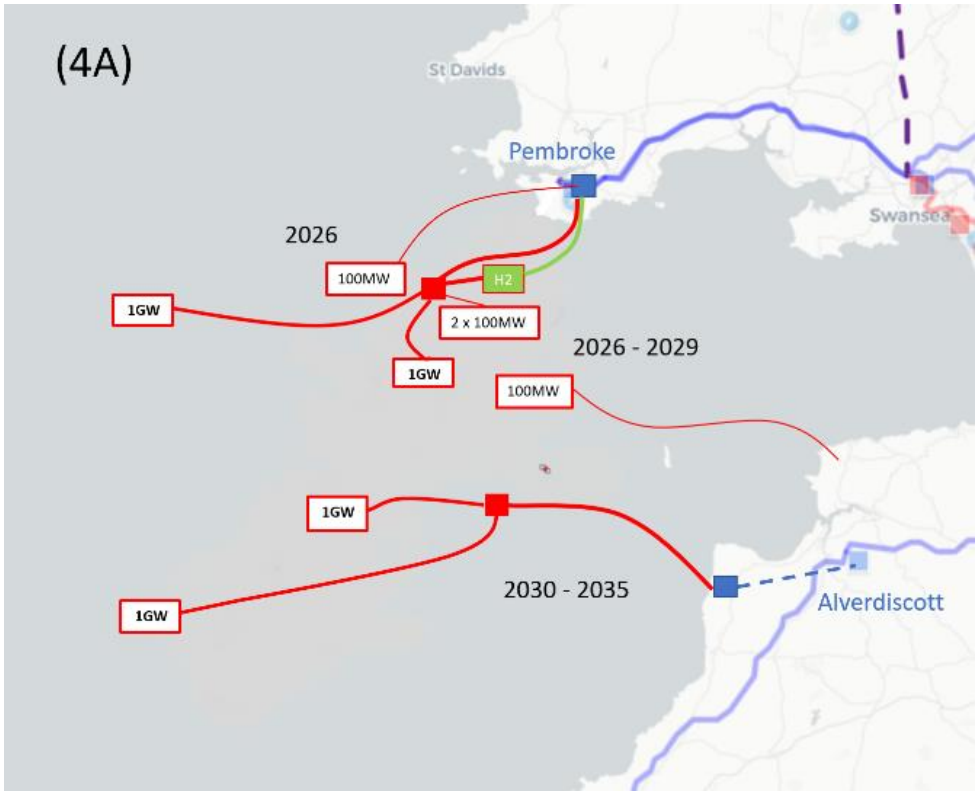

Figure 8: (4A) Alternative scenario: (integration with green hydrogen to existing point of connection): by 2026 system 2x 100 MW; 2026-2029 system 2x 100 MW; 2030-2035 system 4x 1 GW with 2x 1 GW completely separate system to the remaining systems connection in Devon.

3 OFFSHORE WIND ARRAY CONFIGURATIONS

3.1 Introduction

Offshore wind farms (OWFs) must include the necessary electrical infrastructure to transmit generated power from increasing distance offshore to the onshore National Grid. These components must include turbine-based generator, converter and transformer, inter-array cabling, switch gear, conversion technologies for HVAC/HVDC transmission, and transmission export cables. This section investigates the required power, cabling and electrical infrastructure needed to connect OWFs in the Celtic Sea to the onshore National Grid.

3.2 Technical Distribution of Energy

The transmission of energy generated by an OWF requires the electrical infrastructure of inter-array cabling, collector cabling and substation, and export cable of HVAC or HVDC where it connects to the onshore National Grid. This chapter only explores the distribution of the generated energy from offshore wind turbines to onshore substations.

The distribution of energy within the OWF requires a suitable array configuration design with feasible dynamic inter-array cables to withstand constant dynamic loading and ancillary equipment necessary which are described in this section. The energy generated within the wind farm must be collected at an offshore substation and then exported to an onshore infrastructure. Wind farm inter-array cable routing depends on the array configuration which is decided at the wind farm design stage.

To reduce wake effect of the wind direction through each turbine, floating offshore wind turbines (FOWTs) are generally spaced about 8 times the rotor diameter (for example, a rotor diameter of 236 m x 8 = 1,89 kms) which also minimizes the impact of floating structure offsets. For example, the Vestas V236-15.0 MW turbine; powered by the industry's largest swept area of 43,742 m^2; a single turbine is capable of producing up to 80 giga-watt hours per year (GWh/yr); enough energy for over 20,000 households; the 115.5 m blades (with a rotor diameter equaling 236 m) drive a capacity factor of over 60% explained in more detail further on in this report, in section 4 [12].

3.3 Array Topologies

Connection of OWTs in a wind farm are designed in one of four options, namely: tapered radial strings (daisy-chain); tee's (branches); tapered ring loops; or redundant rings. Each topology has been used on at least one UK offshore wind project for fixed bottom wind farms, and potential considerations for floating offshore wind farms are being considered from lessons learnt. This is subject to cost analysis, site conditions and developer risk and/or availability attitudes. Table 2 shows the schematic and description of each topology, while Table 3 lists the advantages and disadvantages of each topology.

Table 2: Array topology schematics and relevant descriptions [13].

Array Topology	Description	Schematic
Tapered Radial Strings	Each turbine, with exception to the last one in each string, has two cables into the base, one cable from the previous turbine or platform and one cable to the next turbine	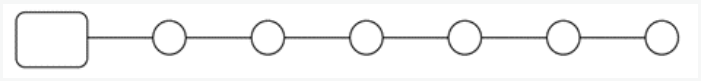
Tee (Branch)	The first (or second) turbine has three cables into the base, that allows for a single cable into the platform but two strings out, normally in a T-shape	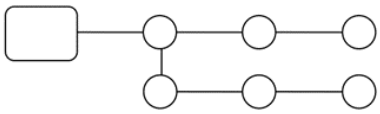
Option 1: Loops (Tapered Ring)	Turbines are arranged in strings, with cable size reducing as the turbines get further from the platform, connecting each pair of strings at the far ends by a joining cable (provide a redundant route for the export of limited power in the event of a cable fault)	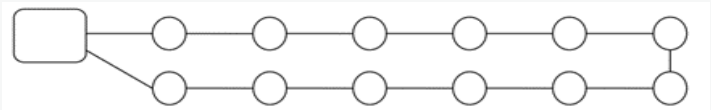
Option 2: Redundant Rings	Turbines are arranged in fully redundant rings, with the cable size remaining same throughout the whole array, to provide a redundant route for the export of all power in the event of a cable fault	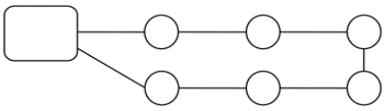

Table 3: Array topology advantages and disadvantages [13].

Array Topology	Advantages	Disadvantages
Tapered Radial Strings:	• Further from the platform the cable size can be reduced • Connections can be very straightforward • Simplified protection • Reduced CSA would cost less for the cable (depending on the vessel it is likely the different sizes can be loaded onto the same vessel)	• Faults in the cable can affect availability • In the event of fault, back-up power is not available
Tee (Branch):	• From substation platform to the first turbine, cable size is reduced	• More complicated protection

	• Fewer cable sizes used • Very flexible with easy connections to substation in compact layouts • Fewer turbines connected with each cable size	• Cable faults cause more availability effects • No back-up power • During O&M stages the connection and routes of cables are not obvious
Loops (Tapered Ring):	• Further from the substation platform the cable size is reduced • Reduced CSA would cost less for the cable (depending on the vessel it is likely the different sizes can be loaded onto the same vessel)	• Arrangement is not possible with odd numbered strings connected to the substation • Difficult to connect turbines may be difficult to configure unless in uniform lines • Turbines at the end of a string may be far from other end turbines causing an increase in cost if you require very long lengths of cable between the last turbines
Redundant Rings:	• Cable fault does not affect availability • Reduced electrical loss • Back-up power available	• Cables into the substation are doubled in number • Increased cable cost • Less flexible arrangement than strings or branches

3.4 Configurations

The *daisy chain* configuration includes "strings" of several FOWTs each connected to the previous turbine via dynamic cables, this design means each dynamic cable carries the total current of the number of turbines previously in the string. Therefore, the cable rating and size may increase towards the end of the string to the offshore substation.

This configuration is most used, however raises issues that each turbine in a string is connected in series, therefore in the event of failure or short-circuit of a single turbine, or cable, then the whole string must be shut-off until maintenance is complete.

In a *fishbone* configuration, each FOWT uses one dynamic cable which connects to a central string static cable which exports to the subsea substation. This requires a high rated static cable at the cables positioned nearer the substation to carry the current; but only one same size dynamic cable to a connection point on the seafloor.

The *star* configuration also requires one same size dynamic cable for each turbine connection to a static cable via a junction box along with several turbines on the seabed (dependent on turbine ratings). This configuration requires the most area to avoid clashing as well as the wake effect from turbine spacing. This configuration is generally the least preferred due to the large requirements for cable connectors and increased cable lengths. Based on the above descriptions, these possible array configurations are shown in more detail in Table 4.

Table 4: Array configurations and relevant schematics.

Configuration	Schematic
Based on 15.0 MW turbines; with a 236 m rotor diameter (i.e., 115.5 m blades), it is expected that turbines are spaced 8x the rotor diameter due to the wake effect of the prevailing wind direction (therefore expressed by calculation, 8 x 236 = 1.89 circa 2 kms) [12]. *For a 66 kV cable rated string, the maximum number of 15 MW FOWTs allowable in a string is 5 (based on the industry standard equates to less than 80 MW). **For a 132 kV cable rated string, the maximum number of 15 MW FOWTs allowable is 10 (based on the industry standard equates to less than 160 MW)	
1: Non-Redundant Daisy Chain Layout Daisy Chain: ~1 GW (max 990 MW) offshore wind array layout *option 1 - 5 turbines per string @ 66 kV, total turbines (5 x 11 strings) = 55 turbines **option 2 - 6 turbines per string @ 132 kV, total turbines (6 x 11 strings) = 66 turbines Due to no redundancy this configuration is unlikely to be a realistic consideration for floating offshore wind	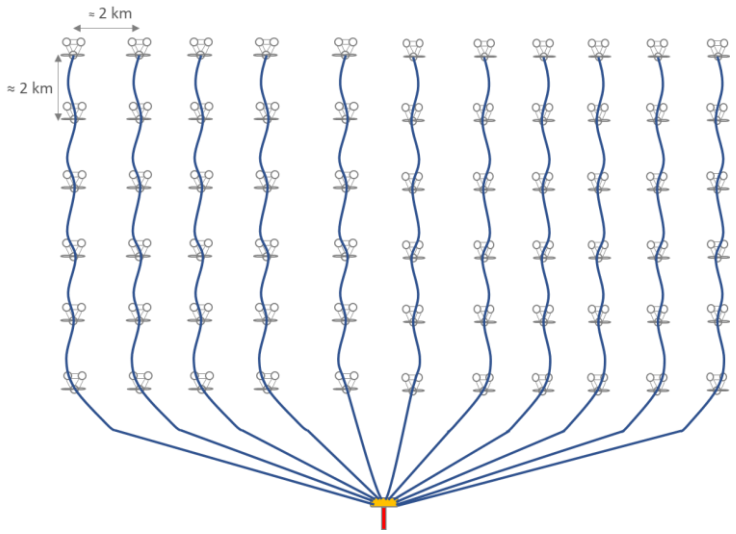
2: Daisy Chain Ring Layout Daisy Chain Ring: ~1 GW (max 990 MW) offshore wind array layout (Cable CSA expectation in 3x mm^2 to reduce cost) *option 1 - 5 turbines per string @ 66 kV, total turbines (5 x 11 strings) = 55 turbines **option 2 - 6 turbines per string @ 132 kV, total turbines (6 x 11 strings) = 66 turbines	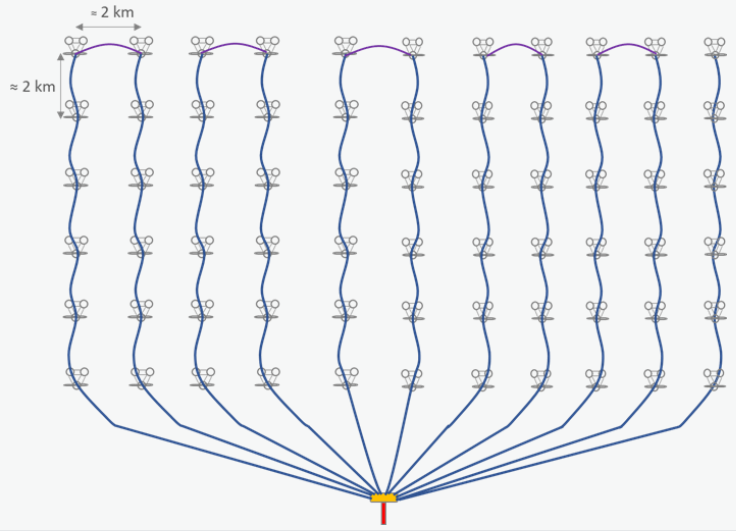

3: Daisy Chain Return Layout

Daisy Chain Return: ~1 GW (max 990 MW) offshore wind array layout

*option 1 - 5 turbines per string @ 66 kV, total turbines (5 x 11 strings) = 55 turbines
**option 2 - 6 turbines per string @ 132 kV, total turbines (6 x 11 strings) = 66 turbines

Not viable for fixed arrays, but may be worth a sensitivity for floating offshore wind (Note this may be a more viable option where the substation is at the array centre for a more realistic array)

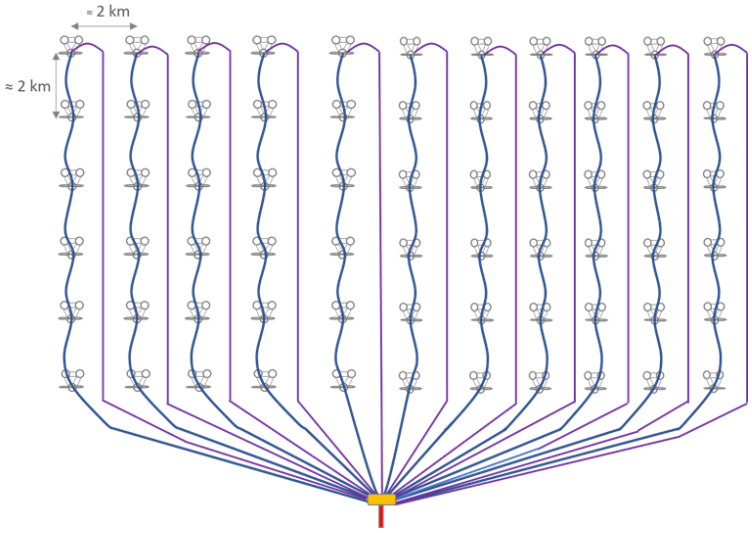

4: Fishbone Layout

Fishbone Layout: ~1 GW (max 990 MW) offshore wind array layout

*option 1 - 5 turbines per string @ 66 kV, total turbines (5 x 11 strings) = 55 turbines
**option 2 - 6 turbines per string @ 132 kV, total turbines (6 x 11 strings) = 66 turbines

The static cable along the sea floor can vary in CSA as it is segmented between connectors.

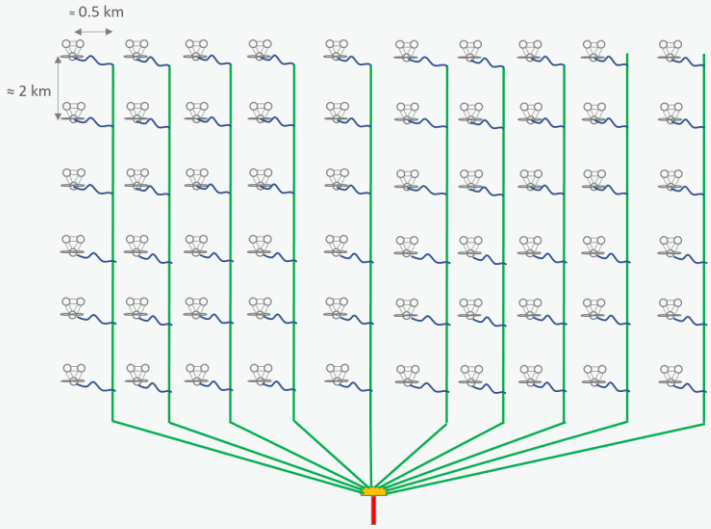

5: Fishbone-Daisy Chain Hybrid

Fishbone-Daisy Chain Hybrid Layout: ~1 GW (max 990 MW) offshore wind array layout

*option 1 - 5 turbines per string @ 66 kV, total turbines (5 x 11 strings) = 55 turbines
**option 2 - 6 turbines per string @ 132 kV, total turbines (6 x 11 strings) = 66 turbines

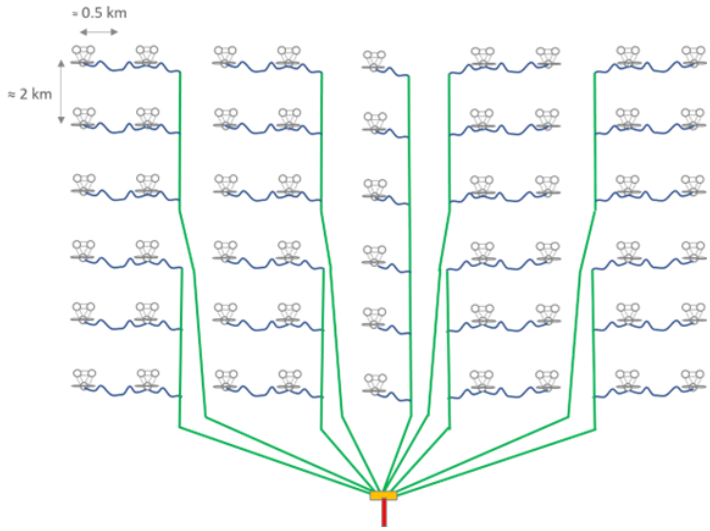

6: Star layout (four-connection groups) Star Layout (4 connection star cable layout): ~1 GW (max 940 MW) offshore wind array layout *option 1 - 4 turbines per string @ 66 kV, total turbines (4 x 10 strings) = 40 turbines **option 2 - 8 turbines per string @ 132 kV, total turbines (8 x 8 strings) = 64 turbines	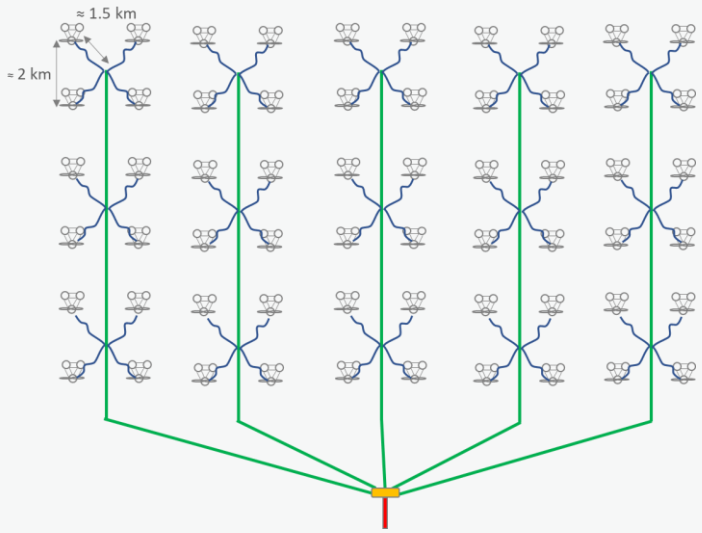
7: Star layout (six-connection groups) Star Layout (6 connection star cable layout only at 132 kV): ~1 GW (990 MW) offshore wind array layout **option 1 - 6 turbines per string @ 132 kV, total turbines (6 x 11 strings) = 66 turbines	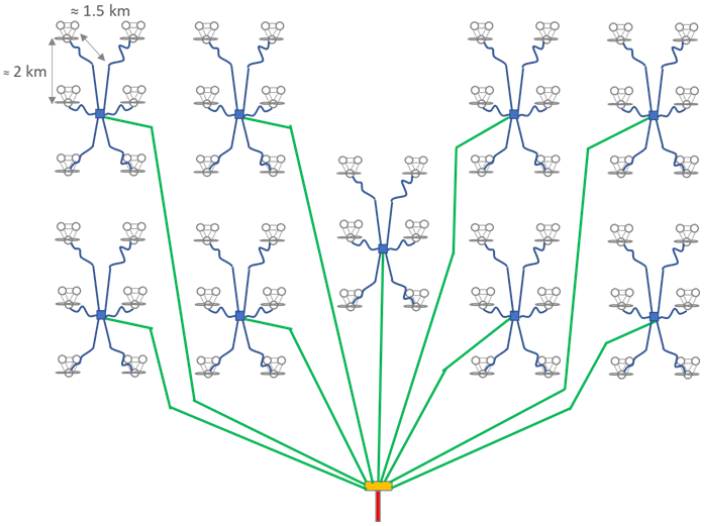

4 ELECTRICAL OUTPUT POWER

4.1 Power output from a wind turbine

To establish the power output from a wind turbine there are fundamental requirements needed that are discussed in the following equations. Wind turbines have performance characteristics such as power output versus wind speed, or versus rotor angular velocity that must be optimized to complete the wind resource availability. Achieved through kinetic energy in a parcel of air of mass, by considering a wind turbine that has a diameter D in meters (m) and a swept area A in meters squared (m^2), if the wind speed is u in meters per second (m/s). The available or 'theoretical' wind kinetic energy per unit time, i.e., the wind power P_{in} can then be evaluated from *equation 1* derivation as shown,

$$P_{in}(U) = \frac{d}{dt}\left(\frac{1}{2}mu^2\right) = \frac{1}{2}\frac{dm}{dt}\,u^2 = \frac{1}{2}\rho AQu^2 \qquad \textit{(Watts)} \qquad \textit{equation 1}$$

However, by replacing Q, with the designated area and velocity Au, as Q is the volumetric flow rate of the wind and ρ (rho) is the air density in kilograms per cubed meters (standard air density used as 1.225 kg/m^3). Hence, the primary reason power available, P_{in} is so effective, is that the power of wind varies with velocity cubed, as represented in *equation 2*,

$$P_{in} = \frac{1}{2}\rho Au^3 \qquad \textit{(Watts)} \qquad \textit{equation 2}$$

It must be noted that for a given turbine, the swept area is a constant, but the air density will vary with elevation and with barometric changes at a given site. In addition, both wind speed and direction will vary over time effecting the power output of each turbine.

4.1.1 Wind Turbine Power Coefficient (C_P)

Often used by the wind power industry is the term power coefficient (C_P) which is a measure of wind turbine efficiency. Power coefficient is the ratio of actual electrical power produced by a wind turbine P_{out} divided by the total wind power flowing into the turbine P_{in} at specific wind speed, as shown in *equation 3*. This overall efficiency of a turbine only forms part of the available/theoretical energy that can be harvested by a wind turbine. The power coefficient therefore must be included as follows,

$$C_p = \frac{P_{out}}{P_{in}} = \frac{(actual\ electrical\ power\ produced)}{(wind\ power\ into\ turbine)} \qquad \textit{equation 3}$$

When defined in this way, the power coefficient represents the combined efficiency of the various wind power systems through a combination of aerodynamic, mechanical, and electrical efficiencies.

4.1.2 Betz Limit

Theoretically, the maximum power coefficient of a horizontal axis wind turbine is 59.3%, which is called the Betz limit (law). The factor is described as a factor of 0.593, or alternatively we can write the maximum power coefficient as $C_p = \frac{16}{27} = 0.593$. The Betz limit was named after the German physicist Albert Betz. Therefore, theoretically a horizontal axis wind turbine cannot extract more than 59.3 percent of the power in an undisturbed tube of air of the same area. In reality power coefficient is lower than factor 0.593, and at most wind speeds, the factor is much lower.

4.1.3 Power Curve

The efficiency, or power coefficient, of wind turbines is not constant, and depends on the wind speed as mentioned in section 4.1.1. Therefore, a power curve depicts how the power of a wind turbine varies with the wind speed. A typical power curve can then be shown in Figure 10, representing a 15 MW power curve layout.

Whilst generating electricity wind turbines are unable to generate at very low or extremely high velocities, either limited to overcome friction for low velocities or severe damage potential at extremely high velocities. Therefore from Figure 9, incorporated into the turbine design is a cut-in speed (in this case 3 m/s) and a cut-out speed (in this case 30 m/s). As discussed earlier the power output increases rapidly because of the velocity cubed relationship, limited by the rated wind speed (in this case 12 – 14 m/s), known as the rated power output P_{out}. This is the maximum level that the electrical generator can still operate, by adjusting the blade angles known as a pitch system.

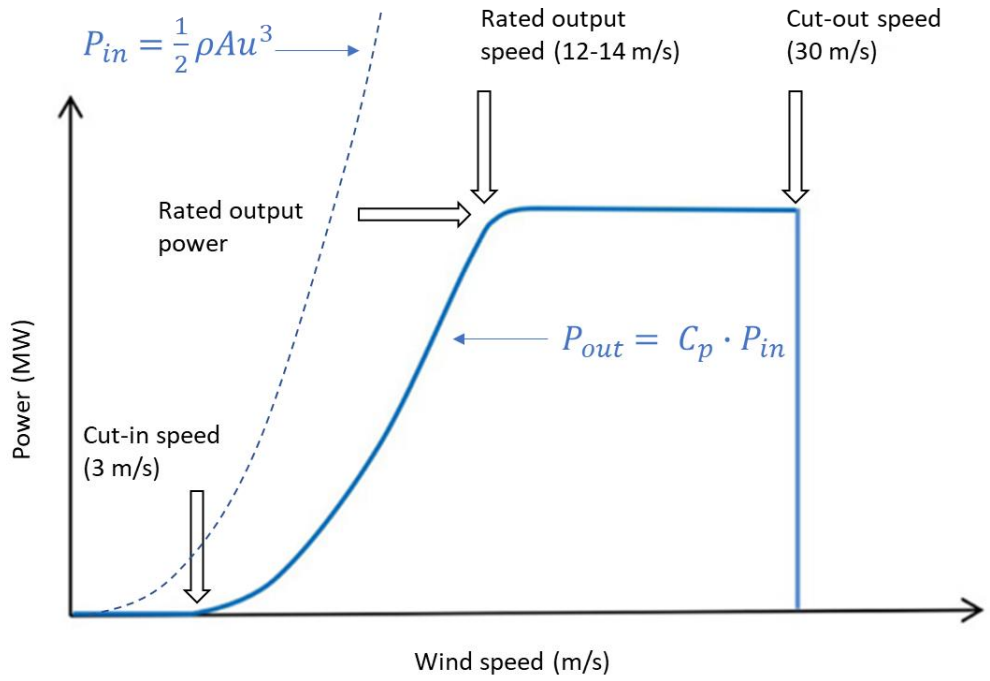

Figure 9: Power curve for a typical 15 MW wind turbine representing power and wind speed.

4.1.4 Power and energy output example to a generic offshore wind farm @ 495 MW

To put this into perspective it is best to consider a typical year that has 365 days or 8,760 hours into an example. The total power predictions can be calculated by how many hours the wind blows with a certain speed, over a period of time and to compute the output power using the power curve (a) and power coefficient (b) plots in Figure 10. There are questions asked when planning the output power of OWF, which can be replicated or increased accordingly to suit the required size of the OWF.

For example, if the OWF was a 495 MW deployment taken from sections 5.1.3 and 5.1.4 and having FOWTs at a rated power output of 15 MW for each turbine. For an OWF of this size the overall FOWTs required would be a total of 33 turbines in the string layouts discussed earlier for the various array configurations in section 3.4.

Calculating the wind turbine power output is dependent upon the velocity of the wind that is rotating the turbine blades. However, the power is not proportional to the wind velocity, as each turbine is different. To determine the output of a specific turbine at a given wind velocity, the power curve and power coefficients is required as shown in Figure 10.

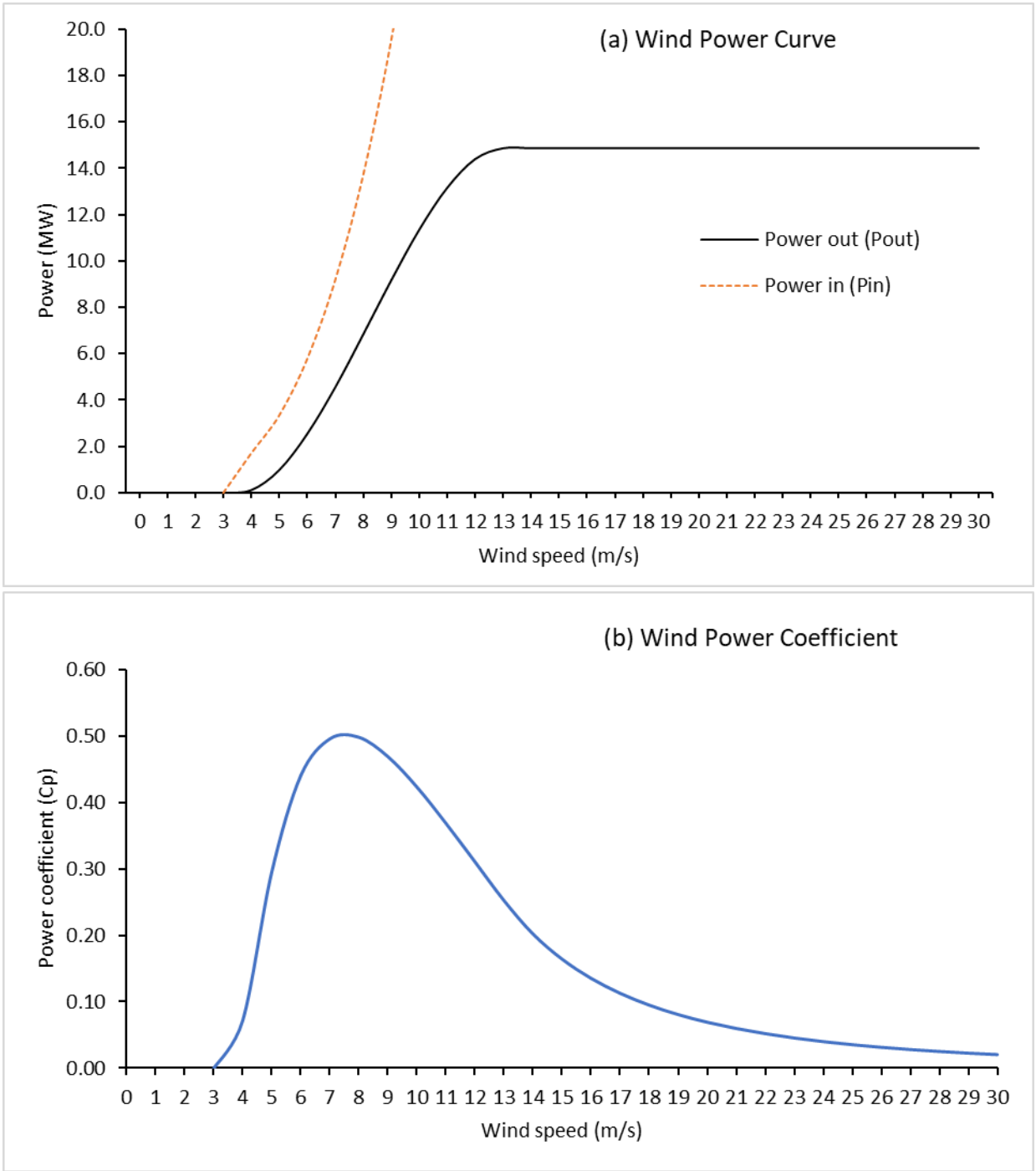

Figure 10: (a) Wind power curve comparing power (MW) to wind speed (m/s). (b) Wind power coefficient curve comparing power coefficient (factor) to wind speed (m/s). Both plots represent a 15 MW turbine.

As the Celtic Sea has a mean yearly wind speed of 9 m/s at 100 m above mean sea level (AMSL) [14], and the power coefficient, $C_p = 0.47$, resulting in the percentage value being 47%. Then by using *equation 2*, P_{in} the wind power formula, and having a standard air density at sea level of 1.225 kg/m^3; and 115.5 m

blades (i.e., rotor diameter equal to 236 m, swept area equals $A = \pi r^2$, shown in Figure 11). The wind power P_{in} flowing into the turbine can then be calculated as follows,

$$P_{in} = \frac{1}{2}\rho A u^3 = \frac{1}{2}(1.225)(43{,}743.536)(9^3) = 19.53\ MW$$

Therefore, the available wind power at a 9 m/s wind speed, will equate to $P_{in} = 19.5\ MW$.

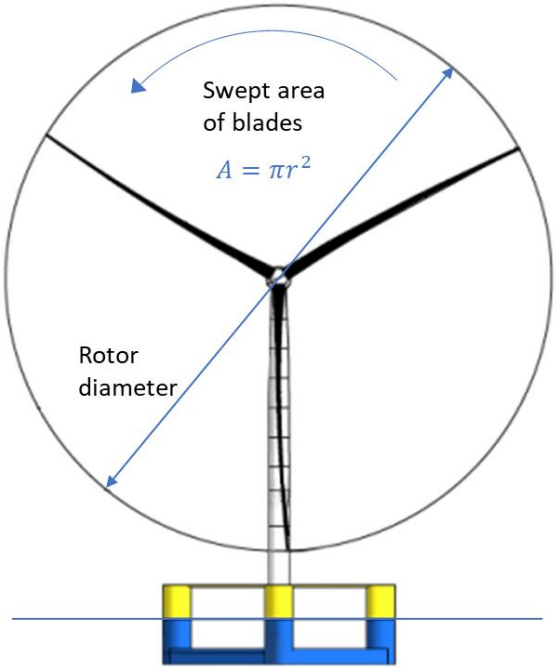

Figure 11: Schematic representation of the swept area of blades for a floating offshore wind turbine.

Furthermore, the actual electrical power output P_{out} of the wind turbine can then be calculated from *equation 3*, as follows,

$$P_{out} = C_p\ (0.47)\ x\ P_{in}\ (19.5) = 9.16\ MW$$

Giga-watt hours per year (GWh/year) is a measure frequently used for FOWT output. This value is important to get the rate of electricity production for the year to the FOWTs. So lastly, each turbine energy production can then be calculated from, *equation 4*,

$$Energy = P_{out}\ x\ time\ (8760) \qquad \text{(GWh/year)} \qquad \textit{equation 4}$$

$$Energy = P_{out}\ (9.16)\ x\ time\ (8{,}760)$$

$$= 80{,}241\ MWh/yr\ or\ 80.2\ GWh/yr$$

remember that 365 days a year multiplied by 24 hours results in 8,760 hours per year.

In Table 5, there are scenarios based on a 495 MW OWF example, incorporating the calculations from the worked-out example above. In presenting Table 5, comparisons can be drawn from various wind speeds within the Celtic Sea, firstly identified by the mean yearly wind speed @ 100 m AMSL (in m/s).

Table 5: Scenario based designs for a 495 MW OWF having a rated power output of 15 MW per FOWT, representing the associated power coefficient and yearly energy production.

OWF example size (in MW)	Total turbines numbers & (rated power (in MW) each)	Wind speed u (m/s)	Turbine rotor diameter A (m)	Power coefficient C_p	Actual mean power output per turbine P_{out} (MW)	Yearly energy production per turbine E (GWh/yr)	Yearly energy production per 495 MW OWF E (GWh/yr)
(1) Mean yearly wind speed Celtic Sea @ 100 m AMSL (m/s)							
495	33 & (15)	9 [14]	236	0.47	9.2	80	2,648
(2) Comparison wind speeds							
495	33 & (15)	6	236	0.44	2.6	22	737
495	33 & (15)	12	236	0.31	14.4	126	4,158
495	33 & (15)	18	236	0.10	14.9	130	4,294

Annual energy output from a wind turbine as seen in Table 5, and Figure 12 express the GWh/year at certain wind speeds. Therefore, by calculating the relationship between wind speeds and annual energy output from a wind turbine previously explained. The plot in Figure 12 can then be generated to the energy production, using *equation 4*, which is then used to calculate the annual power output for each 15 MW turbine.

Figure 12, therefore aligns with the 15 MW specifications from a leading manufacturer, i.e., Vestas from their V236-15.0 MW turbine; powered by the industry's largest swept area of 43,744 m²; a single turbine that can produce up to 80 GWh/year [12], that this sections model is based on. Which aligns with the 9 m/s wind speed calculated (also representing wind speeds in a range from 4 – 12 m/s as the rated output speed), representing the value 80.2 GWh/year as the annual energy output of the turbine.

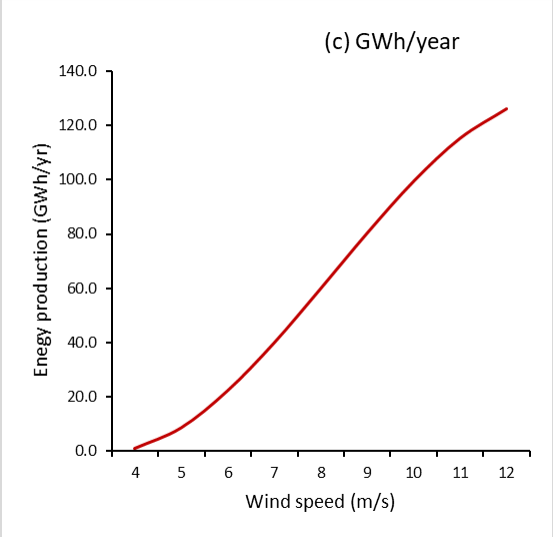

Figure 12: Annual energy output from a wind turbine for a 15 MW turbine expressed in GWh/year compared to wind speeds.

4.1.5 Tip speed ratio lambda

In a wind turbine, there is an optimum value also known as the tip speed ratio lambda λ, where lambda is expressed in *equation 5*,

$$\lambda = \frac{blade\ tip\ speed}{wind\ speed} \qquad \textit{equation 5}$$

The tip speed ratio λ optimum, for which power coefficient C_p is a maximum will be the power maximised for a given wind speed, as expressed in Figure 13. In other words, the peak power for each wind speed (in m/s) occurs at the point where C_p is maximised. To determine the blade tip speed, the model in this section used a rotational speed of the turbine, of 7 revolution per minute (rpm), therefore the blade tip speed value was 86.5 m/s used for lambda, in *equation 5*. It is desirable for the FOWT to have a power characteristic that will follow the maximum C_p line, to maximise the generated power out.

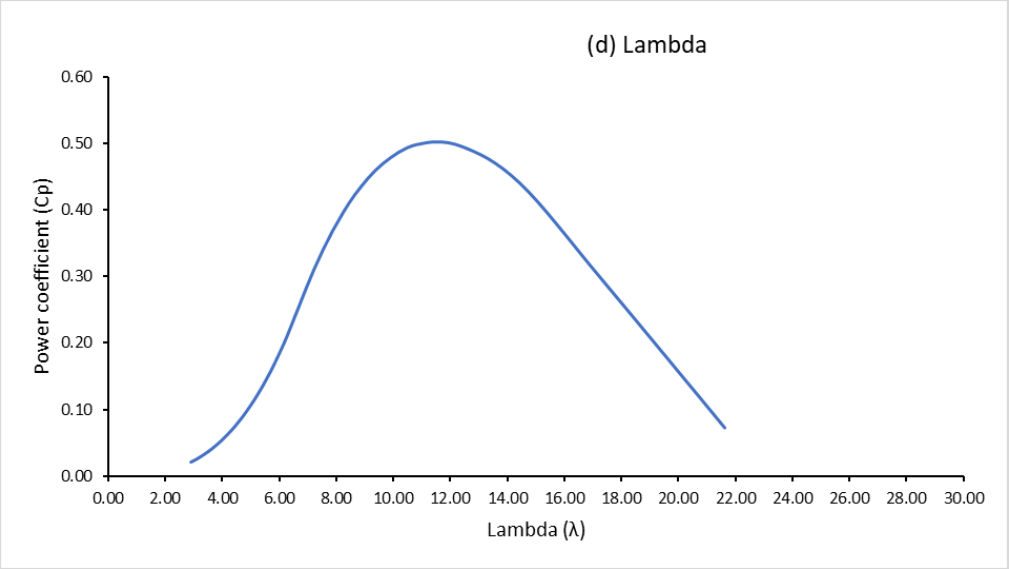

Figure 13: Lambda represented in comparison with the power coefficient to the 15 MW turbine.

4.1.6 The Capacity Factor

Finally, in this section, capacity factor CF measures a power plant's actual generation compared to the maximum amount it could generate in a given period without any interruption. The important point is that the capacity factor decreases rapidly with increasing values of rated wind speed in relation to the power coefficient. As the rated wind speed is increased beyond the optimal rated power output range, the turbine will operate fewer hours at rated power and more hours at partial power or below cut-in speeds.

This decrease in capacity factor must be balanced against an increase in total energy production to obtain the desired economic ideal in GWh. From *equation 6*, by capacity factor this means its actual annual energy output divided by the theoretical maximum possible output, if the FOWT were running at its rated maximum power during all the 8,760 hours of the year (based on 365 days per year).

$$CF = \frac{P_{out}\ (actual\ energy\ output)}{P_{out}\ (maximum\ possible\ output)} \qquad \textit{equation 6}$$

For example: If based on the 495 MW OWF scenario, from 33 by 15 MW turbines this produces 2,647.7 GWh in a year (at a yearly mean wind speed of 9 m/s), the maximum possible output is 4,293.5 GWh in a year, therefore the capacity factor is,

$$CF = \frac{2{,}647.5\ (GWh/yr)}{4{,}647.7\ (GWh/yr)}$$

$$CF = 0.616 = 61.6\%$$

Capacity factors may theoretically vary from 0 to 100 per cent, but in practice they will usually range from 20 to 70%, which aligns with Vestas V236-15.0 MW turbine, driving a capacity factor of over 60% [12]. In summary, there is a capacity factor paradox, that larger CF is not always an economic advantage. As FOW is a very windy location, for instance, it may be an advantage to use a larger FOWT with the same rotor diameter. This would tend to lower the capacity factor, as the calculation above was based on the Celtic Sea annual mean wind speed, resulting in a substantially larger annual production.

4.2 Electrical Conductor Power Losses

The main objective of power cables is to transmit maximum generated power from an offshore wind turbine generator to the National Grid located onshore to be used by consumers. It is obvious that to achieve maximum transmitted power, electrical losses must be kept at a minimum while factoring in economics and environmental concerns. All electrical components will experience a degree of power loss, but a good design will reduce these considerably.

Power losses in HVAC transmission are higher than that of HVDC transmission through radiation loss and induction loss which depend on the HVAC conductor core magnetic field variation. There is also the skin effect which keeps the current density towards the outer diameter of the core with less running through the centre requiring large diameter cores to compensate the larger current; and corona losses where the air surrounding the core ionises to produce sparks when the voltage exceeds a specific limit [15].

The main cause of power loss in a cable is the resistance, which can be reduced by increasing the voltage to reduce the current for a given power rating. The higher the voltages in a transmission line, the lower the losses but also depend on the type of conductor material, length and cross sectional area and configuration. As HVDC is generally able to cover voltages up to 800 kV, losses in these cables are lower than that of an HVAC cable.

4.2.1 Calculation for a typical HVAC 3-core subsea cable

A typical inter-array cable is a HVAC 3-core subsea cable with armoured wiring and a core typical cross-section ranging from 300 mm^2 to 1,000 mm^2, buried in the seafloor of 1 m depth between turbines. Therefore, the electrical cable loss calculation is conducted with the site conditions surrounding the cable and the cable datasheet. So, the calculation of losses in an armoured cable are therefore calculated by using *equations 7 to 10*, showing the sequential calculation steps [16], to achieve each parameter. Added to this are worked examples shown in APPENDIX A, B and E, to cross reference the electrical conductor loss calculations [17].

Power cables have resistance, therefore power lost in the conductors can be calculated as $P = I^2R$ with R as the resistance of the cables and I as the current that passes through them. Power at the load is $P = UI$, so if the voltage U increases by $2x$, only half the current I will be needed to deliver the same power. Therefore in $P = I^2R$, if half the current passes through the same conductors, the system will lose only a quarter of the power.

This example covers the electrical loss calculation steps for a 132 kV, three core CSA at 800 mm^2 submarine inter-array cable. The resistivity of copper is used at 1.77x10^{-8} Ω.m for the three conductor at resistance R, the power generated by the wind turbine is 15 MW, and length equal to 23 kms. Therefore, the required current flowing through the conductors is calculated in section 5.1.4 as 72.69 A per turbine, and 726.96 A for 10 turbines in a string that will be used in this example. The lay configuration is as follows: cable buried in seafloor at a 1 m depth; seabed soil temperature 15°C; soil thermal resistivity 0.7 K.m/W; solidly bonded sheaths; one circuit thermally independent.

Therefore, the following *equations* are worked calculations as shown,

Conductor Losses: $P_{core} = nRI^2$ *equation 7*

where $R = \frac{\rho L}{A} = \frac{1.77x10^{-8} \cdot 1}{800x10^{-6}}$ *= 2.212x10^{-5} Ω/m*

AC resistance of conductor R, Permissible current rating I

$$P_{core} = 3(2.212x10^{-5})(726.96)^2$$

$$P_{core} = 35.077\ W/m$$

Conductor losses result from Joule heating of electrical currents in the conductors, measured in Watts per metre.

Screen Losses: $P_{screen} = n\lambda_1 RI^2$ *equation 8*

Add circulating losses and eddy current losses for foil to find constant λ_1, AC resistance of conductor R, Permissible current rating I

$$P_{screen} = 3(0.1628367815)(2.212x10^{-5})(726.96)^2$$

$$P_{screen} = 5.7118\ W/m$$

Screen losses are caused by circulating currents, only occurring in single core cables, measured in Watts per metre. Screen losses are only applicable to alternating current cables.

Armour Losses: $P_{armour} = n\lambda_2 RI^2$ *equation 9*

Loss factor of the armour constant λ_2, AC resistance of conductor R, Permissible current rating I

$$P_{armour} = 3(0.4206526837)(2.212x10^{-5})(726.96)^2$$

$$P_{armour} = 14.7553\ W/m$$

Armour losses are only applicable to alternating current cables, measured in Watts per metre.

Dielectric Losses: $W_{d_t} = 3W_d$ *equation 10*

Dielectric loss per unit length in each phase constant W_d

$$W_{d_t} = 3(0.1316852157)$$

$$W_{d_t} = 0.39506\ W/m$$

Dielectric losses is the electrical power that is wasted by heating the dielectric in the electric field, measured in Watts per metre. In addition, energy losses occur at the constant and variant current in the dielectric.

The power generated P_{in} by the wind turbine is 15 MW, and the total length equals to 23 kms, therefore the following $P_{total-losses}$ is calculated as follows,

$$P_{total-losses} = P_{core} + P_{screen} + P_{armour} + W_{d_t}$$

$$P_{total-losses} = (35.077x23000) + (5.7118x23000) + (14.7553x23000) + (0.39506x23000)$$

$$P_{total-losses} = 806.773\ kW + 131.372\ kW + 339.371\ kW + 9.086\ kW$$

$$P_{total-losses} = 1286.603\ kW$$

From the total power losses calculated across the system, the final power P_{out} can be worked out as follows, in MW.

$$P_{out} = P_{in} - P_{total-losses} = 150\ MW\ (15x10) - 1.286\ MW = 148.714\ MW$$

Power has a representation in a right angle triangle showing the relation between active power P, in MW, reactive power Q, in $MVAr$ and apparent power S, in MVA (found in sections 5.1.3 and 5.1.4). By implementing the systems losses the efficiency η and power factor PF can be determined. It must be stated that the PF is broken down into three areas, namely 1.0 to 0.95 good, 0.95 to 0.85 poor, 0.85 and below poor. A the perfect PF would be 1.0, however in reality this is almost impossible to achieve.

Therefore, efficiency is:

$$\eta = \frac{P_{out}}{P_{in}} \cdot 100\% = \frac{148.714\ MW}{150\ MW} \cdot 100\% = 99.14\%$$

So, power factor is:

$$PF = \frac{P\ (actual)}{S\ (apparent)} = \frac{148.714\ MW}{157.894\ MW} = 0.94$$

Therefore, the transmission of electrical power is carried out at high voltage due to the following main advantages, and that the PF of the system is always aiming to achieve 0.95 or above:

- When the transmission is carried out at higher voltages, the power losses in the transmission system are reduced significantly and the efficiency of the transmission system is enhanced.
- When the transmission is carried out at higher voltages, the current in the transmission system is reduced significantly, therefore, the CSA of the conductors required is also reduced to carry the reduction of current.

5 OFFSHORE INTERCONNECTION CABLE DESIGN

5.1 Sizing Alternating Current Offshore Array Cables

The cable requirements are defined early in the wind farm design process depending on the FOWT used, array configuration design, and wind farm capacity. For example, if a daisy chain array configuration is used, each turbine in a string contributes current to the dynamic cable infrastructure and so cable ratings are important to consider. Wind farms currently deployed - use cable ratings of either 33 kV or 66 kV, with future intention to increase these to 132 kV when higher farm capacity is designed, that should be considered for FOW. Lower voltage rating cables can carry lower currents so depending on the FOWT used, higher cable rating may be needed. An example of a daisy chain string current calculation is described below.

5.1.1 Copper (Cu) and Aluminium (Al) Conductor

Dynamic cables have been manufactured using copper which have certain cross-sectional areas (CSA) depending on their ratings, these are shown in Table 6. Some state-of-the-art dynamic cables do have aluminium cores, but these have not yet been used for FOW. The CSA shown in Table 6 are for static cable cores, however there is negligible difference when looking at dynamic core design. Copper and aluminium are the most common materials for cable cores, and each have their advantages and disadvantage. For the Cornwall FLOW Accelerator (CFA) Project, a copper conductor core will be used for initial analysis, and cross-linked polyethylene cable (XLPE) widely used as electrical insulation in power cables. Especially for medium to high and extra-high voltage power cables operating at a maximum temperature of 90°C.

Table 6: Cable sizes and ratings for Copper (Cu) and Aluminium (Al), cable current carrying capacity for XLPE Submarine Cable Systems [18].

Cross Section (mm^2)	10 - 90 kV XLPE 3-core cables		100 - 300 kV XLPE 3-core cables	
	Copper (Cu) @ 66 kV	Aluminium (Al) @ 66 kV	Copper (Cu) @ 132 kV	Aluminium (Al) @ 132 kV
	A	A	A	A
95	300	235		
120	340	265		
150	375	300		
185	420	335		
240	480	385		
300	530	430	530	430
400	590	485	590	485
500	665	540	665	540
630	715	600	715	600
800	775	660	775	660
1000	825	720	825	720

5.1.2 Cable Ratings

The following Table 7, shows the cable ratings used in calculations when designing the AC copper inter-array cable. Depending on the voltage rating of either 66 kV or 132 kV and cable cross-section area of the conductor cores, the current rating changes to allow for the number of FOWT in a string to be increased.

Examples of using a 66 kV and a 132 kV both copper cable designs, for an array of 15 MW floating offshore wind turbines, are explained in sections 5.1.3 and 5.1.4. For a 66 kV cable rated string, the maximum number of 15 MW FOWTs allowable in a string is 5 (stated by the industry as less than 80 MW maximum); and for a 132 kV cable rated string the maximum number of 15 MW FOWTs allowable in a string is 10 (stated by the industry as less than 160 MW maximum). Therefore, from Table 7, a string for a 132 kV cable, with a maximum of 10 FOWTs, the maximum current permissible is 730 A, which signifies an 800 mm^2 cross section for the cable, as seen in Table 6.

This can be achieved by incorporating the de-rating factors due to the following criteria; power factor 0.95; minimum operating voltage factor 0.95; operating temperature 90°C; maximum seabed temperature 20°C; laying depth in seabed 1.0 m; seabed thermal resistivity 1.0 K.m/W – the final equivalent current carrying capacity (A); and CSA (mm^2) can be determined, as shown, in Table 7 [18].

Table 7: AC Copper cable data incorporating de-rating factors representing values that includes minimum operating voltage factor [18].

Cable No.	Cross-section area (mm^2)	Current carrying capacity (A) for Cu	Rated current I_n (A) per WT	Voltage U (kV)	Minimum Operating Voltage $U_{op,min}$ (kV) *	WT nominal power P_n (MW)	Apparent power S_n (MVA) **	Capacity number of FOWT per string
@ 66 kV								
#1	240	480	145.39	66	62.7	15	15.8	3
#2	630	715	145.39	66	62.7	15	15.8	4
#3	800	775	145.39	66	62.7	15	15.8	5
@ 132 kV								
#4	240	480	72.69	132	125.4	15	15.8	6
#5	630	715	72.69	132	125.4	15	15.8	9
#6	800	775	72.69	132	125.4	15	15.8	10

(*) Minimum operating voltage 0.95
(**) 3-phase AC core with power factor 0.95
De-rating factors (operating temperature 90°C; maximum seabed temperature 20°C; laying depth in seabed 1.0 m; seabed thermal resistivity 1.0 K.m/W)

5.1.3 Floating Offshore Wind Turbine 15 MW at 66 kV

For a 495 MW wind farm example, the wind turbines are rated at 15 MW per turbine with a minimum operating voltage, $U_{op,min}$ of 0.95 per unit voltage, *puV*, and a power factor, *pf* of 0.95. As the cables are 3-phase AC, the power correction of each turbine is calculated by the following *equations 11 to 13*. To work out the apparent power S_n using the rated turbine power P_n *use equation 11.* To calculate the corrected voltage, use the *puV* from *equation 12*. Finally, to determine the rated current flowing in the cable I_n, for each turbine in the wind farm string, use *equation 13*.

$$S_n = \frac{P_n}{pf} \quad \textit{equation 11}$$

$$U_{correct} = U_{op,min} \cdot U \quad \textit{equation 11}$$

$$I_n = \frac{P_n}{\sqrt{3} \cdot U_{correct} \cdot pf} \quad \textit{equation 12}$$

Therefore the calculations are as follows,

$$S_n = \frac{P_n}{pf} = \frac{15MW}{0.95} = 15.8\ MVA$$

$$U_{correct} = U_{op,min} \cdot U = (0.95)(66kV) = 62.7\ kV$$

$$In = \frac{P_n}{\sqrt{3} \cdot U_{correct} \cdot pf} = \frac{15MW}{(1.732 \cdot 62.7kV \cdot 0.95)} = 145.39\ A \textit{ (Current per turbine)}$$

Each turbine of rated power, namely 15 MW with a corrected operational voltage, and rated current flow of 62.7 kV and 145.39 A respectively. This means that each turbine in a daisy chain string contributes up to 145.39 A of current into the subsequent turbine, which contributes another 145.39 A, until the end of the chain which connects the whole string to a substation connection box. From manufacture specifications and industry practice, a string of wind turbines using 66 kV cables is limited to 80 MW [13].

Using the above calculations, a single string of wind turbines operating with 66 kV cables can carry a current of up to 726.96 A (5x 145.39). Therefore, the maximum number of 15 MW FOWTs that can be in a single string equals 5 (equalling 75 MW @ 726.96 A). So, a 495 MW wind farm consisting of 33 FOWTs can therefore be arranged in an array of 5 strings with 5 FOWTs and 2 strings with 4 FOWTs, as shown, in Figure 14.

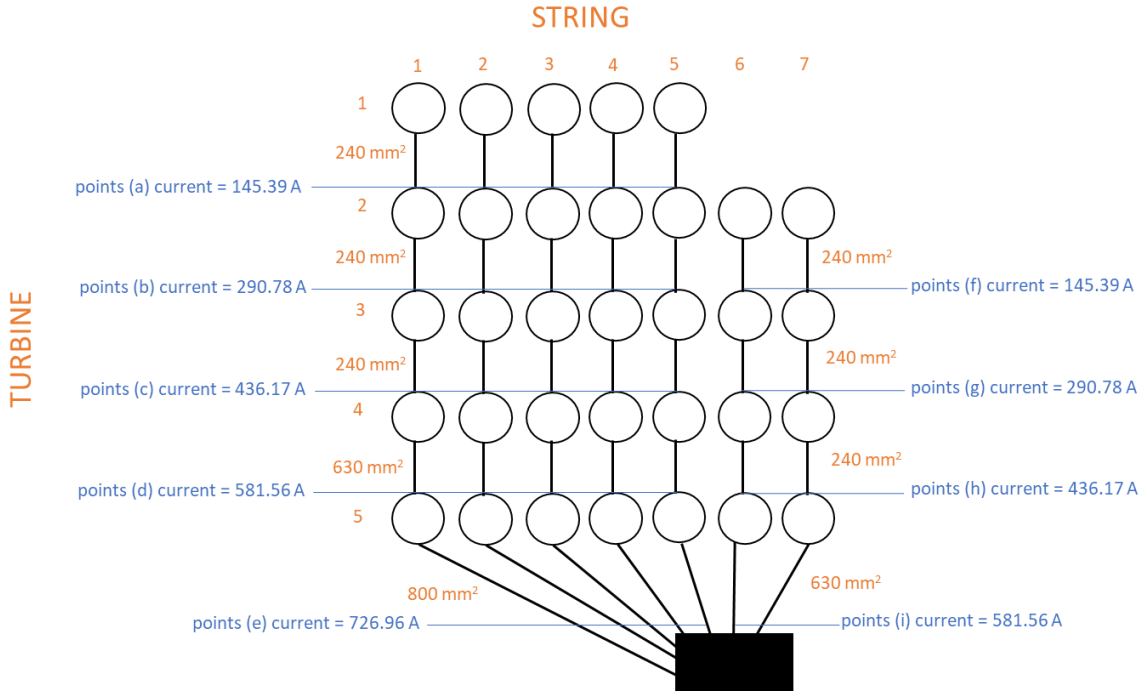

Figure 14: Layout for a 495 MW wind farm of 33 by 15 MW FOWTs connected via 66 kV copper cables; points (a) to (i) signify current on the relevant numbered strings (1 – 7).

As developers would expect cost reduction to cable sizing, the key would be to reduce the cross section moving away from the substation (connection point). In this layout there would be three CSAs to reduce costs 800 mm^2, 630 mm^2 and 240 mm^2 for 66 kV cables.

The first 3 turbines (1 – 3) in strings (1 – 5), from Figure 14, are connected via a 240 mm^2 copper cable to point (c) (able of carrying a maximum current of 480 A); but carrying 436.17 A for the 3 turbines at 15 MW each. Turbine (4) is connected by a 630 mm^2 copper cable to point (d) (able of carry a maximum current of 715 A); but carrying turbines (1 – 4) amounting to 581.56 A. Turbine (5) is connected by a 800 mm^2 copper cable to point (e) (able of carry a maximum current of 775 A); but carrying turbines (1 – 5) amounting to 726.96 A.

Finally, the strings that consist of 5 turbines are connected via cross section 240 mm^2, 630 mm^2 and 800 mm^2 copper cables @ 726.96 A. Using the same principle, the last two strings (6 – 7) that consist of 4 turbines are connected via cross section 240 mm^2 and 630 mm^2 copper cables @ 581.56 A.

5.1.4 Floating Offshore Wind Turbines 15 MW at 132 kV

As the cables are 3-phase AC, the power correction of each turbine is calculated by the following *equations 11 to 13*. To work out the apparent power S_n using the rated turbine power P_n *use equation 11.* To calculate the corrected voltage, use the *puV* from *equation 12*. Finally, to determine the rated current flowing in cable I_n, for each turbine in the wind farm string, use *equation 13*.

Therefore the calculations are as follows,

$$S_n = \frac{P_n}{pf} = \frac{15MW}{0.95} = 15.8\ MVA$$

$$U_{correct} = U_{op,min} \cdot U = (0.95)(132kV) = 125.4\ kV$$

$$I_n = \frac{P_n}{\sqrt{3} \cdot U_{correct} \cdot pf} = \frac{15MW}{(1.732 \cdot 125.4kV \cdot 0.95)} = 72.69\ A \text{ (Current per turbine)}$$

Each turbine of rated power 15 MW with a corrected operational voltage and rated current flow of 125.4 kV and 72.69 A respectively. This means that each turbine in a daisy chain string contributes up to 72.69 A of current into the subsequent turbine, which contributes another 72.69 A, until the end of the chain which connects to a substation connection box. From manufacture specifications and industry practice, a string of wind turbines using 132 kV cables is limited to 160 MW [13].

Using the above calculations, a single string of wind turbines operating with 132 kV cables can carry a current of up to 726.96 A (10x 72.69). Therefore, the maximum number of 15 MW FOWTs that can be in a single string equal 10 (equalling 150 MW; 726.96 A). So, a 495 MW wind farm consisting of 33 FOWTs can therefore be arranged in an array of 4 strings with 8 FOWTs and 1 string with 9 FOWTs, as shown, in Figure 15.

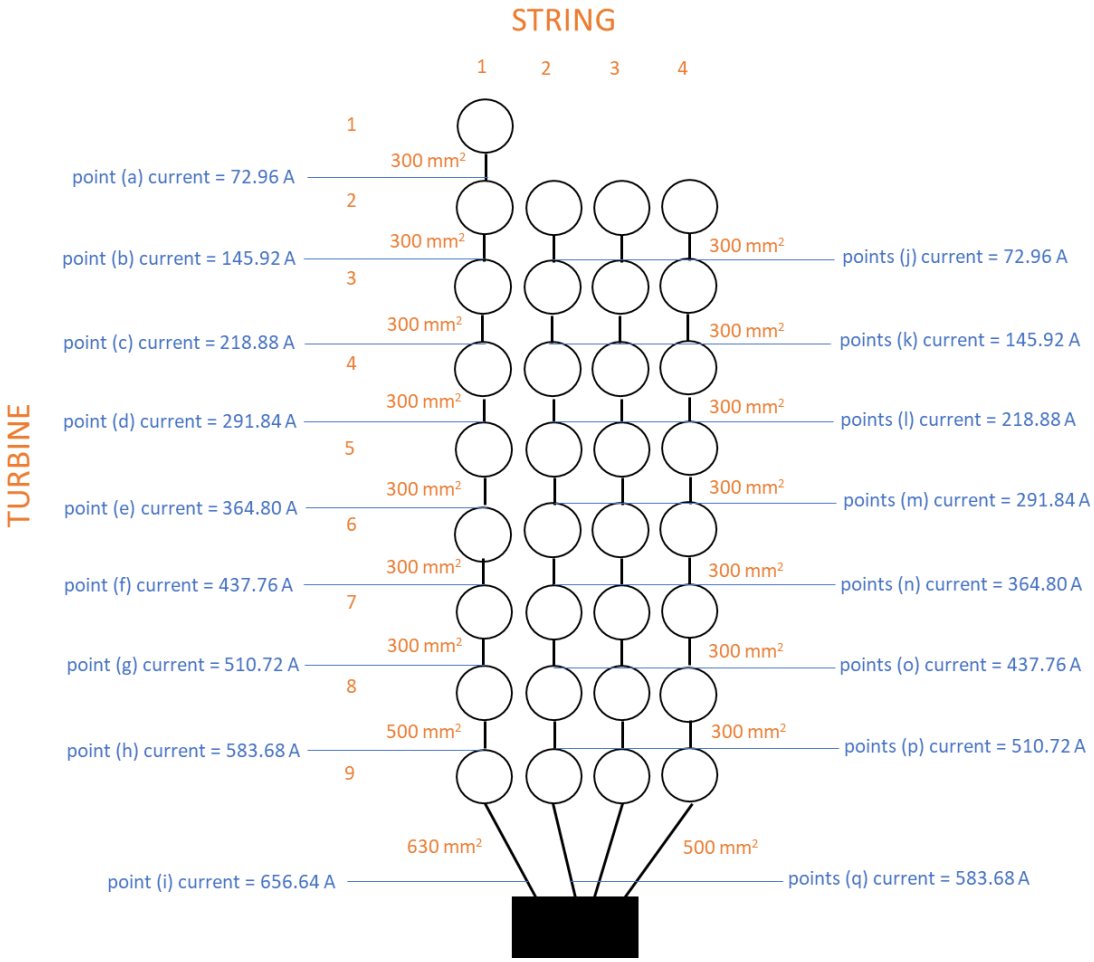

Figure 15: Layout for a 495 MW wind farm of 33 by 15 MW FOWTs connected via 132 kV copper cables; points (a) to (q) signify current on the relevant numbered strings (1 – 4).

As developers would expect cost reduction to cable sizing, the key would be to reduce the cross section moving away from the substation (connection point). In this layout there would be three CSAs to reduce costs 630 mm^2, 500 mm^2 and 300 mm^2 for 132 kV cables.

The first 7 turbines (1 – 7) in strings (1), from Figure 15, are connected via a 300 mm^2 copper cable to point (g) (able of carrying a maximum current of 530 A); but carrying 510.72 A for the 7 turbines at 15 MW each. Turbine (8) is connected by a 500 mm^2 copper cable to point (h) (able of carry a maximum current of 655 A); but carrying turbines (1 – 8) amounting to 583.68 A. Turbine (9) is connected by a 630 mm^2 copper cable to point (i) (able of carry a maximum current of 715 A); but carrying turbines (1 – 9) amounting to 656.64 A.

Finally, the first string that consist of 9 turbines are connected via cross section 300 mm^2, 500 mm^2 and 630 mm^2 copper cables @ 656.64 A. Using the same principle, the last three strings (2 – 4) that consist of 8 turbines are connected via cross section 300 mm^2 and 500 mm^2 copper cables @ 583.68 A.

6 OFFSHORE SUBSTATION AND COLLECTOR SYSTEM

6.1 Offshore Substations

Conventional substations sit between collection system of individual turbine and transmission system. Power from each individual turbine in offshore wind is collected through collector system before connection to the offshore substation. The inter-array cables connecting individual turbines range from 33 to 66 kV, but industry thinking is extending this to 132 kV in the future before connecting to the offshore substation. The primary function of the substation is to accommodate the high voltage and medium voltage electrical components required for transmitting the power collected from the turbines. This high voltage power is transmitted via offshore export cables from the substation to shore and linked to the electrical grid by an onshore substation. Further detail on offshore substations publication in this series by Offshore Renewable Energy Catapult, for the Celtic Sea Cluster (under the Cornwall FLOW Accelerator Project) can be found under this title: '*The Future Potential Role of Offshore Multipurpose Connectors*'.

Reliability and redundancy considerations must take place during the electrical design of the substation. This will include electrical safety from switchgear and circuit breakers to ensure faults can be disconnected if they occur. Step up transformers will convert the cable voltage to 132, 275 or 400 kV to balance safety and efficiency of the system.

6.1.1 Bottom-fixed offshore substations

Support structures comprise of a typical jacket or monopile bottom-fixed offshore substation structure, with piled foundations, which works into the jacket design being considered for the PDZ ranging from a platform size, of 1 to 2.4 giga-watts. The majority of wind farm HVAC offshore substation structure are jacket style which have been deployed to date (similar to those used for support of bottom-fixed wind turbines). Wind farm capacity for these types of offshore substation ranges from just a small 60 MW up to larger 1.2 GW, with larger wind farms having multiple offshore substations. These jacket substructures range in weight from 500 to 7,000 tonnes from small to very large offshore substations (greater than 1 GW in capacity).

6.1.2 Floating offshore substations

A floating offshore substation (FOSS) structure will combine a floating substructure, (also known as a floater), and a station-keeping mooring and anchoring system. When considering a floating offshore substation structure another major difference is the requirement and connection for dynamic inter-array and export cables. Sites like the Celtic Sea under consideration for floating offshore substations, will also have the dynamic cables to consider both for inter-array cables from floating offshore wind turbines, and export cables from floating offshore substations. At present the maturity and technology for high voltage dynamic export cables is not currently commercially ready.

6.2 Collector System

In an offshore wind farm, there are two electrical systems to transfer power, these first being the interconnection of all wind turbines in the wind farm known as the collection system, and the other being

the transmission system operating at higher voltage with the connection from offshore wind farm to the onshore grid.

A typical representation of an offshore wind farm collection system is shown in Figure 16 [19], with a HVDC transmission system. The collector system begins with a transformer within the FOWT tower which usually steps up the generator from 690 V to the inter-array cabling voltage, typically 33 kV on most fixed wind projects however 66 kV is the most common for FOW systems and up to 132 kV are being developed and investigated for future projects. These inter-array cables are typically AC as this is the most well-established technology. This is due to the small distances between turbines, the ability to step up voltages, well established electrical protection and voltage rating suitable for lower power capacity. These cables then connect the FOWTs to the offshore substation where transformers step up the voltage suitable for HVDC transmission through converters.

Depending on the array configuration used in a project, shown in Table 4, subsea connectors are required for fishbone and star arrangements to connect to the central collector cable. Also, large farms may require multiple substations to facilitate the power. Although current offshore wind farms are all AC inter-array collection systems, DC collection systems have been looked at, in various concepts.

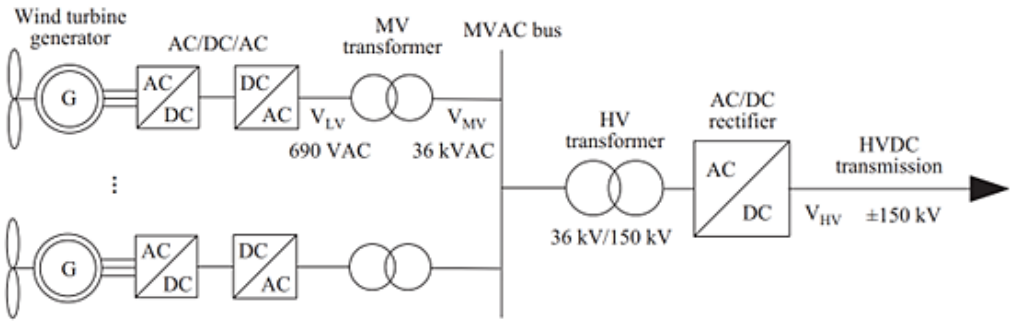

Figure 16: Typical representation of components in an AC electrical collection and transmission system [19].

7 OPTIMISATION IN DYNAMIC CABLE SYSTEMS

7.1 Dynamic Cable Systems

With the increasing growth of FOW in deeper waters around the world, dynamic cables between floating turbines and seabed are being increasingly researched. The floating system consists of three main parts, floating structure, mooring system, and dynamic cable system. All experience dynamic loading from wind, wave and tidal current below the surface which creates additional mechanical stress. Dynamic cables are designed to be flexible to withstand these loads and provide protection to reduce component failure from high stresses. These cables differ from subsea static cables used on B-F offshore wind turbines which are not designed to cope with dynamic motion and have higher risks of failure in subsea environments.

The role of a dynamic cable system is to provide a route for the electrical energy generated by the FOWT from the floating structure to the seabed where it connects to a static section of cable through connectors or a factory joint. This static cable can then either be connected to further dynamic cables to another FOWT, or to a dynamic cable to the floating offshore substation of the wind farm where it is exported to shore. Figure 17 demonstrates the schematic of a dynamic cable system along with FOWTs, array cable and substation in a floating wind farm.

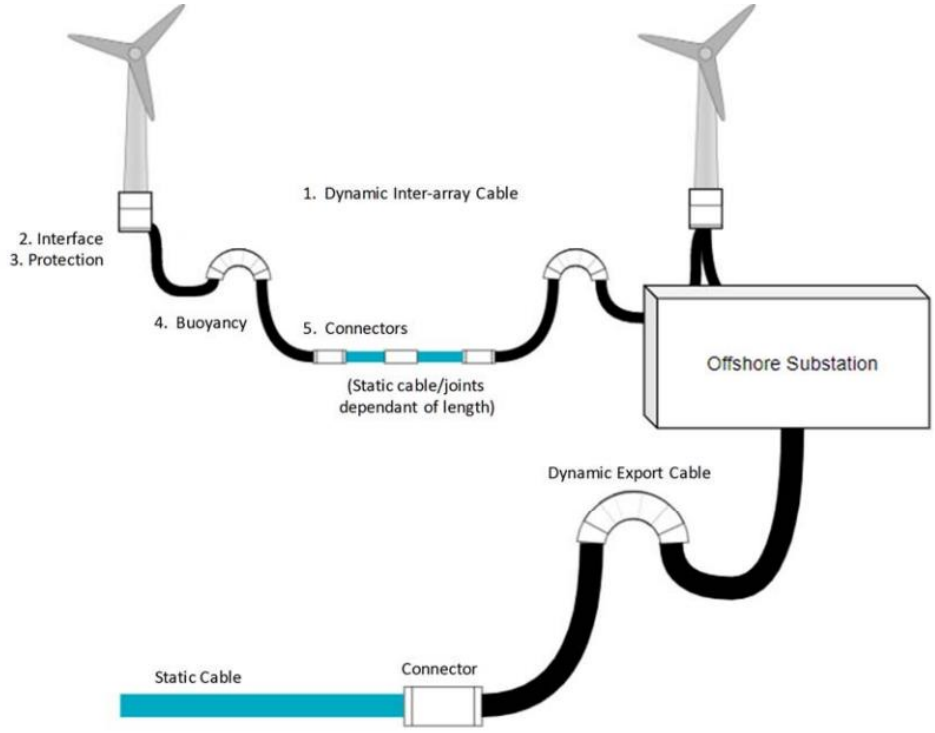

Figure 17: Dynamic cable system schematic for inter-array cabling [13].

A chart of the components and ancillary equipment necessary to design a flexible dynamic cable system is shown in Figure 18, including floater interfaces, protection for the cable, added buoyancy to achieve the designed route configuration, subsea connectors to static seabed cables, and sensors for dynamic cable analysis and monitoring.

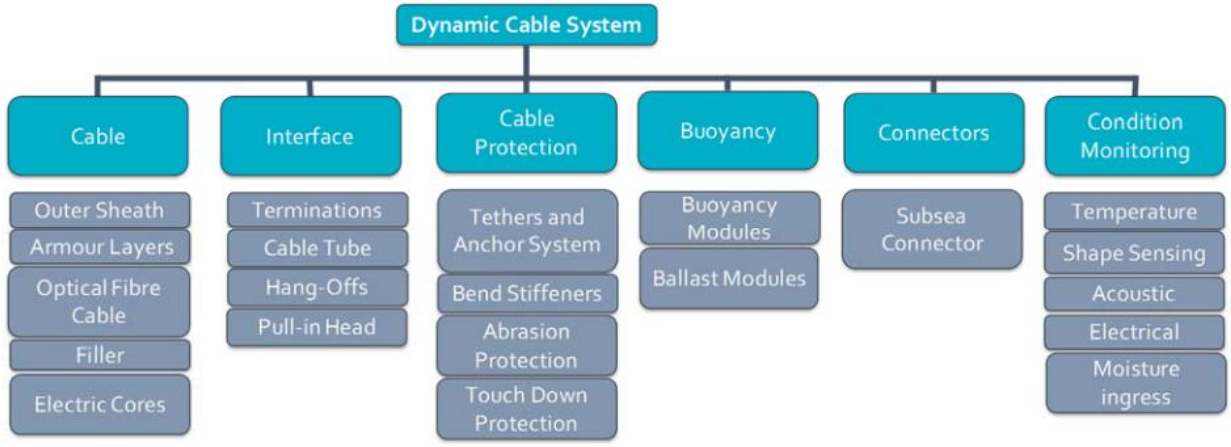

Figure 18: Key components and ancillary equipment of a dynamic cable system [13].

As the floating offshore wind industry has recently increased in growth and interest, there are no official standards which directly apply to the design, analysis or testing of dynamic submarine cables. The O&G industry use standards for subsea power cables and umbilical power cables which reach water depths over 1,000 m. These standards are typically qualified according to The International Electrotechnical Commission (IEC) and The International Council on Large Electric Systems (CIGRE) and are used in the offshore wind dynamic cable industry as guidance.

7.2 Dynamic Cable Configurations

The dynamic cable configuration is the cable layout in between the floater on the surface and the connecting point on the seabed. It is a combined result of cable cross section, ancillary equipment, and operational environment, heavily depending on the site conditions in terms of tidal range, seabed condition and bathymetry. Extreme environmental conditions regarding wind speed, mean significant wave height and subsurface current with depth also play a great role in finalising the configuration.

Three most common configurations are described in Table 8 with their advantages and disadvantages.

Table 8: Dynamic cable configuration advantages & disadvantages [20].

Name	Catenary (Free Hanging)	Lazy Wave	Tethered Wave
Description	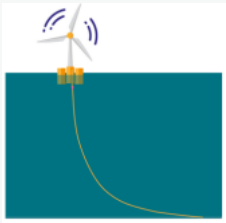 A line extends in a catenary shape from the floater to the seabed.	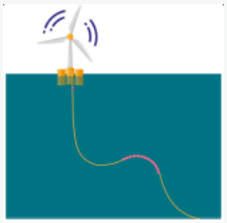 A lazy wave provides lift to a midwater cable section by attached buoyancy modules.	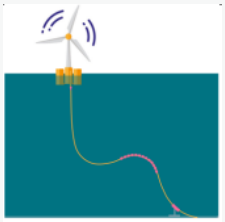 A tethered wave is similar to a lazy wave with the addition of a tether restraining the touchdown point.
Advantages	Simplest configuration	Simple configuration buoyant section which decouples reasonable dynamic	Buoyant section which decouples FOWT motions from fixed subsea end.

		FOWT motions from fixed subsea end. Accommodate reasonable levels of marine growth relative to depth. For shallow waters it may be possible to accommodate higher levels of marine growth by adding buoyancy modules during the lifetime of the system. Proven use for deep water application.	Tether reducing touchdown point migration under cross current. Accommodate reasonable levels of marine growth relative to depth. For shallow waters it can accommodate higher levels of marine growth without the need for adding extra buoyancy modules during the lifetime of the system.
Disadvantages	Vessel motions are not decoupled. No restriction of lateral motion. Likely to require a bend control at the floating structure entrance.	No restraint on lateral motion. Change in configuration shape with marine growth. Requirement for a bend control at the floating structure entrance. Requirement for Buoyancy modules.	Requirement for hold-down tether and clamp which will increase complexity and time of installation. Requirement for a bend control at the floating structure entrance. Requirement for Buoyancy modules.
Overall Comment	Lowest cost cable solution - likely suitable for minimal dynamic motion. Unsuitable for applications where reasonable or significant dynamic motion is expected.	Low-cost cable solution - suitable for applications where reasonable dynamic motion is expected. May be unsuitable for applications with significant dynamic motion and offsets. May be unsuitable where there is a significant field size constraint restricting distance between the floating structure and touchdown point. Unsuitable where strong currents lead to touchdown point migration.	Mid-range cost cable solution.

For the CFA project with an average water depth of 107.7 m and semi-submersible floating structure, a lazy wave configuration will be selected and designed. The general concept of this configuration is shown in Figure 19 including:

A. Sag Bend/Upper Section – the cable length between the hang off point on the floating structure and the start of the buoyancy module section, which is a sag bend profile in a lazy wave configuration.
B. Buoyancy Section – the cable length which uses buoyancy modules to produce a hog bend in a lazy wave configuration, buoyancy modules are spaced along the length to produce this bend.

C. Lower Section – the cable length from the end of the buoyancy section to the touchdown point.
D. Horizontal distance to touch down point – the horizontal total distance from the hang off point on the floating structure to the touchdown point to give indication of distance from the floating structure which the dynamic cable follows.
E. Horizontal distance to end point – the distance from the touchdown point to the anchor end point which must be sufficiently long to avoid over abrasion and to cope with platform offsets.

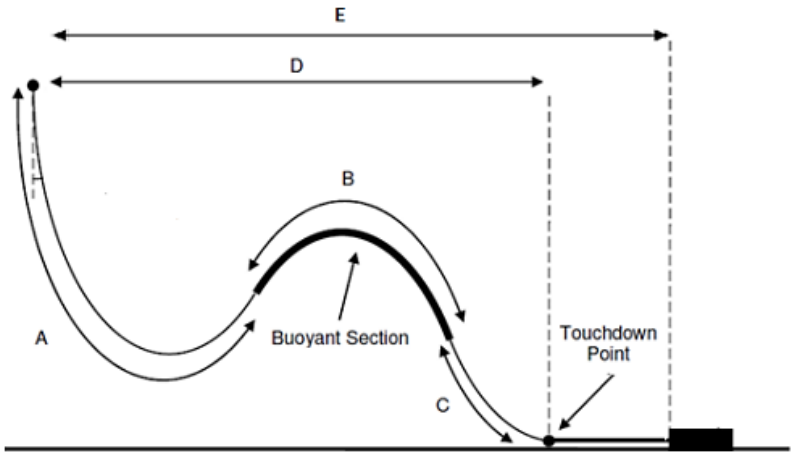

Figure 19: Dynamic cable lazy wave configuration sections.

7.3 Ancillary Equipment

To achieve the required dynamic cable configuration from the floating structure to the seabed, ancillary equipment must be used. For a lazy wave route, the ancillaries needed include a hang off system, bend stiffener, buoyancy modules and buoyancy ballasts, mechanical protection at the seabed touchdown point, and various equipment to secure the dynamic cable for connection to a static cable. Depending on the conditions and analysis, a tether system may be incorporated later in the design process to support the dynamic cable and ensure low stress and curvature at the touchdown point.

The ancillary equipment which will be used for a lazy wave configuration are described further below in Table 9, with relevant equipment shown in Figure 20.

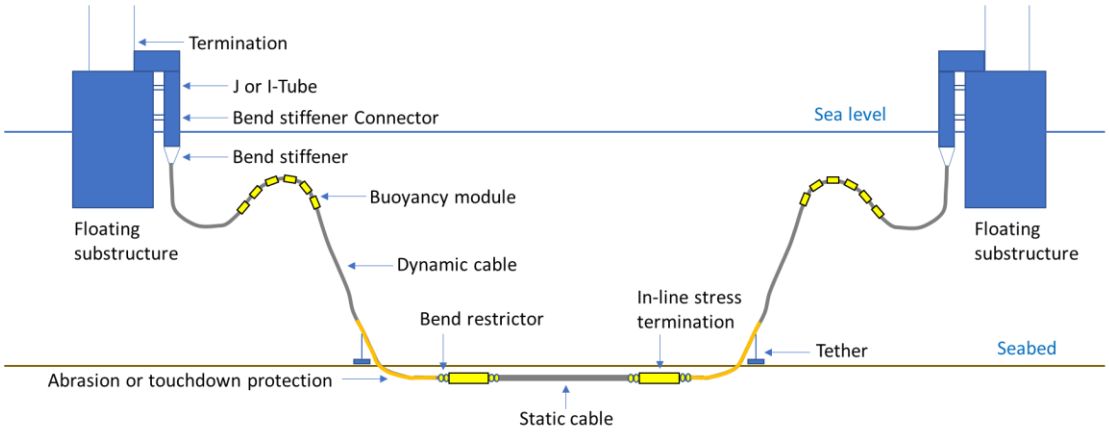

Figure 20: Lazy wave shape and ancillary equipment [21].

Table 9: Dynamic cable ancillary equipment descriptions.

Ancillary Equipment	Description
Hang-off System	To create a fixed connection between the cable and floating platform and to transfer tensile loads from dynamic cables to the platform. Double layered armour of the dynamic cable is terminated and allows the static sections (cores and optical components) to continue.
Bend Stiffener	Located below the floating platform and hang-off system, a long-tapered device to gradually increase bend stiffness of the dynamic cable before entering the hang-off system. Minimum bend radius must not be exceeded so dimensions must be sufficient to support this in extreme weather and sea conditions.
Buoyancy Modules	Attached to the cable near the mid-section (Section B in Figure 19) to give buoyancy to the cable creating the hog bend. The length of cable between the floating platform and touch down point is increased to allow sufficient length for platform offsets. Number of modules depends on the cable properties such as mass and bend radius, to relieve tension from the cable and to decouple the touch down point.
Ballast Modules	Used to balance the forces acting to destabilize the cable, the buoyancy (upward) and cable weight (downward) forces.
Mechanical Protection	Commonly used to prevent abrasive damage or impact from clashes and dropped objects and is usually a stiff mechanical sleeve covering a section of cable.
Hold Back Structure	Used to reduce the cable tension when resting on the seabed by an anchor clamping the cable at the touch down point to prepare the cable for seabed static cable connections.
Tether Clamp	Used if a tether wave configuration is implemented which reduces abrasive movements at the touchdown point. The clamped cable is connected to the tether which is anchored to the seabed and is used to stabilize the cable laterally and axially before connection at the touch down point.

7.4 Dynamic Cable Cross Section

Floating offshore wind farms currently deployed use cable ratings of either 33 kV (only small farms and demonstrators) or 66 kV, with future intention to increase these to 132 kV when higher farm capacity is designed.

The design of the cable cross section components depends on voltage rating, current level and mechanical stress. Generally, the dynamic cable will consist of three power cores, a fibre optical cable for data communication, core insulation and sheaths and tapes, filler material to reinforce the circular cross section shape, and layers of armour steel shielding designed to add strength and stiffness and protection to the conductor cores. The general cross-sectional configuration and representation of a dynamic cable is shown in Figure 21, and Figure 22 [21] [18].

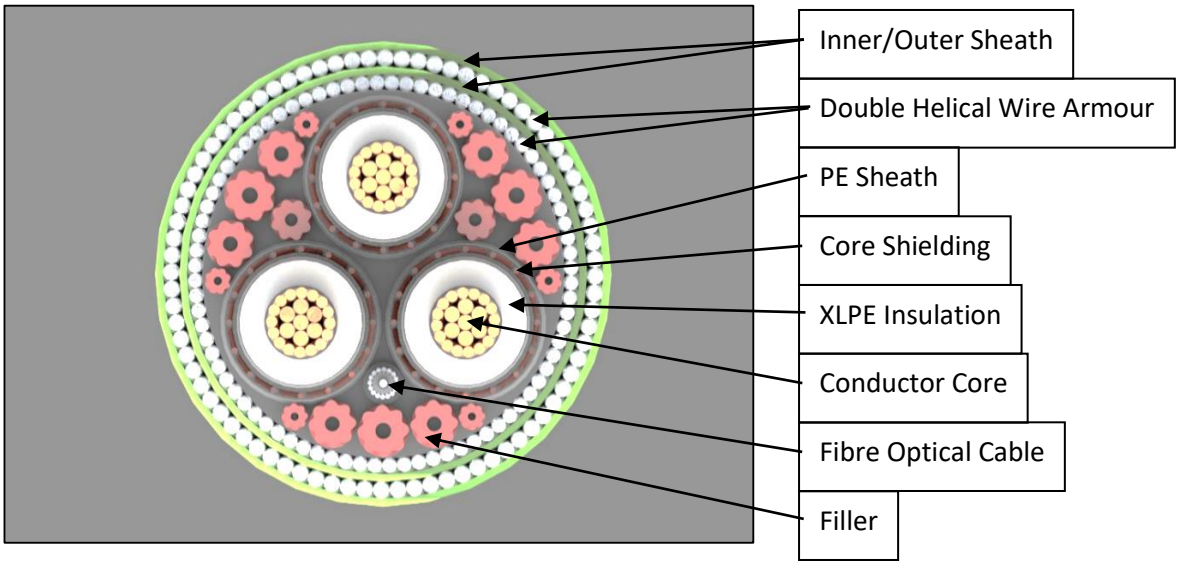

Figure 21: General cross section components of a dynamic cable [21].

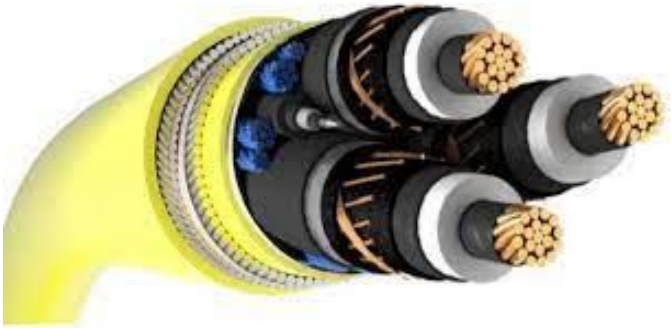

Figure 22: A dynamic cable representation [21].

8 ALTERNATING AND DIRECT CURRENT TRANSMISSION

8.1 Offshore Comparison of HVAC versus HVDC

8.1.1 Fundamental principles

This section describes the comparison between HVAC and HVDC and their suitability and necessary electrical infrastructure.

As offshore wind is expected to expand, connecting offshore wind farms to the National Grid is important while considering economic and environmental factors to increase efficiency. There are two alternatives for interconnecting wind farms, namely: HVAC and HVDC, however it must be stressed that HVDC is maturing, the transmission alternative is extremely costly.

As transmission decisions come to fruition for FOW considerations to use either HVAC or HVDC cables in a wind farm, the decision will be judged by distance and electrical loss through the cable. HVAC has an important limitation, the HVAC cables. This type of cable has a high capacitance per length, measured in micro-Farads per km (*μF/km*), further detail can be found in Appendix B and C. Therefore, in addition to the delivery of electrical current in HVAC cables, there is also a capacitive current. Resulting in long distance HVAC cables to require excessive reactive power, not a limitation factor found in HVDC transmission.

Currently, offshore wind projects are generally close to shore at distances of up to 40 km [22] and mostly use HVAC inter-array cables and export cables to shore. HVAC cables are mostly used for short distances whereas HVDC are more attractive for longer distances, so with wind farms being developed further from shore and floating (increasing the export cable distance), HVDC could be more widely used in the future.

New HVDC innovation and the benefits to HVDC transmission are now being considered for FOW, as HVDC is used to transmit electricity over longer distances to FOW farms greater than 50 kilometres (circa 50 – 80 km) offshore or between HVAC power systems of different and varying frequencies, as seen in Figure 23, showing the clear transition and/or expenditure crossovers and break even distances between the two HVs [23] [24]. In comparison, it shows that at longer distances, HVDC lines are more cost effective than HVAC. Transmitting power at long distances is certainly a challenge that must be overcome in FOW to consider a trade-off between efficiency and investment cost.

As the electrical power needs to be transmitted over long distances with OW developing further from shore, the main factor to account for is electrical loss from the line parameter during the HVAC transmission. To reduce power loss when transmission is over a long distance, increasing the transmission voltage can reduce the current while remaining at the rated power; hence export cables from offshore substation to the onshore substation is of higher voltage rating than the inter-array cabling offshore.

HVAC transmission is used when transmission voltages range from 33 kV to 275 kV; consisting of at least three conductor cores to carry three-phase electrical power.

HVDC is the transmission of higher voltage than HVAC, ranging between 100 kV to 800 kV requiring only two cables each one core design; hence could support the cost-effective argument for longer distance transmission with less power loss due to the higher voltages.

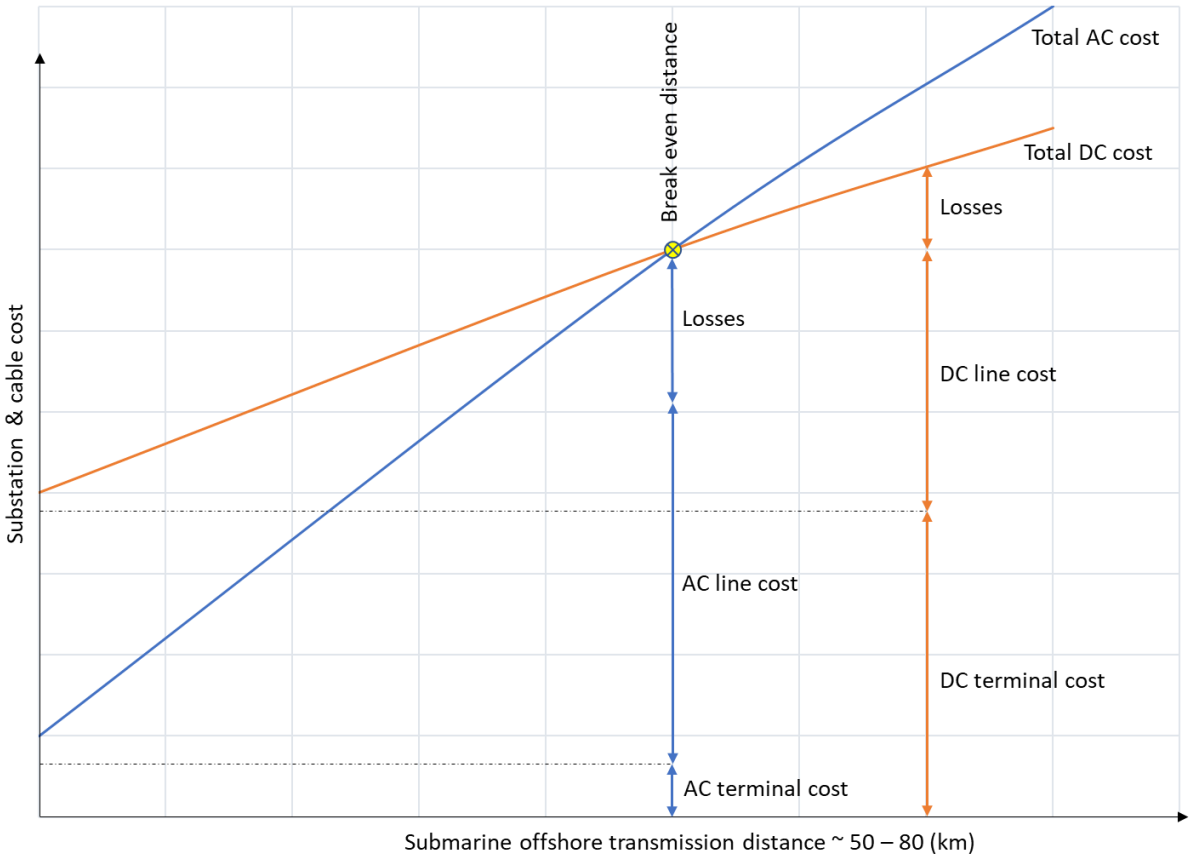

Figure 23: Cost trend comparison between HVAC and HVDC with increased distance from shore, break even distance to FOW farms >50 kilometres (circa 50 – 80 km).

To shape the argument further, the main differences between HVAC and HVDC must be considered as follows,

- HVAC requires a voltage transformation through a transformer (either step up and/or step down); However, going from AC-DC-AC still required transformers, the function of DC uses a rectifier and inverter to convert the transmission from AC to DC in converter station;
- HVAC is used mainly for shorter distances compared to HVDC used for long distances for higher power;
- Corona loss is higher for HVAC compared to HVDC;
- HVDC has no skin effect due to the uniform current density in the cores compared to an uneven current density in HVAC resulting in skin effect, meaning a larger core diameter is necessary;
- HVAC can cause interference when in close proximity to neighbouring lines;
- HVDC circuit breakers are more expensive and more complex than HVAC;
- HVAC is generally cheaper for power transmission than HVDC due to the large converters required for DC, however longer distances HVAC reactive power compensation can become very costly and therefore becomes more expensive to keep the system optimised.

8.1.2 HVDC technologies

For discussion purposes, HVDC transmission for a high-power alternative. Generally long-distance transmission has more advantages compared to HVAC, and so will be investigated further for connecting the OWF to the onshore substation. The two HVDC technologies available are Line-Commutated Converter (LCC-based) and Voltage Source Converter (VSC-based) HVDC, with the LCC-based HVDC more widely used globally, but more studies focusing on VSC-based HVDC for OWF grid integration. A general HVDC connection from OWF to main onshore grid, is shown in Figure 24.

New challenges face HVDC offshore, in the form of the carbon footprint that come with significant impacts in weight, space and investment costs. HVDC transmission efficiency for offshore projects could be more affordable by minimizing power losses in the system. As shown in Figure 24, a solution to HVDC would consist of three main components, that incorporate a rectifier (converter substation), two-core subsea HVDC cable, and an inverter (converter substation) either close offshore, or onshore. The HVDC subsea cables would address the HVAC high capacitance per kilometre effect, as discussed earlier.

For larger OWFs, HVDC collection systems may be the preferred choice in the future for FOW due to increased distances export cables need to travel. Therefore, lower power loss as the energy is not driven by frequency, and reduced cost due to the use of only two conductor cores in comparison to HVAC three core design. However, HVDC converter stations onshore are extremely expensive in comparison to conventional HVAC substations. However, the HVAC collection system is preferred in current offshore wind farm projects globally due to HVDC collection challenges including DC-DC converters and grid code compliance.

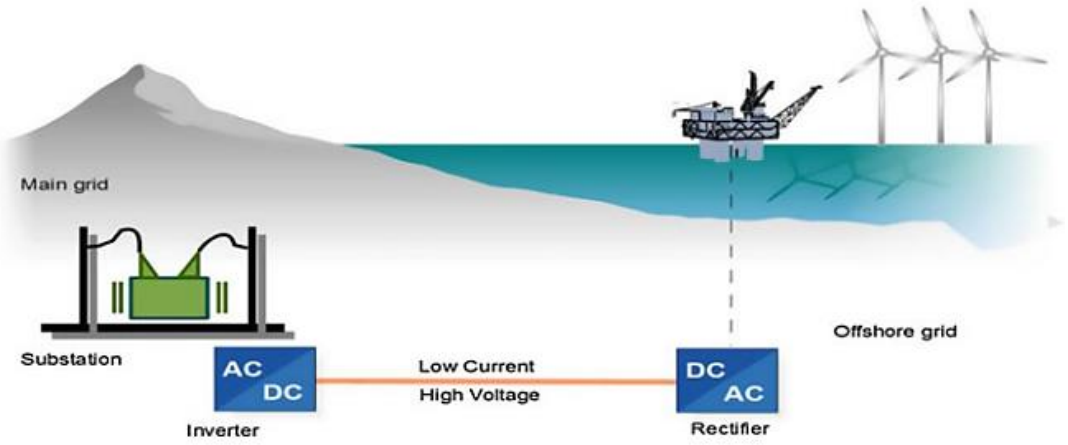

Figure 24: Schematic representation of possible HVDC transmission from offshore wind farm to onshore main grid [24].

8.1.3 Offshore grid configurations for HVAC and HVDC options

As show in Figure 25 (a), that by connecting the OWF through HVDC cables in an AC grid offshore concept connects the offshore grid and onshore substation with high voltage, low current cables. Instead of having the last stage of conversion to AC offshore, perhaps a solution would be to implement a DC grid offshore, as shown in Figure 25 (b). If HVDC were to be used in a project, it is essential for there to be adequate

converter stations to convert the power from an AC voltage to DC transmission offshore, then converter stations to convert from DC to AC again onshore for distribution around the National Grid [26].

In Figure 25, the permanent magnet synchronous generator (PMSG) would represent the HVAC wind turbine, as the turbine must be equipped with a power electronic converter. The reason for the power electronic converter (i.e., AC-DC-AC) is to control the rotational speed, and therefore, able to extract the maximum power from the available wind.

The most widely used HVDC converters globally, are LCC-based which uses the line voltage of an AC system for conversion, using uncontrolled thyristor switching devices that can be turned on. The switching frequency must match the line frequency, namely between 50 & 60 Hz. They are suitable for bulk power transmission, and cheaper than other systems with simple control and fewer losses (previously discussed). However, are large structures which increase the footprint of an offshore platform.

The other HVDC technology widely used, is the VSC-based transmission converters, which use Insulate-Gate Bipolar Gate Transistors (IGBT) in series [27], having several advantages over LCC-based transmission. The operation can be performed without the need for an external voltage source, compared to LCC-based which requires an AC voltage to operate. Due to the IGBTs there is lower distortion from harmonics in VSC-based systems. However, VSCs are more expensive and achieve greater losses. A comparison between LCC-based and VSC-based HVDC converters, is shown in Table 10. Company ABB use this VSC technology, that enable the offshore converter to transmit all the wind farm generated power to the onshore converter, while maintaining a stable voltage and stable frequency [24].

As discussed previously, it was stated that there are pros and cons to either HVAC compared to HVDC, however, a HVDC grid could be a more efficient solution since it increases the exploitation of subsea cables offshore. In HVAC systems, related to their respective sinusoidal waveforms, subsea cables must carry both active and reactive power. Reactive power increases current and consequently transmission losses, in HVAC systems. The total losses are a combination of transmission losses and the efficiency of the converter stations.

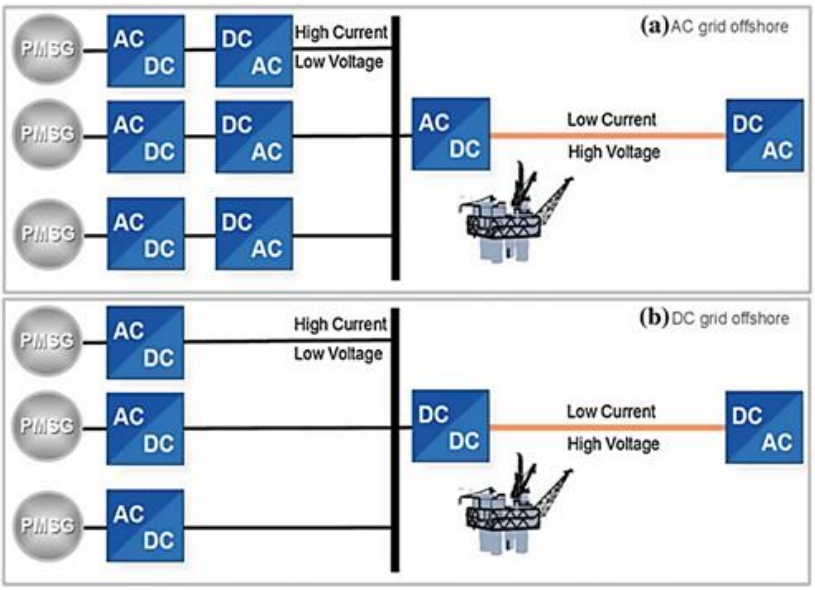

Figure 25: Possible schematics for offshore grid configurations. Top a) AC offshore grid schematic. Bottom b) DC offshore grid schematic [25].

Two alternate HVDC concepts, are shown in Figure 26, (a) in parallel, and (b) in series [25]. In a DC grid for a parallel connection, there could be one, or several stages of DC/DC conversion, emulating conventional AC grids. If turbines were to be connected in series, both the offshore grid and the transmission have the same low current in this configuration, as seen in Figure 26 (b). That would increase the overall efficiency and have a high voltage to the system. Eliminating the centralised DC converter station, reducing the cost, and reliability is not compromised over the same transmission distance, as per the parallel connection.

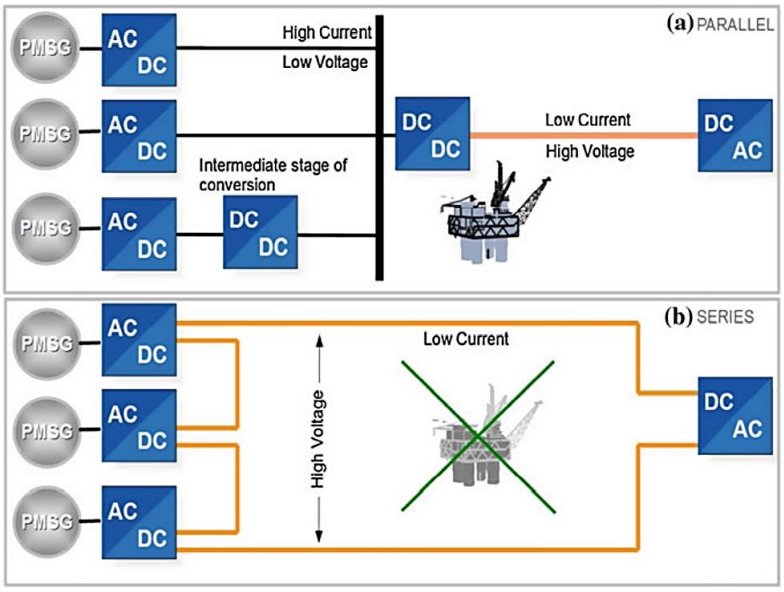

Figure 26: Possible schematics for DC grid configurations. Top a) Parallel DC grid connection. Bottom b) Series DC grid connection [25].

Table 10: LCC-based and VSC-based HVDC converter comparison [26]

	VSC-Based HVDC	LCC-Based HVDC
Switch Device	IGBT	Thyristor
Commutation	Self-Commutated (up to a few kHz)	Line Dependent (50-60 Hz)
Station Power Loss	~1%	0.6-0.8%
Power-flow Reversal Mechanism	Current direction reversal	Voltage polarity reversal
Network Strength Dependency	Independent	Dependent
Converter Station Footprint	Smaller	Larger
Inherent VAR Consumption	None	50-60% of rated MW
Reactive/filtering Equipment	High	Low
Inherent VAR control	Yes	No
Inherent AC Grid Black Start	Yes	No
AC & DC Side Harmonic Level	Lower	Higher
Applications	Offshore projects	High-power, long distance
Multi-Terminal HVDC Suitability	Highly suitable	Limited
Station Cost	Higher	Lower

In summary, inter-array cabling at the offshore wind farm location are suitable for HVAC transmission due to the short distances and FOWT current rating. Whereas the export cable from offshore wind farm to shore is more suitable to be HVDC, due to the long distances and higher power capacity needed, to carry the power from an entire wind farm. HVDC is more suitable because of the decrease in electrical power losses. However, require adequate conversion technologies to convert the transmission from AC to DC and vice versa when onshore. In this section, the most common conversion technologies have been explored in detail with their advantages and disadvantages through comparison.

9 CONCLUSION AND RECOMMENDATIONS

9.1 Conclusion

From earlier considerations floating offshore wind should be integrated into the South West and South Wales transmission network. To consider both technically and spatially, how the distribution of energy from both short and long-term floating wind deployments can be best delivered in the Celtic Sea. The types of major infrastructure, alternative solutions, scenarios, models, and investment required for integrating floating offshore wind developments into the Celtic Sea energy network, are discussed. Currently, in the Celtic Sea there are no offshore cable routes to connect offshore wind farms, nor to connect South Wales to South West England directly without having to transmit through the National Grid onshore infrastructure. This research has brought to the forefront the importance of the electrical infrastructure that must accompany floating offshore wind to the South West region.

Around South Wales and South West England, there are six 400 kV substations onshore, namely: Pembroke, Swansea North, Rhigos, Cilfynydd, Hinkley Point and Alverdiscott, as potential connecting points to floating offshore wind. The Pembroke substation is located very close to the Celtic Sea and is a focal point for offshore-onshore connection, however, it will not be enough to cope with the additional generations from future offshore wind projects.

The Holistic Network Design developed by the National Grid is a design to provide onshore and offshore recommendations to facilitate the UK Governments ambition. However, it assumes that the Celtic Sea will facilitate just 1 GW of floating wind, but in reality, the Celtic Sea has the potential for much more capacity. Therefore, this oversite will need to be addressed to meet the ambitions. Onshore works to facilitate the Holistic Network Design include a substation for new connections at Pembroke, uprating circuits and installing flow control devices to manage power flow. Alternative designs recommended by the National Grid, using high-voltage direct current links between one of the floating offshore wind farms to the substation at Alverdiscott, should be reconsidered. Further alternative scenarios have also been explored by ORE Catapult and Celtic Sea Power feeding evidence back to the National Grid which assumes a greater, more realistic capacity in the Celtic Sea by 2030.

The distribution of energy within offshore wind farms requires suitable array configuration design with feasible dynamic inter-array cables, to withstand constant dynamic loading and ancillary equipment necessary. Thereby, the energy generated within the wind farm can be collected at an offshore substation and then exported to an onshore infrastructure. The inter-array cable routing depends on the array configuration of wind farms. By using one or more of the following array topologies, i.e., tapered radial strings (daisy-chain), tee's (branches), tapered ring loops, and redundant rings this can be achieved. Each topology has been used on UK offshore projects of bottom fixed wind farms, and potential considerations for floating offshore wind farms are being considered from lessons learned. The decisions would be subject to cost analysis, site conditions and developer risk and/or availability opinions.

Research has found that there are three main configurations when connecting offshore wind turbines in appropriate strings. These are daisy chain, fishbone, and star configurations, with various derivatives to suit the application. The daisy chain configuration is most commonly used; however, it raises an issue that the rest of string must be shut-off until the failure has been fixed once it happens to the turbine in a string.

Therefore, the importance of taking redundancy into account with offsets for all offshore wind farm developments is emphasized.

Array cable voltage ratings for floating offshore wind farms are either 33 kV or 66 kV, with future intention to increase these voltages to 132 kV, when higher farm capacity are designed or higher power wind turbines are considered. Copper and aluminium are the most common materials for array cable cores, as each has their advantages and disadvantage. For floating offshore wind, array cables with copper core are deployed for initial analysis, and cross-linked polyethylene is widely used as electrical insulation in these cables, especially for medium to high and extra-high voltage power cables operating at the maximum core temperature of 90°C.

From the examples based on a 495 MW floating wind farm of 15 MW turbines, developers would anticipate cost reduction regarding cable size. The key could be to reduce the cross-section area while moving away from the substation (collection point). For a 66 kV array cable layout, there would be three cross-section areas to reduce costs, namely, 800 mm^2, 630 mm^2 and 240 mm^2. For a 132 kV subsea dynamic cables layout, there would be another three sets with reduced cross-section areas, namely, 630 mm^2, 500 mm^2 and 300 mm^2, all based on conventional layout configurations.

Substations sit commonly between transmission system and collection system through which the power from each turbine is collected and connected to the offshore substation. The primary function of the substation is to accommodate the high-voltage and medium-voltage electrical components required to transmit the power collected from offshore turbines. This high-voltage power is transmitted through subsea export cables from offshore to shore and fed into the electrical grid by the onshore substation. Reliability and redundancy must therefore be considered during the substation design phase. This includes electrical safety from switchgears and circuit breakers to ensure that failure can be disconnected if it occurs. Although offshore wind farms are all alternating current inter-array collection systems, the direct current collection systems have been explored in various concepts.

Dynamic cables are designed to be flexible to withstand mechanical loading and provide protection to the inner components from high stresses. These cables differ from the subsea static cables that are used on bottom fixed offshore wind turbines. A dynamic cable system has been explored in terms of configuration and route from the floating structure to the seabed. Lazy wave or tethered wave configuration can be achieved with appropriate ancillary equipment. Despite the recent development and increased interest in the floating offshore wind industry, there are no official standards that can be directly applied to dynamic cable design, analysis, or testing.

There are two alternatives for wind farm energy transmission to shore, i.e., high-voltage alternating current and high-voltage direct current. It must be stressed that high-voltage direct current is maturing, however, this alternative is still extremely costly. The decision to use either type of transmissions will be judged based on distance and conductor losses in the cable. High-voltage direct current can be used to transmit electricity over longer distances to floating offshore wind farms that are greater than 50 kilometres offshore. To conclude, larger offshore wind farms might opt to use high-voltage direct current collection systems as the preferred choice in the future for floating offshore wind.

9.2 Recommendations

A follow-on study could look at a holistic view of electrical infrastructure, or potential technical bottlenecks into turbine and transmission systems. Added to the follow-up, it could involve modular electrical systems for easier replacements and more considerations at the design phase for offshore wind farm redundancy.

In terms of the future of the Celtic Sea transmission network, it is recommended to consider potential generation than previously stated in the Holistic Network Design in preparation for the Detailed Network Design. It is also desired to use all the available electrical infrastructure around the Celtic Sea onshore area, rather than connecting to Pembroke's only onshore substation.

In terms of the dynamic array cable and the static inter-array cabling for offshore wind, it is recommended to consider site specific design for future projects in terms of the socioeconomics, industry collaboration, standardisation, and environmental factors. The sizing of cabling must be thoroughly investigated incorporating configurations and topology, and future project redundancy which may use the same cables.

It is recommended to propose a functioning floating offshore wind transmission system in the Celtic Sea. Through functional systems, dynamic array cable and export cable manufacturers can standardise fatigue and failure rate analysis, re-risking the sector for future developers. In addition, a functioning floating offshore wind farm could provide combined efficiency of the various wind power systems through a combination of aerodynamic, mechanical, and electrical efficiencies in the Celtic Sea.

Finally, cabling must be designed for high-voltage alternating current or high-voltage direct current, and it is recommended that specific research is published regarding high-voltage direct current transmission as floating offshore wind farms are to be located further distances from shore.

10 REFERENCE LIST

[1] APPG, “Ten point plan for climate and nature,” APPG Environment Green Alliance (UK Secretariat), London, 2022.

[2] BEIS, “British energy security strategy-Policy Paper,” 2022. [Online]. Available: https://www.gov.uk/government/publications/british-energy-security-strategy/british-energy-security-strategy. [Accessed 31 October 2022].

[3] nationalgridESO, “South Wales and South England Boundaries,” 2021. [Online]. Available: https://www.nationalgrideso.com/research-publications/etys/electricity-transmission-network-requirements/south-wales-england-boundaries. [Accessed November 2022].

[4] NationalGrid, “Holistic Network Design,” February 2022. [Online]. [Accessed November 2022].

[5] T. C. Estate, “Celtic Sea Floating Wind: October 2022 update,” October 2022. [Online]. Available: https://www.thecrownestate.co.uk/en-gb/what-we-do/on-the-seabed/floating-offshore-wind/celtic-sea-floating-wind-october-2022-update/. [Accessed November 2022].

[6] NGESO, “National Grid,” 2023. [Online]. Available: www.nationalgrid.com. [Accessed 27 January 2023].

[7] J. Hardisty, The British Seas: an introduction to the oceanography and resources of the north-west European continental shelf, Taylor & Francis, 1990.

[8] Regen, “Floating offshore wind opportunity study for the Heart of the South West,” 13 May 2022. [Online]. Available: https://www.regen.co.uk/publications/floating-offshore-wind-opportunity-in-the-celtic-sea/. [Accessed November 2022].

[9] O. Catapult, “Offshore Wind and Grid in Wales in Collaboration with Welsh Government,” September 2021. [Online]. Available: https://gov.wales/sites/default/files/publications/2021-09/grid-report-non-technical-summary.pdf. [Accessed November 2022].

[10] P. Government, “Milford Haven: Energy Kingdom,” 2022. [Online]. Available: https://www.pembrokeshire.gov.uk/mh2-energy-kingdom/mh2-education-resources. [Accessed November 2022].

[11] C. S. Power, “Cornwall Floating Offshore Wind Accelerator, Pembrokeshire Demonstration Zone,” Cornwall Council Company, 2022. [Online]. Available: https://celticseapower.co.uk/our-projects-5/. [Accessed 29 November 2022].

[12] Vestas, “V236-15.0 MW,” 2022. [Online]. Available: https://www.vestas.com/en/products/offshore/V236-15MW/V236-15MW. [Accessed 05 November 2022].

[13] O. Catapult, “Floating Offshore Wind - Dynamic Cables ORE/20/89 Design Requirements,” ORE Catapult, 2021.

[14] G. W. Atlas, “Danmarks Tekniske Universitet, Technical University of Denmark,” Global Solar Atlas, Energy Database, Powered by WAsP, 2022. [Online]. Available: https://globalwindatlas.info/en. [Accessed 03 December 2022].

[15] L. Team, “Linquip Technews: HVDC vs HVAC Transmission Systems - Difference between them,” 11 Feb 2021. [Online]. Available: https://www.linquip.com/blog/hvdc-vs-hvac-transmission-systems/#:~:text=HVDC%20stands%20for%20High%20Voltage,energy%20transmission%20over%20long

%20distances. [Accessed Oct 2022].

[16] CIGRE, “Power cable rating examples for calculation tool verification,” in *B1 Technical Brochure Insulated Cables 880*, CIGRE, 2022.

[17] Cigre, “Insulated Cables - Power cable rating examples for calculation tool verification (B1 Reference 880),” Cigre, 2022.

[18] ABB, “XLPE Submarine Cable Systems (REV5); Attachment to XLPE Land Cable Systems - User's Guide,” ABB’s high voltage cable unit, Sweden, 2010.

[19] R. S. a. J. L. Padmavathi Lakshmanan, “Electrical Collection Systems for Offshore Wind Farms: A Review,” *CSEE JOURNAL OF POWER AND ENERGY SYSTEMS,* vol. 7, no. 5, pp. 1078-1092, 2021.

[20] Corewind, “D3.1 Review of the state of the ART OF DYNAMIC CABLE SYSTEM DESIGN,” 2020.

[21] J. Cables, Artist, *Lazy wave dynamic cable configuration with ancillary equipment.* [Art]. 2021.

[22] H. Diaz and C. Guedes Soares, “Review of the current status, technology and future trends of offshore wind farms,” *Ocean Engineering, Elsevier,* vol. 209, no. https://doi.org/10.1016/j. oceaneng.2020.107381, pp. 1-21, 2020.

[23] E. Technology, “Electrical Technology,” 2020. [Online]. Available: https://www.electricaltechnology. org/. [Accessed 14 November 2022].

[24] ABB, “HVDC technology for offshore wind is maturing,” 2018. [Online]. Available: https://new.abb. com/news/detail/8270/hvdc-technology-for-offshore-wind-is-maturing #:~:text=The%20most% 20straightforward%20HVDC%20offshore%20wind%20farm%20configuration, HVDC%20connection %20schemes%20for%20offshore%20wind%3A%20Point-to-point%20connection. [Accessed 14 November 2022].

[25] A. G. a. G. B. Raymundo Enrique Torres Olguin, “HVDC Transmission for Offshore Wind,”Large Scale Renewable Power Generation, Springer, Singapore, 2014.

[26] P. M. Mircea Ardelean, “HVDC submarine power cables in the world,” Joint Research Center, 2015.

[27] S. B. O. E. G. A. C. M. Abdulrahman Alassi, “HVDC Transmission: Technology Review, Market Trends and Future Outlook,” Renewable and Sustainable Energy Reviews 112, 2019.

[28] CIGRE, “B1 Technical Brochure Insulated Cables,” CIGRE, 2022.

[29] R. Taylor, “Design Guide for Drag Embedment Anchors,” Defence Technical Information Centre, 1984.

[30] LIFES50+, “Deliverable D7.2 Design Basis,” 2015.

[31] First Marine Solutions, “Floating Offshore Wind Mooring & Anchoring Systems - Design Requirements,” ORE Catapult, 2021.

[32] LIFES50+, “D4.1 Simple numerical models for upscaled design,” 2020.

[33] Orcina, “OrcaFlex Documentation - Version 11.2a”.

[34] G. Ji, “On-Bottom Stability of Umbilicals and Power Cables for Offshore Wind Applications,” *Energies,* vol. 12, 2019.

[35] A. Gray, “Initial Predictions for Offshore Wind Farms in the ScotWind Leasing Round,”ORE Catapult, 2021.

[36] ITP Energised, “Floating Offshore Wind Constraint Mapping in the Celtic Sea,” ORE Catapult, 2020.

[37] PhysE Ltd, “Wave Mapping in UK Waters - RR392,” HSE, 2005.

[38] HSE, “Environmental Considerations - Offshore Technology Report 2001/010,” 2001.

[39] B. Jonkman, “Turbsim User's Guide version 1.50,” NREL.

[40] O. C. CoE, “Floating Offshore Wind - Dynamic Cable ORE/20/89,” ORE Catapult, 2021.

[41] O. R. E. Catapult, “Offshore wind and grid in Wales in collaboration with Welsh Government,” Celtic Sea Cluster, South Wales, 2021.

[42] 4COffshore, “Offshore Transmission and Cables,” TGS Company, Lowestoft, 2023.

APPENDIX A. XLPE CABLE AND CABLE SYSTEM STANDARDS

ABB´s XLPE cable systems are designed to meet requirements in international and/or national standards. Some of these are listed below.

IEC

XLPE cable systems specified according to IEC (International Electrotechnical Commission) are among many other standards accepted. IEC standards are considered to express an international consensus of opinion. Some frequently used standards are:

IEC 60228

Conductors of insulated cables.

IEC 60287

Electric cables - Calculation of the current rating.

IEC 60332

Tests on electric cables under fire conditions.

IEC 60502

Power cables with extruded insulation and their accessories for rated voltage from 1 kV (Um=1,2 kV) up to 30 kV (Um=36 kV).

IEC 60840

Power cables with extruded insulation and their accessories for rated voltage above 30 kV (Um=36 kV) up to 150 kV (Um=170 kV). Test methods and requirements.

IEC 60853

Calculation of the cyclic and emergency current rating of cables.

IEC 61443

Short-circuit temperature limits of electric cables with rated voltages above 30 kV (Um=36 kV).

IEC 62067

Power cables with extruded insulation and their accessories for rated voltage above 150 kV (Um=170 kV) up to 500 kV (Um=550 kV). Test methods and requirements

CENELEC

In Europe, cable standards are issued by CENELEC. (European Committee for Electrotechnical Standardization.) They are as a rule implementations of the IEC specifications. Special features in design may occur depending on national conditions.

HD 620

Distribution cables with extruded insulation for rated voltages from 3.6/6 (7.2) kV up to and including 20.8/36 (42) kV.

HD 632

Power cables with extruded insulation and their accessories for rated voltage above 36 kV (Um=42 kV) up to 150 kV (Um=170 kV). Part 1- General test requirements. Part 1 is based on IEC 60840, and follows that standard closely. HD 632 is completed with a number of parts and subsections for different cables intended to be used under special conditions which can vary nationally in Europe.

ICEA

For North America cables are often specified according to ICEA (Insulated Cable Engineers Association, Inc.).

S-97-682

Standard for utility shielded power cables rated 5-46 kV.

S-108-720

Standard for extruded insulated power cables rated above 46 through 345 kV.

ISO Standards

ABB has well-developed systems for quality and environmental management which put the needs and wishes of the customer first. Our systems comply with the requirements of ISO 9001 and ISO 14001 and are certified by Bureau Veritas Quality International

APPENDIX B. XLPE CABLE SYSTEMS FORMULAE

1. Formulae for capacitance

$$C = \frac{\varepsilon_r}{18 \cdot ln\,(\frac{r_o}{r_i})}[\mu F/km]$$

ε = relative permittivity of the insulation
r_o = external radius of the insulation (mm)
r_i = radius of conductor, including screen (mm)
ε_r XLPE = 2.5 (Value from IEC 60287)

2. Formula for dielectric losses

$$W = \frac{U^2}{3} 2\pi f \cdot C \cdot \tan(\delta)\,[W/km]$$

U = rated voltage (kV)
f = frequency (Hz)
C = capacitance $(\mu F/km)$
tan δ = loss angle

3. Formula for inductance

$$L = 0.05 + 0.2 \cdot \ln \frac{K \cdot s}{r_c}[mH/km]$$

trefoil formation: K = 1
flat formation: K = 1.26
s = distance between conductor axes (mm)
r_c = conductor radius (mm)

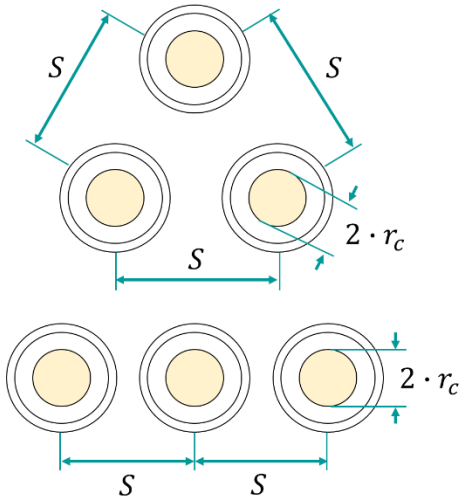

4. Formula for inductive reactance

$$X = 2\pi f \cdot \frac{L}{1000}[\Omega/km]$$

f = frequency (Hz)
L = inductance (mH/km)

5. Formula for electric stress

Conductor screen: $E_{max} = \frac{U_O}{r_i \ln(\frac{r_o}{r_i})}\ [kV/mm]$

Insulation screen: $E_{min} = \frac{U_O}{r_o \ln(\frac{r_o}{r_i})}\ [kV/mm]$

r_i = radius of conductor screen
r_o = radius of XLPE insulation
U_O = voltage across insulation

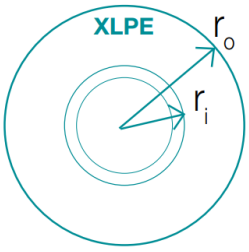

6. Formula for maximum short circuit currents

$$I_{sh} = \frac{I_1}{\sqrt{t_{sh}}}[kA]$$

I_{sh}= short-circuit current during time t_{sh}
I_1 = short-circuit current rating during 1 second. See the 1 second value in tables 14 for the conductor and in table 15 for the metallic screen from ABB XLPE land cable system user's guide.
t_{sh} = short-circuit duration (sec)
For XLPE insulated conductors the maximum allowable short circuit temperature is 250 °C.

7. Formula for calculation of dynamic forces between two conductors

$$F = \frac{0.2}{S} \cdot I_{peak}^2[\mathrm{N/m}]$$

I_{peak} = 2.5 I_{sh} [kA]
I_{sh}= short-circuit current [kA] RMS
S = centre to centre spacing between conductors [m]
F = maximum force [N/m]

APPENDIX C. XLPE CABLE SYSTEM WORKED EXAMPLES

This example uses formulae from Appendix B, and the data from the cable used in the Appendix E worked example (CSA @ 630 mm^2).

1. Formula for capacitance

$$C = \frac{\varepsilon_r}{18 \cdot \ln\left(\frac{r_o}{r_i}\right)} [\mu F/km]$$

$$C = \frac{(2.5)}{18 \cdot ln\left(\frac{24.25}{16.25}\right)} [\mu F/km]$$

$$C = 0.346[\mu F/km]$$

2. Formula for dielectric losses

$$W = \frac{U^2}{3} 2\pi f \cdot C \cdot \tan(\delta) [W/km]$$

$$W = \frac{(30)^2}{3} 2\pi(50) \cdot (0.346) \cdot (0.004)[W/km]$$

$$W = 130.438[W/km]$$

3. Formula for inductance

$$L = 0.05 + 0.2 \cdot \ln\frac{K \cdot s}{r_c} [mH/km]$$

$$L = 0.05 + 0.2 \cdot \ln\frac{(1) \cdot (52.5)}{(30)} [mH/km]$$

$$L = 0.1619[mH/km]$$

4. Formula for inductive reactance

$$X = 2\pi f \cdot \frac{L}{1000} [\Omega/km]$$

$$X = 2\pi(50) \cdot \frac{0.1619}{1000} [\Omega/km]$$

$$X = 0.0508[\Omega/km]$$

5. Formula for electric stress

Conductor screen: $E_{max} = \frac{U_O}{r_i \ln\left(\frac{r_o}{r_i}\right)} [kV/mm]$

Conductor screen: $E_{max} = \frac{(30)}{(16.25)\ln\left(\frac{24.25}{16.25}\right)} [kV/mm]$

$$E_{max} = 4.6116[kV/mm]$$

Insulation screen: $E_{min} = \frac{U_O}{r_o \ln\left(\frac{r_o}{r_i}\right)} [kV/mm]$

Insulation screen: $E_{min} = \frac{(30)}{(24.25)\ln\left(\frac{24.25}{16.25}\right)} [kV/mm]$

$$E_{min} = 3.090[kV/mm]$$

6. Formula for maximum short circuit currents

$$I_{sh} = \frac{I_1}{\sqrt{t_{sh}}} [kA]$$

$$I_{sh} = \frac{90.1}{\sqrt{1}} [kA]$$

$$I_{sh} = 90.1[kA]$$

7. Formula for calculation of dynamic forces between two conductors

$$F = \frac{0.2}{s} \cdot I_{peak}^2 [\mathrm{N/m}]$$

$$F = \frac{0.2}{52.5} \cdot (2.5 \cdot 90.1)^2 [\mathrm{N/m}]$$

$$F = 193.2857[\mathrm{N/m}]$$

APPENDIX D. ELECTRICAL LOSS SEQUENTIAL CALCULATION STEPS

1. Calculation of lay-up core factor

Parameter	Reference
Lay length of core stranding, L_{core} (mm)	Cable datasheet
Core diameter, D_e (mm)	Cable datasheet

$$f_{layup} = \sqrt{1 + \left[\frac{1.29\pi D_e}{L_{core}}\right]^2}$$

2. Calculation of conductor AC resistance at operation temperature

Parameter	Reference
Conductor DC resistance at 20°C, R_0 (Ω/m)	Cable datasheet
External diameter of conductor, d_c (mm)	Cable datasheet
Conductor material	Cable datasheet
Type of conductor	Cable datasheet
Skin effect factor used for calculating x_s, k_s	
Proximity effect factor used for calculating x_p, k_s	
Temperature coefficient per Kelvin at 20°C, α_{20} (K^{-1})	
Maximum operating temperature of conductor, θ (°C)	Cable datasheet
Axial separation of conductors, s (mm)	Cable datasheet
System frequency, f (Hz)	System design

$$R' = R_o[1 + \alpha_{20}(\theta - 20)]$$

$$x_s^2 = \frac{8\pi f}{R'} 10^{-7} k_s$$

$$y_s = \frac{x_s^4}{192 + 0.8x_s^4}$$

$$x_p^2 = \frac{8\pi f}{R'} 10^{-7} k_p$$

$$y_p = \frac{x_s^4}{192 + 0.8x_s^4}\left(\frac{d_c}{s}\right)^2\left[0.312\left(\frac{d_c}{s}\right)^2 + \frac{1.18}{\frac{x_s^4}{192 + 0.8x_s^4} + 0.27}\right]$$

$$R = R'\left(1 + 1.5(y_s + y_p)\right)$$

3. Dielectric losses

Parameter	Reference

Diameter over insulation, D_i (mm)	Cable datasheet
External diameter of conductor including screen, d_c (mm)	Cable datasheet
Relative permittivity of insulation, ε	
Loss factor for the insulation, *tanδ*	
Voltage to earth, U_0 (V)	System design
System frequency, *f* (Hz)	System design
Capacitance of each core, *C* (F/m)	Calculate
Angular frequency of system, ω	Calculate
Dielectric loss per unit length per phase, W_d (W/m)	Calculate

$$C_{core} = \frac{\varepsilon}{18 \ln\left(\frac{D_i}{d_c}\right)} 10^{-9}$$

$$C = C_{core} f_{layup}$$

$$\omega = 2\pi f$$

$$W_d = \omega C U_o^2 tan\delta$$

4. Sheath loss factor calculation

Parameter	Reference
AC resistance of sheath at 20°C, R_{SO} (Ω/m)	Calculated
Mean diameter of the sheath, *d* (mm)	Cable datasheet
Cross sectional area of the metallic sheath, A_{PB} (mm²)	Calculated
Sheath resistivity at 20°C, ρ_{sh} (Ωm)	
Sheath temperature coefficient at 20°C per Kelvin, α_{20}	
Distance between conductor axes, S (mm)	System design
System frequency, f (Hz)	System design
AC resistance of conductor at operating temp, R (Ω/m)	Calculated
Calculation of the cross-sectional area of the sheath	
Maximum operating temperature of the cable sheath, to be determined iterative, θ_{sc} (°C)	
Resistance of sheath at operating temperature, R_s (Ω/m)	
Reactance per unit length of sheath, X (Ω/m)	
Loss factor circulating losses for sheath, λ_1'	
Loss factor for eddy current losses λ_1''	
Loss factor of the sheath λ_1	

$$A_{PB} = \pi t_{sh}(d + t_{sh})$$

$$R_{so\_core} = \frac{\rho_{sh}}{A_{PB}}$$

$$R_{so} = R_{so\_core} f_{layup}$$

$$\theta_{sc} = \theta - (I^2R + 0.5W_d)T_1$$

$$R_s = R_{so}[1 + \alpha_{20}(\theta_{sc} - 20)]$$

$$d = (D_{sh} - t_{sh})$$

$$X_{1\_core} = 2\omega 10^{-7} \ln\left(\frac{2s}{D_{sh} + t_{sh}}\right)$$

$$X_1 = X_{1\_core} f_{layup}$$

$$\gamma_1' = \frac{R_S}{R} \frac{1.5}{1 + \left(\frac{R_S}{X}\right)^2}$$

$$m = \frac{\omega}{R_s} 10^{-7}$$

$$\gamma_0 = 3\left(\frac{m^2}{1 + m^2}\right)\left(\frac{d}{2s}\right)^2$$

$$\Delta_1 = (1.14m^{2.45} + 0.33)\left(\frac{d}{2s}\right)^{0.92m+1.66} \qquad \Delta_2 = 0$$

$$\beta_1 = \sqrt{\frac{4\pi\omega}{10^7 \rho_s(1 + \alpha_s(\theta_s - 20))}}$$

$$g_s = 1 + \left(\frac{t_s}{D_s}\right)^{1.74} (\beta_1 D_s 10^{-3} - 1.6)$$

$$\gamma_1'' = \frac{R_s}{R}\left[g_s\gamma_0(1 + \Delta_1 + \Delta_2) + \frac{(\beta_1 t_s)^4}{12x10^{12}}\right]$$

$$M = N = \frac{R_{s_{PB}}}{X_{core}}$$

$$F = \frac{4M^2N^2 + (M + N)^2}{4(M^2 + 1)(N^2 + 1)}$$

$$\gamma_1 = \gamma_1' + F\gamma_1''$$

5. Armour loss factor calculation

Parameter	Reference
AC resistance of sheath at 20°C, R_{A0} (Ω/m)	Calculated
Mean diameter of the armour, d_A (mm)	Cable datasheet
Number of armour wires, n_1	Cable datasheet
Diameter of armour wires, d_f (mm)	Cable datasheet
Cross sectional area of the armour, A (mm²)	Calculated
Lay length of armour, $laylength_{arm}$ (mm)	Cable datasheet

Increment factor for estimation of the AC resistance of the armour based on the DC armour resistance, *K*	Calculated
Armour resistivity at 20°C, ρ_a (Ωm)	
Armour temperature coefficient at 20°C per Kelvin, α_{arm}	
Distance between conductor axes/Diameter over single core, S (mm)	Cable datasheet
Diameter over assembled three cores, D_{cable} (mm)	Cable datasheet
System frequency, f (Hz)	System design
AC resistance of conductor at operating temp, R (Ω/m)	Calculated
Calculation of the cross-sectional area of the armour	
Ratio of length of wires to length of cable, *S/L*	
Maximum operating temperature of the cable armour, to be determined iterative, θ_{arm} (°C)	
Calculation of value c, the distance between axis of conductors and axis of cable for three-cores, *c* (mm)	
Resistance of armour at operating temperature, R_{arm} (Ω/m)	
Loss factor of the armour λ_2	

$$A = n_1 \pi \left(\frac{d_f}{2}\right)^2$$

$$f_{layup\_armour} = \frac{S}{L} = \sqrt{1 + \left(\frac{\pi d_A}{laylength_{arm}}\right)^2}$$

$$R_{Ao}^* = \frac{\rho_a}{A}$$

$$R_{Ao} = kR_{Ao}^* f_{layup\_armour}$$

$$\theta_{arm} = \theta - (I^2R + 0.5W_d)T_1 - (I^2R(1+\lambda_1) + W_d)nT_2$$

$$R_A = R_{Ao}[1 + \alpha_{arm}(\theta_{arm} - 20)]$$

$$c = \frac{D_{cable}}{2} - \frac{S}{2}$$

$$\gamma_2 = 1.23\frac{R_A}{R}\left(\frac{2c}{d_A}\right)^2 \frac{1}{\left(\frac{2.77R_A 10^6}{\omega}\right)^2 + 1}\left(1 - \frac{R}{R_s}\lambda_1'\right)$$

6. Conductor and Screen thermal resistance calculation

Parameter	Reference
Conductor diameter, d_c (mm)	Cable datasheet
External diameter over the sc tape of conductor, d_{wb_con} (mm)	Cable datasheet
External diameter of sc conductor screen, d_{sc} (mm)	Cable datasheet
External diameter of insulation, D_i (mm)	Cable datasheet

External diameter of sc insulation screen, D_{si} (mm)	Cable datasheet
External diameter of sc-water blocking tape, D_{uwb} (mm)	Cable datasheet
Thermal resistivity of semiconducting tapes, ρ_{sc_t} (K.m/W)	
Thermal resistivity of sc screen, ρ_{sc} (K.m/W)	
Thermal resistivity of insulation, ρ_i (K.m/W)	
Thermal resistivity of water blocking tape, ρ_{wb} (K.m/W)	
Thermal resistance of sc tape over conductor, $T_{1\_sc\_con}$ (K.m/W)	Calculated
Thermal resistance of sc conductor screen, T_{1_csc} (K.m/W)	Calculated
Thermal resistance of insulation, T_{1_i} (K.m/W)	Calculated
Thermal resistance of sc insulation screen, T_{1_isc} (K.m/W)	Calculated
Thermal resistance of sc water blocking tape, T_{1_uwbt} (K.m/W)	Calculated
Thermal resistance between conductor and screen per core length, T_{1_core} (K.m/W)	Calculated
Thermal resistance between conductor and screen, T_1 (K.m/W)	Calculated

$$T_{1\_wb\_con} = \frac{\rho_{sc\_t}}{2\pi} \ln\left(\frac{d_{sc}}{d_c}\right)$$

$$T_{1\_csc} = \frac{\rho_{sc}}{2\pi} \ln\left(\frac{d_{sc}}{d_c}\right)$$

$$T_{1\_i} = \frac{\rho_i}{2\pi} \ln\left(\frac{D_i}{D_{sc}}\right)$$

$$T_{1\_isc} = \frac{\rho_{sc}}{2\pi} \ln\left(\frac{d_{si}}{D_i}\right)$$

$$T_{1\_wbt} = \frac{\rho_{wb}}{2\pi} \ln\left(\frac{D_{si}}{D_i}\right)$$

$$T_{1\_core} = T_{1\_wb\_con} + T_{1\_csc} + T_{1\_i} + T_{1\_isc} + T_{1\_wbt}$$

$$T_1 = \frac{T_{1_{core}}}{f_{layup}}$$

7. Sheath, fillers and bedding thermal resistance calculation, T_2

Parameter	Reference
External diameter of metallic sheath, D_s (mm)	Cable datasheet
External diameter of sc PE sheath, D_e (mm)	Cable datasheet
Thermal resistivity of sc PE sheath, ρ_{scPE} (K.m/W)	
Geometric factor, G	Calculated
Thermal resistivity of fillers and binding tapes, ρ_{fill_bt} (K.m/W)	
Thermal resistance of sheath around each core per core length, T'_{2_core} (K.m/W)	Calculated
Thermal resistance of sheath around each core per cable length, T'_2 (K.m/W)	Calculated

Thermal resistance of fillers and bedding for SL-type cables, T"$_2$ (K.m/W)	Calculated
Thermal resistance of the sheath, T_2 (K.m/W)	Calculated

$$T'_{2\_core} = \frac{\rho_{wb}}{2\pi} \ln\left(\frac{D_e}{D_s}\right)$$

$$T'_2 = \frac{T'_{2\_core}}{f_{layup}}$$

$$X = \frac{\left(\frac{D_{armour} - D_{cable}}{2}\right)}{D_e}$$

$$G = 2\pi(0.00022619 + 2.11429X - 20.4762X^2)$$

$$T''_2 = \frac{\rho_T}{6\pi} G$$

$$T_2 = \frac{T'_2}{3} + T''_2$$

8. Outer covering thermal resistance calculation, T_3

Parameter	Reference
External diameter of armour, D'$_a$ (mm)	Cable datasheet
Thickness of the serving, t_3 (mm)	Cable datasheet
Thermal resistivity of outer covering, ρ_T (K.m/W)	
Thermal resistance of outer covering, T_3 (K.m/W)	Calculated

$$T_3 = \frac{\rho_T}{2\pi} \ln\left(1 + \frac{2t_3}{D'_a}\right)$$

9. External thermal resistance calculation, T_4

Parameter	Reference
External diameter of one cable, D_e (mm)	Cable datasheet
Distance from the surface of the ground to the cable axis, *L* (mm)	System design
Thermal resistivity of the soil, ρ_{soil} (K.m/W)	System design
External thermal resistance, T_4 (K.m/W)	Calculated

$$u = \frac{2L}{D_e}$$

$$T_4 = \frac{1}{2\pi} \rho_T [\ln\left(u + \sqrt{u^2 - 1}\right)]$$

10. Permissible current rating calculation, *I*

$$I = \left[\frac{\Delta\theta - W_d[0.5T_1 + n(T_2 + T_3 + T_4)]}{RT_1 + nR(1 + \lambda_1)T_2 + nR(1 + \lambda_1 + \lambda_2)(T_3 + T_4)}\right]^{0.5}$$

11. Losses calculation

Conductor Losses:

$$P_{core} = nRI^2$$

$$P_{core} = 3(4.211x10^{-5})(838.34)^2$$

$$P_{core} = 88.786\ W/m$$

Screen Losses:

$$P_{screen} = n\gamma_1 RI^2$$

$$P_{screen} = 3(0.16284)(4.211x10^{-5})(838.34)^2$$

$$P_{screen} = 14.458\ W/m$$

Armour Losses:

$$P_{armour} = n\gamma_2 RI^2$$

$$P_{armour} = 3(0.42065)(4.211x10^{-5})(838.34)^2$$

$$P_{armour} = 37.348\ W/m$$

Dielectric Losses:

$$W_{d_t} = 3W_d$$

$$W_{d_t} = 3(0.13168)$$

$$W_{d_t} = 0.395\ W/m$$

APPENDIX E. ELECTRICAL LOSS WORKED EXAMPLE

This example covers the electrical loss calculation steps for a 30 kV, three core 630 mm^2 submarine inter-array cable with the datasheet shown. The lay configuration is as follows:

Cable buried in seafloor at a 1 m depth

Seabed soil temperature 15°C

Soil thermal resistivity 0.7 K.m/W

Solidly bonded sheaths

One circuit thermally independent

Dimensional characteristics :

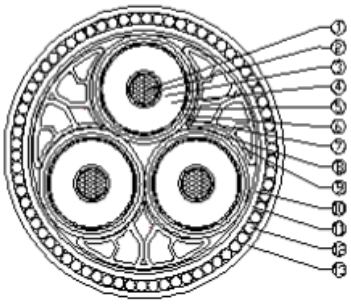

		Diameter (mm)
1.	Copper round stranded compacted class 2 according to IEC 60228 of nominal cross-section equal to 630 sq.mm, longitudinally water sealed.	30 (approximate)
2.	Semiconducting tape(s) applied with overlap.	30.5 (approximate)
3.	Conductor non-metallic extruded screen: Extruded semiconducting compound bonded to inner surface of insulation.	32.5 (approximate)
4.	Insulation: XLPE super-clean according to IEC 60502 of 8.0 mm nominal thickness.	48.5 (approximate)
5.	Core non-metallic extruded screen: Extruded semiconducting compound bonded to outer surface of insulation.	50.3 (approximate)
6.	Semiconducting waterblocking tape(s) applied with overlap.	52.5 (approximate)
7.	Metallic sheath: Lead alloy of 2.3 mm nominal thickness.	57.1 (approximate)
8.	Semiconducting PE sheath of 2.5 mm approximate thickness. Sheath colour: Black	62.1 (approximate)
9.	Extruded polyethylene profile fillers at the outer interstices between cores in order to give the cable a circular cross-section.	134.9 (approximate, after cabling)
10.	Binding synthetic tape(s) helically applied with overlap.	135.3 (approximate)
11.	One layer of polypropylene yarns of approximate thickness of 1 mm.	137.3 (approximate)
12.	Armour consisting of helically applied bitumen compound coated galvanized steel round wires of grade 34, class A, 6.0 mm diameter, according to EN 10257-2. Number of wires: 71, Length of lay: 1.785 mm	149.3 (approximate)
13.	Two layers of polypropylene yarns with total approximate thickness of 3.0 mm. Over the inner (first) layer bitumen compound is applied. Also, the outer (second) layer shall consist of black and yellow polypropylene yarns as to form a helical yellow stripe.	Cable OD = 155.3 (approximate)

Electrical Data:		
Frequency:	50	Hz
Maximum conductor's temperature at continuous operation:	90	°C
Maximum conductor's temperature at short-circuit (5 s maximum duration):	250	°C
Maximum conductor DC resistance at 20°C:	0.0283	Ω/km

Figure 27: Cable datasheet

1. Calculation of lay-up factor of the cores, f_{layup}

Parameter	Value	Reference

Lay length of core stranding, L_{core} (mm)	2152	Cable datasheet
Core diameter, D_e (mm)	62.1	Cable datasheet

$$f_{layup} = \sqrt{1 + \left[\frac{1.29\pi D_e}{L_{core}}\right]^2} = \sqrt{1 + \left[\frac{1.29\pi(62.1)}{(2152)}\right]^2} = 1.00682\ mm$$

2. Calculation of conductor AC resistance at operation temperature, *R*

Parameter	Value	Reference
Conductor DC resistance at 20°C, R_0 (Ω/m)	$0.0283x10^{-3}$	Cable datasheet
External diameter of conductor, d_c (mm)	30	Cable datasheet
Conductor material	Copper	Cable datasheet
Type of conductor	Round stranded compacted	Cable datasheet
Skin effect factor used for calculating x_s, k_s	1	
Proximity effect factor used for calculating x_p, k_s	1	
Temperature coefficient per Kelvin at 20°C, α_{20} (K^{-1})	$3.93x10^{-3}$	
Maximum operating temperature of conductor, θ (°C)	90	Cable datasheet
Axial separation of conductors, *s* (mm)	62.1	Cable datasheet
System frequency, *f* (Hz)	50	System design

$$R' = R_o[1 + \alpha_{20}(\theta - 20)] = (0.0283x10^{-3})\left[1 + (3.93x10^{-3})\left((90) - 20\right)\right] = 3.6085x10^{-5}\ \Omega/\mathrm{m}$$

$$x_s^2 = \frac{8\pi f}{R'}10^{-7}k_s = \frac{8\pi(50)}{(3.6085x10^{-5})}10^{-7}(1) = 3.4824$$

$$y_s = \frac{x_s^4}{192 + 0.8x_s^4} = \frac{(3.4824)^4}{192 + 0.8(3.4824)^4} = 0.06012$$

$$x_p^2 = \frac{8\pi f}{R'}10^{-7}k_p = \frac{8\pi(5)}{(3.6085x10^{-5})}10^{-7}(1) = 3.4824$$

$$y_p = \frac{x_s^4}{192 + 0.8x_s^4}\left(\frac{d_c}{s}\right)^2\left[0.312\left(\frac{d_c}{s}\right)^2 + \frac{1.18}{\frac{x_s^4}{192 + 0.8x_s^4} + 0.27}\right]$$

$$= \frac{(3.4824)^4}{192 + 0.8(3.4824)^4}\left(\frac{(30)}{(62.1x10^{-3})}\right)^2\left[0.312\left(\frac{(30)}{(62.1x10^{-3})}\right)^2 + \frac{1.18}{\frac{(3.4824)^4}{192 + 0.8(3.4824)^4} + 0.27}\right] = 0.05118$$

$$R = R'\left(1 + 1.5(y_s + y_p)\right) = (3.6085x10^{-5})\left(1 + 1.5((0.06012) + (0.05118))\right) = 4.211x10^{-5}\ \Omega/\text{m}$$

3. Dielectric losses, W_d

Parameter	Value	Reference
Diameter over insulation, D_i (mm)	48.5	Cable datasheet
External diameter of conductor including screen, d_c (mm)	32.5	Cable datasheet
Relative permittivity of insulation, ε	2.5	
Loss factor for the insulation, *tanδ*	$40x10^{-4}$	
Voltage to earth, U_0 (V)	$\frac{30000}{\sqrt{3}}$	System design
System frequency, *f* (Hz)	50	System design
Capacitance of each core, *C* (F/m)		
Angular frequency of system, ω		
Dielectric loss per unit length per phase, W_d (W/m)		

$$C_{core} = \frac{\varepsilon}{18\ln\left(\frac{D_i}{d_c}\right)}10^{-9} = \frac{(2.5)}{18\ln\left(\frac{(48.5)}{(32.5)}\right)}10^{-9} = 3.469x10^{-10}\ F/m$$

$$C = C_{core}f_{layup} = (3.469x10^{-10})(1.00682) = 3.4931x10^{-10}\ F/m$$

$$\omega = 2\pi f = 2\pi(50) = 314.159\ rad/s$$

$$W_d = \omega C U_o^2 tan\delta = (314.159)(3.4931x10^{-10})\left(\frac{30000}{\sqrt{3}}\right)^2(40x10^{-4}) = 0.1317\ W/m$$

4. Sheath loss factor calculation, λ_1

Parameter	Value	Reference
AC resistance of sheath at 20°C, $Rso\ (\Omega/m)$		Calculated
Mean diameter of the sheath, *d* (mm)	54.8	Cable datasheet
Cross sectional area of the metallic sheath, A_{PB} (mm^2)		Calculated
Sheath resistivity at 20°C, ρ_{sh} (Ωm)	$21.4x10^{-8}$	
Sheath temperature coefficient at 20°C per Kelvin, α_{20}	$4.0x10^{-3}$	
Distance between conductor axes, S (mm)	62.1	System design
System frequency, f (Hz)	50	System design
AC resistance of conductor at operating temp, $R\ (\Omega/m)$		Calculated
Calculation of the cross-sectional area of the sheath		
Maximum operating temperature of the cable sheath, to be determined iterative, θ_{sc} (°C)		
Resistance of sheath at operating temperature, R_s (Ω/m)		
Reactance per unit length of sheath, X (Ω/m)		

Loss factor circulating losses for sheath, λ_1'		
Loss factor for eddy current losses λ_1''		
Loss factor of the sheath λ_1		

$$A_{PB} = \pi t_{sh}(d + t_{sh}) = \pi(0.0023)\big((0.00525) + (0.0023)\big) = 395.966x10^{-6}\ m^2$$

$$R_{so\_core} = \frac{\rho_{sh}}{A_{PB}} = \frac{(21.4x10^{-8})}{(395.966x10^{-6})} = 5.405x10^{-4}\ \Omega/m$$

$$R_{so} = R_{so\_core} f_{layup} = (5.405x10^{-4})(1.00682) = 5.441x10^{-4}\ \Omega/m$$

$$\theta_{sc} = \theta - (I^2R + 0.5W_d)T_1 = (90) - \big((838.34)(4.211) + 0.5(0.1317)\big)(0.3579) = 79.385\ ℃$$

$$R_s = R_{so}[1 + \alpha_{20}(\theta_{sc} - 20)] = (5.4413x10^{-4})\big[1 + (4.0x10^{-3})\big((79.385) - 20\big)\big] = 6.734x10^{-4}\ \Omega/\mathrm{m}$$

$$d = (D_{sh} - t_{sh})\ \big((0.0525) - (0.0023)\big) = 0.0548\ m$$

$$X_{1\_core} = 2\omega 10^{-7} \ln\left(\frac{2s}{d}\right) = 2(314.159)10^{-7} \ln\left(\frac{2(0.0621)}{(0.0548)}\right) = 5.141x10^{-5}\ \Omega/\mathrm{m}$$

$$X_1 = X_{1\_core} f_{layup} = (5.141x10^{-5})(1.00682) = 5.176x10^{-5}\ \Omega/\mathrm{m}$$

$$\lambda_1' = \frac{R_S}{R}\frac{1.5}{1 + \left(\frac{R_S}{X}\right)^2} = \frac{(6.734x10^{-4})}{(4.211x10^{-5})}\frac{1.5}{1 + \left(\frac{(6.734x10^{-4})}{5.176x10^{-5})}\right)^2} = 0.141$$

$$m = \frac{\omega}{R_s}10^{-7} = \frac{(100\pi)}{(6.734x10^{-4})}10^{-7} = 0.0467$$

$$\lambda_0 = 3\left(\frac{m^2}{1 + m^2}\right)\left(\frac{d}{2s}\right)^2 = 3\left(\frac{(0.0467)^2}{1 + (0.0467)^2}\right)\left(\frac{(0.0548)}{2(0.0621)}\right)^2 = 0.00127$$

$$\Delta_1 = (1.14m^{2.45} + 0.33)\left(\frac{d}{2s}\right)^{0.92m + 1.66} = (1.14(0.0467)^{2.45} + 0.33)\left(\frac{0.0548)}{2(0.0621)}\right)^{0.92(0.0467) + 1.66} = 0.0821$$

$$\Delta_2 = 0$$

$$\beta_1 = \sqrt{\frac{4\pi\omega}{10^7\rho_s\big(1 + \alpha_s(\theta_s - 20)\big)}} = \sqrt{\frac{4\pi(100\pi)}{10^7(21.4x10^{-8})\big(1 + (0.004)((79.385) - 20)\big)}} = 38.609$$

$$g_s = 1 + \left(\frac{t_s}{D_s}\right)^{1.74}(\beta_1 D_s 10^{-3} - 1.6) = 1 + \left(\frac{(2.3)}{(57.1)}\right)^{1.74}((38.609)(57.1)10^{-3} - 1.6) = 1.00226$$

$$\lambda_1'' = \frac{R_s}{R}\left[g_s\lambda_0(1 + \Delta_1 + \Delta_2) + \frac{(\beta_1 t_s)^4}{12x10^{12}}\right]$$

$$= \frac{(6.734x10^{-4})}{(4.211x10^{-5})}\left[(1.00226)(0.00127)(1 + (0.0821) + (0)) + \frac{((38.609)(2.3))^4}{12x10^{12}}\right] = 0.0221$$

$$M = N = \frac{R_{S_{PB}}}{X_{core}} = \frac{(6.734x10^{-4})}{(5.176x10^{-5})} = 13.010$$

$$F = \frac{4M^2N^2 + (M+N)^2}{4(M^2+1)(N^2+1)} = \frac{4(13.010)^2(13.010)^2 + ((13.010)+(13.010))^2}{4((13.010)^2+1)((13.010)^2+1)} = 0.994$$

$$\lambda_1 = \lambda_1' + F\lambda_1'' = (0.141) + (0.994)(0.0221) = 0.163$$

5. Armour loss factor calculation, λ_2

Parameter	Value	Reference
AC resistance of armour at 20°C, R_{A0}		
Mean diameter of the armour, d_A (mm)	143.3	
Number of armour wires, n_1	71	
Diameter of armour wires, d_f	6	
Cross sectional area of the armour, A (mm^2)		
Lay Length of the armour, $laylength_{arm}$ (mm)	1785	
Increment factor for the estimation of the AC resistance of the armour based on the DC resistance of the armour, K		
Armour resistivity at 20°C, ρ_a (Ωm)	13.8x10^{-8}	
Armour temperature coefficient at 20°C per Kelvin, α_{arm}	0.0045	
Distance between conductor axes/Diameter over single core, S (mm)	62.1	
Diameter over assembled three cores, D_{cable} (mm)	134.9	
System frequency, f (Hz)	50	
AC resistance of conductor at operating temp., R (Ω/m)		

$$A = n_1\pi\left(\frac{d_f}{2}\right)^2 = (71)\pi\left(\frac{(6)}{2}\right)^2 = 2007.478\,m^2$$

$$f_{layup\_armour} = \frac{S}{L} = \sqrt{1 + \left(\frac{\pi d_A}{laylength_{arm}}\right)^2} = \sqrt{1 + \left(\frac{\pi(0.1433)}{(1.785)}\right)^2} = 1.0313$$

$$R_{A0}^* = \frac{\rho_a}{A} = \frac{13.8x10^{-8}}{2007.478} = 6.874x10^{-5}\ \Omega/m$$

$$R_{Ao} = kR_{Ao}^* f_{layup\_armour} = (1.467)(6.874x10^{-5})(1.0313) = 1.040x10^{-4}\ \Omega/m$$

$$\theta_{arm} = \theta - (I^2R + 0.5W_d)T_1 - (I^2R(1+\lambda_1) + W_d)nT_2$$

$$= (90) - \Big((838.340)^2(4.211x10^{-5}) + 0.5(0.132)\Big)(0.358)$$
$$- \Big((838.340)^2(4.211x10^{-5})\big(1 + (0.163)\big) + (0.132)\Big)3(0.0779) = 71.309\ ℃$$

$$R_A = R_{Ao}[1 + \alpha_{arm}(\theta_{arm} - 20)] = (1.040x10^{-4})\big[1 + (0.0045)\big((71.309) - 20\big)\big]$$
$$= 1.280x10^{-4}\ \Omega/\mathrm{m}$$

$$c = \frac{D_{cable}}{2} - \frac{S}{2} = \frac{(0.1349)}{2} - \frac{(0.0621)}{2} = 0.0364\ m$$

$$\lambda_2 = 1.23\frac{R_A}{R}\left(\frac{2c}{d_A}\right)^2 \frac{1}{\left(\frac{2.77R_A 10^6}{\omega}\right)^2 + 1}\left(1 - \frac{R}{R_s}\lambda_1'\right)$$

$$= 1.23\frac{(1.280x10^{-4})}{(4.211x10^{-5})}\left(\frac{2(0.0364)}{(0.1433)}\right)^2 \frac{1}{\left(\frac{2.77(1.280x10^{-4})10^6}{314.159}\right)^2 + 1}\left(1 - \frac{(4.211x10^{-5})}{(6.734x10^{-4})}(0.141)\right)$$

$$= 0.421$$

6. Conductor and Screen thermal resistance calculation, T_1

Parameter	Value	Reference
Conductor diameter, d_c (mm)	30	Cable datasheet
External diameter over the sc tape of conductor, d_{wb_con} (mm)	30.5	Cable datasheet
External diameter of sc conductor screen, d_{sc} (mm)	32.5	Cable datasheet
External diameter of insulation, D_i (mm)	48.5	Cable datasheet
External diameter of sc insulation screen, D_{si} (mm)	50.3	Cable datasheet
External diameter of sc-water blocking tape, D_{uwb} (mm)	52.5	Cable datasheet
Thermal resistivity of semiconducting tapes, ρ_{sc_t} (K.m/W)	6	
Thermal resistivity of sc screen, ρ_{sc} (K.m/W)	2.5	
Thermal resistivity of insulation, ρ_i (K.m/W)	3.5	
Thermal resistivity of water blocking tape, ρ_{wb} (K.m/W)	12	
Thermal resistance of sc tape over conductor, $T_{1\_sc\_con}$ (K.m/W)		Calculated
Thermal resistance of sc conductor screen, T_{1_csc} (K.m/W)		Calculated
Thermal resistance of insulation, T_{1_i} (K.m/W)		Calculated
Thermal resistance of sc insulation screen, T_{1_isc} (K.m/W)		Calculated
Thermal resistance of sc water blocking tape, T_{1_uwbt} (K.m/W)		Calculated
Thermal resistance between conductor and screen per core length, T_{1_core} (K.m/W)		Calculated
Thermal resistance between conductor and screen, T_1 (K.m/W)		Calculated

$$T_{1\_wb\_con} = \frac{\rho_{sc\_t}}{2\pi}\ln\left(\frac{d_{sc}}{d_c}\right) = \frac{6}{2\pi}\ln\left(\frac{0.0305}{0.03}\right) = 0.01578\ K.m/W$$

$$T_{1\_csc} = \frac{\rho_{sc}}{2\pi}\ln\left(\frac{d_{sc}}{d_c}\right) = \frac{2.5}{2\pi}\ln\left(\frac{0.0325}{0.0305}\right) = 0.02527\ K.m/W$$

$$T_{1\_i} = \frac{\rho_i}{2\pi}\ln\left(\frac{D_i}{D_{sc}}\right) = \frac{3.5}{2\pi}\ln\left(\frac{0.0485}{0.0325}\right) = 0.22299\ K.m/W$$

$$T_{1\_isc} = \frac{\rho_{sc}}{2\pi}\ln\left(\frac{d_{si}}{D_i}\right) = \frac{2.5}{2\pi}\ln\left(\frac{0.0503}{0.0485}\right) = 0.01450\ K.m/W$$

$$T_{1\_wbt} = \frac{\rho_{wb}}{2\pi}\ln\left(\frac{D_{si}}{D_i}\right) = \frac{12}{2\pi}\ln\left(\frac{0.0525}{0.0503}\right) = 0.08176\ K.m/W$$

$$T_{1\_core} = T_{1\_wb\_con} + T_{1\_csc} + T_{1\_i} + T_{1\_isc} + T_{1\_wbt}$$
$$= 0.01578 + 0.02527 + 0.22299 + 0.01450 + 0.08176 = 0.3603\ K.m/W$$

$$T_1 = \frac{T_{1_{core}}}{f_{layup}} = \frac{0.3603}{1.00682} = 0.3579\ K.m/W$$

7. Sheath, fillers and bedding thermal resistance calculation, T_2

Parameter	Value	Reference
External diameter of metallic sheath, D_s (mm)	57.1	Cable datasheet
External diameter of sc PE sheath, D_e (mm)	62.1	Cable datasheet
Thermal resistivity of sc PE sheath, ρ_{scPE} (K.m/W)	2.5	
Geometric factor, G		Calculated
Thermal resistivity of fillers and binding tapes, ρ_{fill_bt} (K.m/W)	6	
Thermal resistance of sheath around each core per core length, T'_{2_core} (K.m/W)		Calculated
Thermal resistance of sheath around each core per cable length, T'_2 (K.m/W)		Calculated
Thermal resistance of fillers and bedding for SL-type cables, T''_2 (K.m/W)		Calculated
Thermal resistance of the sheath, T_2 (K.m/W)		Calculated

$$T'_{2_{core}} = \frac{\rho_{scPE}}{2\pi}\ln\left(\frac{D_e}{D_s}\right) = \frac{(2.5)}{2\pi}\ln\left(\frac{0.0621}{0.0571}\right) = 0.03340\ K.m/W$$

$$T'_2 = \frac{T'_{2\_core}}{f_{layup}} = \frac{0.03340}{1.00682} = 0.03317\ K.m/W$$

$$X = \frac{\left(\frac{D_{armour} - D_{cable}}{2}\right)}{D_e} = \frac{\left(\frac{0.1373 - 0.1349}{2}\right)}{0.0621} = 0.01932$$

$$G = 2\pi(0.00022619 + 2.11429X - 20.4762X^2)$$
$$= 2\pi(0.00022619 + 2.11429(0.01932) - 20.4762(0.01932)^2) = 0.2101$$

$$T''_2 = \frac{\rho_T}{6\pi}G = \frac{6}{6\pi}(0.2101) = 0.06687\ K.m/W$$

$$T_2 = \frac{T'_2}{3} + T''_2 = \frac{0.03317}{3} + 0.06687 = 0.07793\ K.m/W$$

8. Outer covering thermal resistance calculation, T_3

Parameter	Value	Reference
External diameter of armour, D'_a (mm)	149.3	Cable datasheet
Thickness of the serving, t_3 (mm)	3	Cable datasheet
Thermal resistivity of outer covering, ρ_T (K.m/W)	6	
Thermal resistance of outer covering, T_3 (K.m/W)		Calculated

$$T_3 = \frac{\rho_T}{2\pi}\ln\left(1+\frac{2t_3}{D'_a}\right) = \frac{6}{2\pi}\ln\left(1+\frac{2(0.003)}{0.1493}\right) = 0.03763\ K.m/W$$

9. External thermal resistance calculation, T_4

Parameter	Value	Reference
External diameter of one cable, D_e (mm)	155.3	Cable datasheet
Distance from the surface of the ground to the cable axis, L (mm)	1000	System design
Thermal resistivity of the soil, ρ_{soil} (K.m/W)	0.7	System design
External thermal resistance, T_4 (K.m/W)		Calculated

$$u = \frac{2L}{D_e} = \frac{2(1)}{0.1553} = 12.8783$$

$$T_4 = \frac{1}{2\pi}\rho_{soil}[\ln\left(u+\sqrt{u^2-1}\right)] = \frac{1}{2\pi}(0.7)[\ln\left(12.8783+\sqrt{(12.8783)^2-1}\right)] = 0.36176\ K.m/W$$

10. Permissible current rating calculation, I

$$I = \left[\frac{\Delta\theta - W_d[0.5T_1 + n(T_2+T_3+T_4)]}{RT_1 + nR(1+\lambda_1)T_2 + nR(1+\lambda_1+\lambda_2)(T_3+T_4)}\right]^{0.5}$$

$$= \left[\frac{75 - 0.13169[0.5(0.3579) + 3((0.07793)+(0.03763)+(0.36176))]}{(4.211x10^{-5})(0.3579) + 3(4.211x10^{-5})(1+(0.16284))(0.07793) + 3(4.211x10^{-5})(1+(0.16284)+(0.42065))((0.03763)+(0.36176))}\right]^{0.5}$$
$$= 838.34\ A$$

11. Conductor Losses calculation

Conductor Losses: $P_{core} = nRI^2 = 3(4.211x10^{-5})(838.34)^2 = 88.786\ W/m$

Screen Losses: $P_{screen} = n\lambda_1 RI^2 = 3(0.16284)(4.211x10^{-5})(838.34)^2 = 14.458\ W/m$

Armour Losses: $P_{armour} = n\lambda_2 RI^2 = 3(0.42065)(4.211x10^{-5})(838.34)^2 = 37.348\ W/m$

Dielectric Losses: $W_{d_t} = 3W_d = 3(0.13168) = 0.395\ W/m$

CATAPULT
Offshore Renewable Energy

GLASGOW

ORE Catapult
Inovo
121 George Street
Glasgow
G1 1RD

+44 (0)333 004 1400

BLYTH

National Renewable
Energy Centre
Offshore House
Albert Street, Blyth
Northumberland
NE24 1LZ

+44 (0)1670 359555

LEVENMOUTH

Fife Renewables Innovation
Centre (FRIC)
Ajax Way
Leven
KY8 3RS

+44 (0)1670 357649

GRIMSBY

O&M Centre of Excellence
ORE Catapult, Port Office
Cleethorpe Road
Grimsby
DN31 3LL

+44 (0)333 004 1400

ABERDEEN

Subsea UK
30 Abercrombie Court
Prospect Road, Westhill
Aberdeenshire
AB32 6FE

07436 389067

CORNWALL

Hayle Marine Renewables
Business Park
North Quay
Hayle, Cornwall
TR27 4DD

+44 (0)1872 322 119

PEMBROKESHIRE

Marine Energy Engineering
Centre of Excellence (MEECE)
Bridge Innovation Centre
Pembrokeshire Science
& Technology Park
Pembroke Dock, Wales
SA72 6UN

+44 (0)333 004 1400

CHINA

11th Floor
Lan Se Zhi Gu No. 15
Ke Ji Avenue,
Hi-Tech Zone
Yantai City
Shandong Province
China

+44 (0)333 004 1400

LOWESTOFT

OrbisEnergy
Wilde Street
Lowestoft
Suffolk
NR32 1XH

01502 563368